

1. Report No. FHWA/TX-90+1129-2F	2. Government Accession No.	3.  L004886
4. Title and Subtitle ANALYSIS AND DESIGN OF BRIDGE BENT COLUMNS		5. Report Date November 1988
7. Author(s) M. Haque, J. M. Roesset, and C. P. Johnson		6. Performing Organization Code 8. Performing Organization Report No. Research Report 1129-2F
9. Performing Organization Name and Address Center for Transportation Research The University of Texas at Austin Austin, Texas 78712-1075		10. Work Unit No.
12. Sponsoring Agency Name and Address Texas State Department of Highways and Public Transportation; Transportation Planning Division P. O. Box 5051 Austin, Texas 78763-5051		11. Contract or Grant No. Research Study 3-5-86-1129
15. Supplementary Notes Study conducted in cooperation with the U. S. Department of Transportation, Federal Highway Administration Research Study Title: "Bent Column Analysis and Design"		13. Type of Report and Period Covered Final
16. Abstract The behavior of bridge bents under spatial loads was investigated to evaluate the suitability of the current office procedure of the Texas State Department of Highways and Public Transportation (TSDHPT) for analyzing and designing slender concrete bridge bent columns. Two computer codes were developed for this purpose. The linear method of analysis uses the conventional direct stiffness method of solution and considers linear material behavior. The AASHTO moment magnifier method was used to approximate second order effects. The design forces from the linear analysis were compared with those from the TSDHPT approximate procedure. The effect of variation in live load positions over the bridge deck was examined. The nonlinear method of analysis, developed in this study, uses a fiber model and an updated Lagrange finite element formulation to predict the space behavior of multistory concrete bents. The analytical results for typical bents were compared with those from the TSDHPT approximate method and the AASHTO moment magnification procedure. The sensitivity of the results to bent column slenderness and foundation flexibilities were examined in terms of predicted bent behavior.		14. Sponsoring Agency Code
17. Key Words bridge bent, column, behavior, inplane, out of plane, loads, procedures, analysis, design, linear moment magnifier method, three-dimensional	18. Distribution Statement No restrictions. This document is available to the public through the National Technical Information Service, Springfield, Virginia 22161.	
19. Security Classif. (of this report) Unclassified	20. Security Classif. (of this page) Unclassified	21. No. of Pages 76
22. Price		

**ANALYSIS AND DESIGN OF
BRIDGE BENT COLUMNS**

by

M. Haque
J. M. Roesset
C. P. Johnson

Research Report Number 1129-2F

Research Project 3-5-86-1129
Bent Column Analysis and Design

conducted for

**Texas State Department of Highways
and Public Transportation**

in cooperation with the

**U.S. Department of Transportation
Federal Highway Administration**

by the

CENTER FOR TRANSPORTATION RESEARCH

Bureau of Engineering Research
THE UNIVERSITY OF TEXAS AT AUSTIN

November 1988

The contents of this report reflect the views of the authors, who are responsible for the facts and the accuracy of the data presented herein. The contents do not necessarily reflect the official views or policies of the Federal Highway Administration. This report does not constitute a standard, specification, or regulation.

There was no invention or discovery conceived or first actually reduced to practice in the course of or under this contract, including any art, method, process, machine, manufacture, design or composition of matter, or any new and useful improvement thereof, or any variety of plant which is or may be patentable under the patent laws of the United States of America or any foreign country.

PREFACE

The authors would like to express their appreciation to Mr. Richard L. Wilkison of the Bridge Division of the Texas State Department of Highways and Public Transportation for his valuable advice and assistance on the study as a whole, providing the information on the design approach used at present and data on actual bridges in the State of Texas.

The authors would also like to thank Kay Lee and the entire staff of the Center for Transportation Research for their assistance in preparation of the report.

M. Haque
J. M. Roesset
C. P. Johnson

ABSTRACT

The behavior of bridge bents under spatial loads was investigated to evaluate the suitability of the current office procedure of the Texas State Department of Highways and Public Transportation (TSDHPT) for analyzing and designing slender concrete bridge bent columns. Two computer codes were developed for this purpose.

The linear method of analysis uses the conventional direct stiffness method of solution and considers linear material behavior. The AASHTO moment magnifier method was used to approximate second order effects. The design forces from the linear analysis were compared with those from the TSDHPT approximate procedure. The effect

of variation in live load positions over the bridge deck was examined.

The nonlinear method of analysis, developed in this study, uses a fiber model and an updated Lagrange finite element formulation to predict the space behavior of multistory concrete bents. The analytical results for typical bents were compared with those from the TSDHPT approximate method and the AASHTO moment magnification procedure. The sensitivity of the results to bent column slenderness and foundation flexibilities were examined in terms of predicted bent behavior.

LIST OF REPORTS

Research Report No. 1129-1, "Computer Program for the Analysis of Bridge Bent Columns Including a Graphical Interface," by R. W. Stocks, C. P. Johnson, and J. M. Roesset, presented the development of a computer program to determine axial forces and moments in columns of bridge bents accounting for the AASHTO loading combinations of Load Groups I, II, and III and using either the simplified procedure of the Texas State Department of Highways and Public Transportation or an integral frame analysis. A graphical interface was developed for the IBM-AT micro-computer to input the needed data in a user-friendly, self-explanatory way. The computer program was adapted to the

facilities of the Texas State Department of Highways and Public Transportation.

Research Report No. 1129-2F, "Analysis and Design of Bridge Bent Columns," by M. Haque, J. M. Roesset, and C. P. Johnson, presents the results of comparative studies to evaluate the adequacy of the approximate procedure used by the Texas State Department of Highways and Public Transportation. Typical bridge bents are analyzed using this procedure, a linear frame analysis program as developed in the previous report, and a nonlinear analysis program including material and geometric nonlinearities to estimate the ultimate loads.

SUMMARY

The Texas State Department of Highways and Public Transportation uses at present an approximate procedure for the analysis and design of the columns of a bridge bent. In this procedure axial loads due to gravity are uniformly distributed among the columns, the moments due to inplane lateral loads are computed assuming an inflection point at the midheight of the columns, and the moments due to out of plane loads are estimated assuming each column as a cantilever. The column lengths are increased to take into account the flexibility of the foundation including a depth to fixity which is based on engineering judgment and experience. Finally, slenderness or second order geometric effects are considered using a k factor of 1.25.

The purpose of the present study was to assess the validity of these approximations. For this purpose a series of typical bridge bents were considered and analyzed using a linear frame analysis with the k factors suggested by AASHTO and a true nonlinear analysis which incorporates material and geometric nonlinearities to estimate the ultimate loads. In the linear analysis the effect of varying the position of the truck loads over the bridge deck was also investigated. It should be noticed that although a frame analysis is theoretically correct, it assumes rigid joints which may not really exist due the available size for development

length of the rebars. Thus the present approximate procedure, while a simplification, is also based on important practical considerations.

A series of comparative studies have been conducted using both the linear and the nonlinear analysis procedures and the present approximations. The results of these studies indicate that for bents where the girders are symmetrically arranged and for slenderness ratios less than 40 (ratio of the column length to the radius of gyration of the cross section) the approximate procedure yields very reasonable results. When the girders are arranged in a highly unsymmetrical pattern the axial forces in the columns assuming a uniform distribution may be underestimated, particularly if the live loads are moved along the width of the deck. For columns with slenderness ratios larger than 60 some care must be exercised: the ultimate loads may be substantially smaller than those obtained from the nonlinear analyses. Ultimate loads computed using the AASHTO procedure tend to be, on the other hand, conservative and excessively so for very slender frames.

The results indicate also that the use of the depth to fixity to account for the foundation flexibility seems to provide reasonable and conservative results for the range of soil properties considered in the analyses.

IMPLEMENTATION STATEMENT

Comparison between the results obtained using linear and nonlinear frame analysis programs and the approximate procedure used at present by the Texas State Department of Highways and Public Transportation indicates that this procedure gives reasonable design forces for bents with a nearly symmetric arrangement of the girders over the bent cap and for slenderness ratios of the order of 40 or less. The

use of a depth to fixity, based on engineering judgment, to account for the foundation flexibility provided also a reasonably conservative solution for the cases considered.

Some care must be exercised, however, when the procedure is applied to bents with unsymmetric arrangement of the girders, and in particular when dealing with slenderness ratios larger than 60.

TABLE OF CONTENTS

PREFACE	iii
ABSTRACT	iii
LIST OF REPORTS	iii
SUMMARY.....	iv
IMPLEMENTATION STATEMENT.....	iv
CHAPTER 1. INTRODUCTION	
1.1 General.....	1
1.2 Objectives.....	3
1.3 Outline of Contents.....	3
CHAPTER 2. ANALYSIS PROCEDURES	
2.1 General Consideration.....	4
2.1.1 Loading Combinations	4
2.1.2 Moment Magnifier Method.....	4
2.2 Approximate Procedure.....	5
2.3 Linear Analysis of Bents	5
2.4 Nonlinear Analysis of Bents	6
CHAPTER 3. NONLINEAR ANALYSIS FORMULATION	
3.1 Introduction	8
3.2 Derivation of the Stiffness Matrix.....	8
3.3 Geometric Nonlinearity.....	12
3.4 Material Nonlinearity.....	13
3.5 Solution Procedure	15
3.5.1 Computation of Element Distortions	15
3.5.2 Iterative Solution	15
CHAPTER 4. VALIDATION OF COMPUTER PROGRAM	
4.1 Introduction	17
4.2 Effect of Number of Segments Per Member	17
4.3 Effect of the Size of Load Steps.....	17
4.4 Comparison with Analytical Results.....	19
4.5 Comparison with Experimental Results.....	19
4.6 Summary	20
CHAPTER 5. RESULTS AND DISCUSSION	
5.1 Introduction	23
5.2 Bent Configuration	23
5.3 Loads on Bents.....	23
5.4 Approximate Procedure Vs Linear Frame Analysis.....	23
5.4.1 Group I Loads.....	23
5.4.2 Group II Loads.....	24

5.4.3	Group III Loads	24
5.4.4	Discussion of Results.....	24
5.5	Approximate Procedure Vs Nonlinear Analysis.....	34
5.5.1	Load-Deformation Curves.....	34
5.5.2	Predicted Axial Loads Vs Design Axial Forces	34
5.5.3	Predicted Moments Vs Design Moments.....	34
5.5.4	Effect of Slenderness Ratio of Bent Columns	50
5.5.5	Effect of Foundation Flexibility	53
5.6	Summary	54
CHAPTER 6. CONCLUSIONS AND RECOMMENDATIONS		
6.1	Summary of the Study	66
6.2	Approximate Procedure Vs Nonlinear Analysis.....	66
6.1.1	Approximate Procedure Vs Linear Frame Analysis.....	66
6.1.2	Approximate Procedure Vs Nonlinear Analysis.....	66
6.3	Research Needs.....	67
REFERENCES.....		68

CHAPTER 1. INTRODUCTION

1.1 GENERAL

The design of bridge bent columns requires the determination of axial forces and associated moments. The design loads necessary for analyzing bent columns are provided in the American Association of State Highway and Transportation Officials (AASHTO) Specifications [4]. There are twelve loading combinations specified by AASHTO which must be considered in computing the design loads. Of these twelve loading combinations, three groups govern the design of columns for typical Texas highway bridge bents. Figures 1.1 and 1.2 on the following page show a typical highway multi-column bridge bent. The design loads include dead load, live load, impact, earth pressure, buoyancy, wind load on structure, wind load on live load, longitudinal force from live load, centrifugal force, rib shortening, shrinkage, temperature, earthquake, stream flow pressure, and ice pressure.

1.1.1 Current Texas Highway Department Approach

The Texas State Department of Highways and Public Transportation (TSDHPT) has identified AASHTO load groups I, II and III as the critical loading combinations for designing bridge bents. The current office procedure of analysis involves utilizing an approximate method derived for hand analysis. Since the bent cap and column system is an indeterminate frame, simplifying assumptions are made in order to make hand analysis possible. The column moments, due to in-plane lateral loads, are computed assuming an inflection point located at the mid-height of all columns. This assumption may or may not be reasonable depending on the relative stiffness between the bent cap and the columns. Another drawback in the approximate method is that changes in axial loads due to horizontal forces are not taken into account. Neglecting the effect of overturning forces on the axial forces results in final design loads which are not conservative in all cases. A final simplifying assumption is that all columns receive an equal percentage of the total load on the bridge. Although the loads from the superstructure are transferred to bent columns via the girders, the location of these beams over the bent cap is not included in the approximate procedure. No consideration is given for the variation in the live load positions over the bridge deck.

The moments computed for the lateral loads are amplified to include second order effects. There have been several methods advocated for the analysis of compression members [17,18,32,33]. The approximate method of the TSDHPT uses the moment magnifier method of AASHTO [4] to approximate the slenderness effects. The AASHTO provisions are based on the ACI Building Code [1,2] which focuses on strength and do not clearly focus on lateral displacements, although such deflections are implicitly

included in the moment magnification procedure. The extensive experimental and analytical studies [2,6,18] which formed the basis for the code provisions considered typical columns and loading conditions found in buildings. Most buildings have small story drifts, thus lateral deflection is not a primary concern. In bridge bent design, the lateral displacements are considerably higher and therefore lateral deflection may be an important factor. The AASHTO provisions do not explicitly alert designers when deflection might be a problem.

An important aspect of the moment magnification procedure lies in the evaluation of the effective length factor (k) and the reduced column stiffness due to nonlinear effects. The code provides empirical equations for estimating the reduced stiffness of columns and beams. The difficulties in using the effective length approach are associated with the evaluation of the restraints at the column ends. In most Texas highway bridges, little or no restraints are provided at the top of the bent especially in the direction parallel to the bridge axis. Also, the base of the columns are far from fixity. In these conditions, the effective length factor (k) may vary from 1.5 to 3.0 [25]. The degree of fixity at the foundation level is an extremely significant parameter affecting the k values. There is no guidance given in AASHTO on how to evaluate it. The evaluation of rotational and translational restraints for various foundation conditions requires a great deal of judgement. The problem of soil-structure interaction has been addressed by several authors [5,20,22,26,31] for both shallow and pile foundations, under both static and dynamic loadings. The results have been presented in terms of equivalent spring stiffnesses which depend on the soil properties (shear wave velocity) and the type and size of the foundation. The determination of the shear wave velocity is a formidable task. Empirical equations relating the shear wave velocity and number of blow counts have been presented in the literature [28,30].

In the event of uncertainty in the foundation fixity, the current office procedure assumes an increased column length and a fixed base to simulate the soil-structure interaction effects. The increased column length is called "Depth to fixity" (Fig 1.2). Its value ranges from 4 to 10 feet depending on the soil conditions and the engineer's judgment.

With the fixed base, the bent behaves like a cantilever in the out of plane direction and as an unbraced frame under in-plane loads. For this case, the code provisions recommend the use of k values of 2.0 for the out of plane bending. The effective length factor for in-plane behavior should be computed considering the interaction of rotational restraint of beams on columns. The approximate procedure of the TSDHPT assumes an effective length factor of 1.25 for both axes of bending. The value is used irrespective of the relative

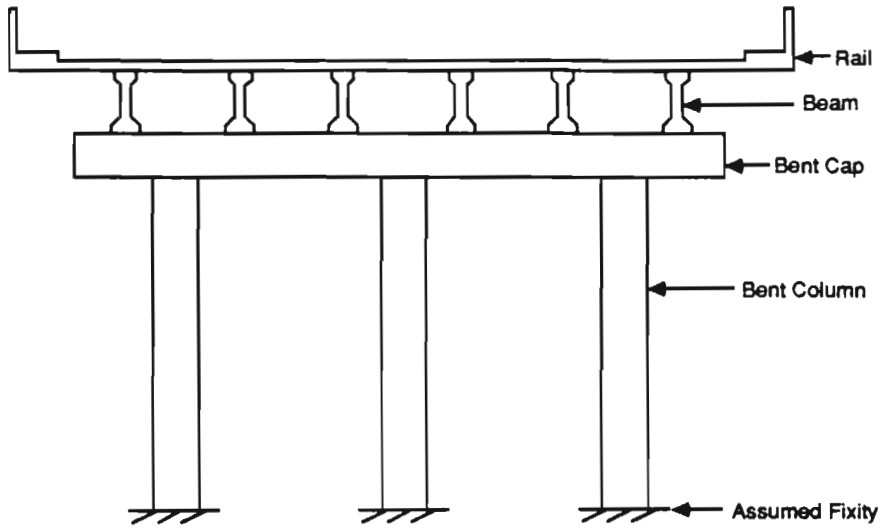


Fig 1.1. Bridge bent.

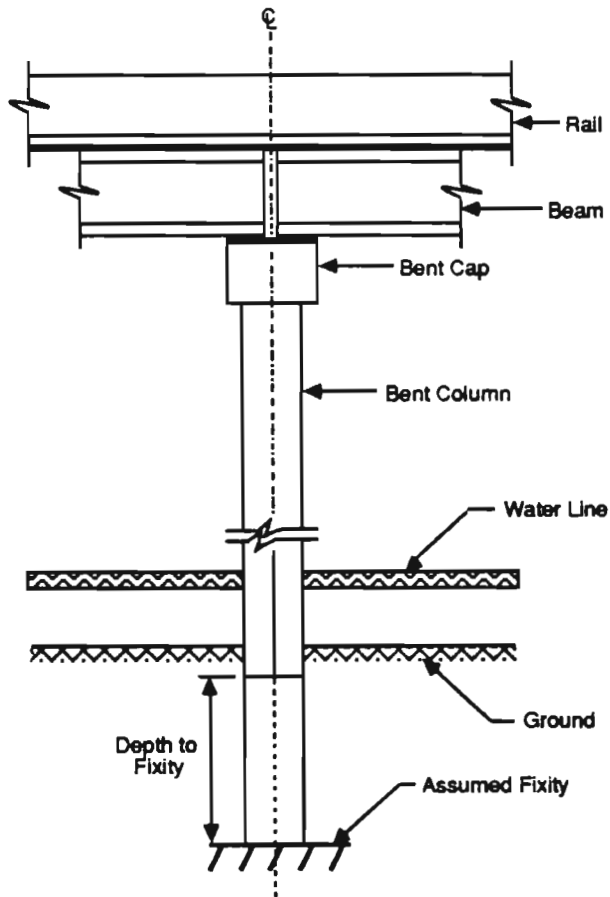


Fig 1.2. Bent column elevation.

sizes of beams and columns, the loading conditions, and the column slenderness. The moment magnification procedure of analysis was originally developed for uniaxial bending. The procedure is greatly complicated when biaxial bending is considered. The ACI Code [1,2] conservatively recommends to amplify the moments about both axes, computed from a linear analysis, independently of their associated moment magnification factors. The present code provisions do not account for the interaction between the two axes of bending. The TSDHPT approximate procedure essentially uses the code method to approximate the biaxial slenderness effects.

1.2 OBJECTIVES

The purpose of this investigation was to study the suitability of the current office procedure of the TSDHPT in predicting the design forces and the behavior of slender bents. The study involved developing two computer programs for the analysis of reinforced concrete bridge bents.

The linear frame analysis program utilizes the direct stiffness method of solution and considers linear material behavior. The moment magnifier method of the code is used to approximate second order effects. The program was used to compute the design forces for bent columns.

The nonlinear analysis program was developed to analyze reinforced concrete bridge bents under spatial loads. The fiber model [3,23] and an updated Lagrange finite element formulation were used to model the geometric and material nonlinearities. The program was used to predict the behavior of typical bents up to failure.

The primary objectives of this study were:

(1) To compare the design loads obtained from the approximate method with those obtained using the linear frame analysis.

(2) To investigate the sensitivity of variations in the live load positions, over the bridge deck, on the computed design forces from the approximate procedure.

(3) To compare the moments obtained from the approximate procedure and the AASHTO moment magnifier method with those obtained from the nonlinear analysis.

(4) To investigate the effect of column slenderness ratio on the behavior of bents and to evaluate the sensitivity of foundation flexibilities, comparing the results for various foundation conditions with the current approach of the approximate procedure.

1.3 OUTLINE OF CONTENTS

Chapter 2 describes the analysis procedures used in this study. Computation of various loads on bridges are briefly discussed. A brief review of the AASHTO moment magnifier method is presented.

Chapter 3 presents a detailed derivation of the equations for the nonlinear analysis. The solution procedure and consideration of geometric and material nonlinearities are described.

In Chapter 4, the accuracy and efficiency of the nonlinear analysis program are verified. The predictions of the program are checked against experimental results and other analytical predictions.

Chapter 5 contains the comparison between the design forces obtained from the linear frame analysis and the approximate procedure. The results of nonlinear analyses are compared with those obtained from the ACI moment magnifier method and the TSDHPT approximate procedure. The effects of column slenderness and foundation flexibility on the bent behavior are included in this chapter.

Chapter 6 summarizes the conclusions and recommendations for further research.

CHAPTER 2. ANALYSIS PROCEDURES

2.1 GENERAL CONSIDERATION

The Texas State Department of Highways and Public Transportation (TSDHPT) uses an approximate procedure, suitable for hand calculations, to compute the design axial forces and associated bending moments in bridge bent columns. The approximate procedure assumes that the column moments are developed due to lateral loads and the axial forces in columns are induced by gravity loads only. The contribution of the lateral loads on the axial forces and that of the gravity loads on the bending moments are neglected. In the linear and nonlinear analyses used in this study, the bent cap and the columns are treated as an integral frame. The gravity loads are equally divided between the girders. Thus moments and axial forces in columns are developed due to both the gravity and lateral loads. To compute the design forces and moments for a particular structure, the bridge must be defined by several variables including bridge geometry, geographic location, and properties of the construction materials.

2.1.1 Loading Combinations

The design of bent columns requires determining the critical axial loads and bending moments considering twelve loading combinations following AASHTO specifications. Of these twelve loading combinations or groups, TSDHPT has identified groups I, II and III as the critical loading combinations which must be considered in the design of typical Texas highway bridge bents. These loading combinations are

$$\text{Group I} = 1.30 * [\beta_D * DL + 1.67 * (LL + I) + CF + SF]$$

$$\text{Group II} = 1.30 * [\beta_D * DL + SF + W]$$

$$\text{Group III} = 1.30 * [\beta_D * DL + (LL + I) + CF + SF + 0.3 * W + WL + LF]$$

The dead load (DL) computations include the weights of bridge rails, slab, beams, bent cap and the columns. The variable β_D is the load combination coefficient for the dead load. A value of 0.75 is assigned when checking a column for the minimum axial load and maximum moment or maximum eccentricity. A value of 1.0 is used when checking a column for the maximum axial load and minimum moment. The live loads (LL) as specified by AASHTO include lane load and truck load. The larger of the two live load values is used in computing the live load plus impact (LL+I). The live load intensity is reduced according to AASHTO Article 3.12 for a multiple lane bridge in view of the improbability of coincident maximum loading. For one or two lanes, no reduction is allowed. For three lanes, the reduction factor is 0.90. For four or more lanes, the reduction factor is 0.75. The value of CF represents the centrifugal force associated with curved bridges. The value of SF represents the stream flow for columns subjected to design water pressure. The wind load (W) includes the effect of wind pressures on the bridge

superstructure, specified in AASHTO Article 3.15.2.1.1, as well as wind forces applied directly to the bridge substructure, specified in AASHTO Article 3.15.2.2. AASHTO recommends the use of five wind directions, relative to the longitudinal axis of the bridge, in computing the wind forces on the bridge. The design wind forces provided by AASHTO are derived on a base wind velocity of 100 miles per hour. According to AASHTO Article 3.15, the design wind forces for load group II must be reduced or increased by the ratio of the square of the design wind velocity to the square of the base velocity. The values of WL represent wind load on moving live loads, specified in AASHTO Article 3.15.2.1.2. The longitudinal force (LF) represents the effect of the acceleration or deceleration of vehicles, and it is taken as a percentage (5%) of the live load, specified in AASHTO Article 3.9.

The column's axial load and associated bending moments are computed for each load group. The moments are compared with the minimum eccentricity moments to ensure that the critical values are used in design. The factored moments are then amplified to include second order effects, commonly called $P\Delta$ effects. There have been several methods of analysis advocated for slender compression members. These include the Reduction Factor Method, the Stability Index Procedure, the Moment Magnifier Method and computer based second order frame analysis. An excellent review of these procedures is given elsewhere [25]. The TSDHPT uses the ACI Moment Magnifier Method to approximate the second order effects in columns. The method has been adopted by AASHTO as a basic approximate procedure for determining slenderness effects in concrete compression members. The moment magnification procedure of the ACI code is briefly described in the next subsection.

2.1.2 Moment Magnifier Method

The ACI Building Code recommends the use of this method to approximate the effect of column slenderness and other nonlinearities on the column forces and moments. The code procedure is based on the evaluation of an effective length factor and a moment magnifier. The moments computed using an elastic frame analysis and linear force-deformation relationships are multiplied by a coefficient, called the moment magnification factor. The magnification factor is a function of the applied axial load, the column critical buckling load, the ratio of column end moments, and the column deflected shape. For unbraced frames, the code recommends the use of the following expression for computing design moments.

$$M_c = \delta_b M_g + \delta_s M_s \quad (2.1)$$

where

δ_b = moment magnification factor for frames braced against sidesway

δ_s = sway moment magnification factor

M_c = equivalent design moment

M_g = moments due to gravity load (nonsway moments)

M_s = lateral load moments (sway moments)

For frames braced against sidesway, Equation (2.1) is used with sway moments as zero. The moments M_g and M_s are computed using an elastic frame analysis where the uncracked section properties of the members are used for the stiffness calculation. The moment magnifiers δ_b and δ_s are

$$\delta_b = C_m / (1 - (P_u / \phi P_c)) \geq 1.0$$

and

$$\delta_s = 1 / (1 - (\Sigma P_u / \phi \Sigma P_c)) \geq 1.0$$

in which

$$P_c = \pi^2 EI / (kL_u)^2$$

where

P_u = axial load in the column

P_c = critical or Euler buckling load of columns

ϕ = capacity reduction factor

C_m = an equivalent moment correction factor
= $0.6 + 0.4 [M_1/M_2]$ ($0.4 \geq C_m \geq 1.0$)

M_1 and M_2 = smaller and larger column end moments respectively, determined from the first order analysis

k = effective length factor

EI = stiffness of the column

L_u = unsupported length of the columns.

The stiffness of the column and the restraining members are the major parameters and as a consequence the accuracy of the magnification factor is highly dependent on the values used. The effective EI of reinforced concrete depends on the magnitude and the type of loading, and the variation of material properties along the column length. The code recommends the following formulas for the effective EI for reinforced concrete compression members.

$$EI = 0.4 E_c I_g \quad \text{for } \rho \leq 2\% \quad (2.2)$$

$$EI = 0.2 E_c I_g + E_s I_s \quad \text{for } \rho > 2\% \quad (2.3)$$

where

E_c = elastic modulus of concrete

E_s = elastic modulus of reinforcement

I_g = moment of inertia of gross concrete section, neglecting reinforcement

I_s = moment of inertia of reinforcement about centroidal axis of member cross section

ρ = reinforcement ratio.

The maximum of the above two values of EI are used in computing the column critical buckling load. The effect of sustained load is included by dividing Equations (2.2) and (2.3) by $(1 + \beta_d)$, where β_d is the ratio of the maximum design dead load moment to the maximum design total load moment. The effective length factor is computed using alignment charts [2].

The following sections include a description of the approximate and the frame analysis procedures.

2.2 APPROXIMATE PROCEDURE

The first step in the TSDHPT analysis procedure is to determine the Euler buckling load of the column needed for computing the ACI moment magnifier. This computation requires the selection of an appropriate effective length factor as defined in AASHTO Article 8.16.5.2.3 [4]. The TSDHPT uses a k -factor of 1.25 for both x -axis (in-plane) and z -axis (out of plane) bending for typical bridge bent columns.

Next, the dead and live loads of the structure are computed. The gravity loads on the structure are divided equally between the columns. The columns are isolated for computing the bending moments. The column moments due to in-plane lateral loads (in-plane moments) are computed by assuming the inflection point at the mid-height of the column. Conservatively, the moments due to out of plane lateral loads (out of plane moments) are computed using the total height of the column. AASHTO has specified the locations at which the lateral forces are applied in computing these moments. The axial loads and moments computed for various forces are combined in accordance with AASHTO load groups I, II and III. The details of the computer code for computation of these loads for a typical bridge bent are given by Stocks [29]. The design bending moments about both axes are computed by magnifying the lateral load moments as

$$M_c = \delta M_s$$

where

$$\delta = 1 / (1 - (P_u / \phi P_c))$$

It may be noted that the magnification factors δ and δ_s are the same for a bent with identical columns since the moments due to gravity loads are neglected in the approximate procedure.

2.3 LINEAR ANALYSIS OF BENTS

In the linear analysis, the bent cap and the columns are treated as a rigid frame. The linear frame analysis utilizes a six-degree-of-freedom linear beam element to represent each member and uses the conventional direct stiffness method of solution. The standard assumption of small deformation, plane sections remaining plane, and true rigid connections between members are made. Also, it is assumed that

members are originally straight and a linear elastic material following Hooke's law is being used.

As with the approximate analysis, AASHTO load groups I, II and III are utilized in computing the design axial forces and moments. A primary difference between the two analysis procedures is that no assumptions are made concerning the location of the inflection points with the integral frame solution. In the frame analysis, the bridge dead load is distributed equally between all the beams and therefore column loads are accurately proportioned. Recall that the approximate procedure distributes the total bridge loads equally between all columns. The live loads on the bridge are approximated in two ways. The first method distributes the total live load on the bridge evenly between the beams. The second approach considers the variable position of the AASHTO live loads over the deck. The position of the truck and lane loads are varied across the width of the deck according to the scheme shown in Fig 2.1. First, one truck or lane load is moved over the entire width of the deck as shown in Fig 2.1(a). Next, each lane of the bridge is loaded with one truck or lane load, and the movement of these live loads is restricted within the AASHTO specified lane width. The loads on the girders are computed assuming the deck slab simply supported between the girders. For each position of live loads, the column axial loads and associated bending moments are recorded. The column design forces consist of either the maximum moment and corresponding axial load or the maximum axial load and corresponding bending moment. The results obtained with both approaches will be compared.

As mentioned in the discussion of the approximate analysis procedure, AASHTO specifies the location on the bridge structure at which the lateral forces must be applied. For some load cases, the design lateral forces are applied on or above the superstructure of the bridge. For the frame solution, forces must be applied on the frame itself. Thus, to approximate the AASHTO requirements, the design forces were increased by the ratio of the height specified by AASHTO to the distance between the cap center line and the assumed fixity depth ($F^*D=f^*d$ i.e. $f=F^*D/d$), as shown in Fig 2.2.

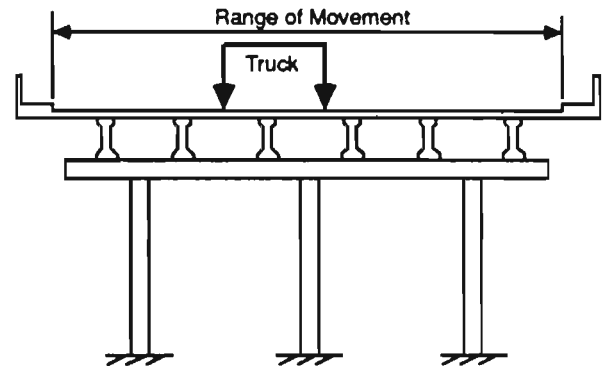
The solution provided by the frame analysis yields the axial load and bending moments for each column. These member forces evolve from an elastic analysis, and therefore must be modified by the AASHTO moment magnifier method to approximate second order effects.

2.4 NONLINEAR ANALYSIS OF BENTS

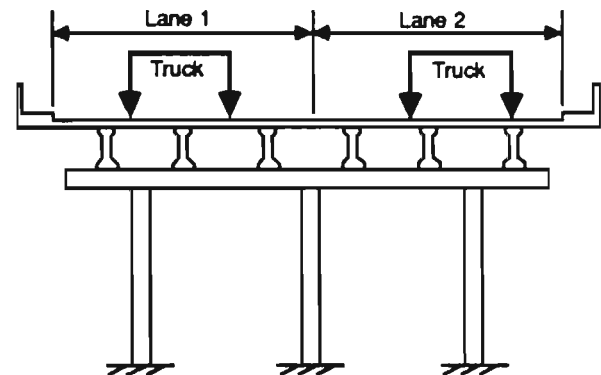
The nonlinear analysis procedure also treats the bent cap and the columns as a rigid frame. In this analysis procedure, the total gravity loads on the bridge are divided equally between the beams. The basic formulation selected in this study uses the fiber model and an updated Lagrange formulation. The basic difference between the linear and

nonlinear analyses lies in the consideration of various nonlinearities. In the linear analysis procedure, the moment magnifier method is used to approximate the amplification of column moments in order to account for the effect of axial loads on these moments. The nonlinear analysis uses realistic moment-curvature relationships based on accurate stress-strain relationships and considers the effect of axial load, variable moment of inertia along the member, and the effect of lateral deflections on moments and forces.

The nonlinear analysis procedure uses a combination of incremental and iterative solutions. For a specified load increment, the iterative solution seeks a configuration which satisfies equilibrium of the structure. The incremental technique is used to find the behavior of bents at various loading stages. The loading on the bent is assumed to be static and monotonic. The details of the nonlinear analysis formulation and the solution procedures are described in the next chapter.



(a) Single truck on the bridge



(b) One truck in each lane

Fig 2.1. Variable position of AASHTO truck.

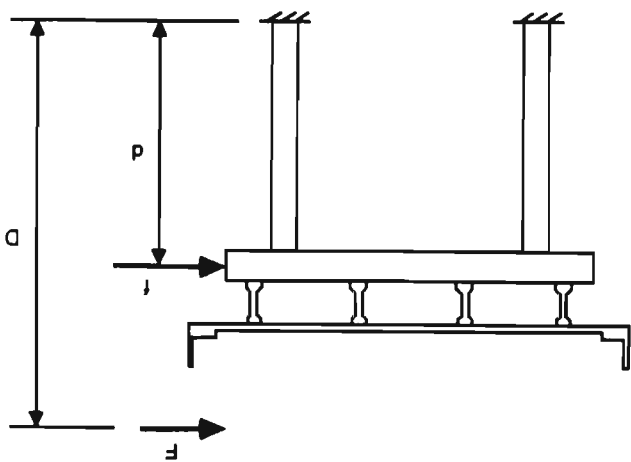


Fig 2.2. Force on bridge superstructure.

CHAPTER 3. NONLINEAR ANALYSIS FORMULATION

3.1 INTRODUCTION

In this study the updated Lagrangian Finite element formulation is used to model the behavior of reinforced concrete bridge bents under spatial loads. The approach uses an iterative solution with moving coordinates of the joints. The local axes move with the element and therefore share its rigid body motion. The current deformed state is used as a reference prior to the next incremental step of solution.

The model uses a tangent stiffness formulation. For an applied load increment, the incremental displacements are calculated using the conventional stiffness method. Nodal displacements are updated and local axes of each element are established. The distortion of the elements and hence the internal forces corresponding to the nodal degrees of freedom are computed. The difference between the externally applied loads and the internal forces are the residual forces. If the residual forces are within specified limits then the next step of incremental load is applied and the process is continued either up to the failure of the structure or to a specified load level. If the residual forces do not satisfy the equilibrium of the structure then the stiffness matrix corresponding to the updated strains is formed, incremental displacements are computed and the process is iterated until convergence is achieved. The material and geometric nonlinearities considered in this study are explained later in this chapter.

The analysis procedure assumes that the members are prismatic. A nonprismatic member can be divided into several prismatic members. Each member is then divided into a series of longitudinal segments or elements, and the cross section of the member into longitudinal fibers as shown in Figure 3.1.

3.2 DERIVATION OF THE STIFFNESS MATRIX

The Finite element displacement model is used to arrive at the force displacement relationship for a beam-column element. It is assumed that the effects of shear and torsion on the deformation are negligible and yielding of the section is a function of the normal stress only. The virtual work principle for this case can be stated as

$$\int_{\text{vol.}} \delta \epsilon^T (\Delta \sigma + \sigma) dv = \int_0^L \delta u^T (T + \Delta T) dL$$

where

- ϵ = state of normal strain in the system
- σ = state of normal stress in the system
- T = applied traction
- $\Delta \sigma$ = increment in normal stress
- ΔT = increment in applied traction
- L = length of the element
- u = displacement function along the element length

The normal strain distribution ϵ can be expressed in terms of axial strain and strains due to bending about two axes. For the local axes of the member shown in Figure 3.2, the normal strain distribution in terms of displacements is

$$\epsilon = \frac{\partial v}{\partial y} - x \frac{\partial^2 u}{\partial y^2} - z \frac{\partial^2 w}{\partial y^2}$$

or

$$\epsilon = v' - xu'' - zw'' \quad (3.2)$$

where prime indicates the derivative of the function with respect to y . In incremental form, Equation (3.2) becomes

$$\Delta \epsilon = \Delta v' - x \Delta u'' - z \Delta w'' \quad (3.3)$$

where

- u = displacement in x -direction
- v = displacement in y -direction
- w = displacement in z -direction
- x = distance of differential element in z -direction
- z = distance of differential element in x -direction

To evaluate the integrals in Equation (3.1), the element nodal forces and deformations are chosen as shown in Figure 3.3. It is assumed that the deflected shape of the element about the x and z axes can be expressed as a third degree polynomial. This satisfies the conditions of constant shear and linearly varying bending moment. The shape function in the y -direction is assumed to be linear. The deflection at any section along the length of the element can be expressed in terms of the nodal degrees of freedom as

$$v = g_1 v_A + g_2 v_B \quad (3.4)$$

$$u = f_1 u_A - f_2 \phi_{ZA} + f_3 u_B - f_4 \phi_{ZB} \quad (3.5)$$

$$w = f_1 w_A + f_2 \phi_{xA} + f_3 w_B + f_4 \phi_{xB} \quad (3.6)$$

where g_1, g_2, f_1, f_2, f_3 and f_4 are conventional Hermite interpolation functions for a beam element. These functions are

$$g_1 = 1 - \frac{y}{L}$$

$$g_2 = \frac{y}{L}$$

$$f_1 = 1 - 3 \left[\frac{y}{L} \right]^2 + 2 \left[\frac{y}{L} \right]^3$$

$$f_2 = y \left\{ 1 - \left[\frac{y}{L} \right] + \left[\frac{y}{L} \right]^2 \right\}$$

Fig 3.2. Global and local coordinates.

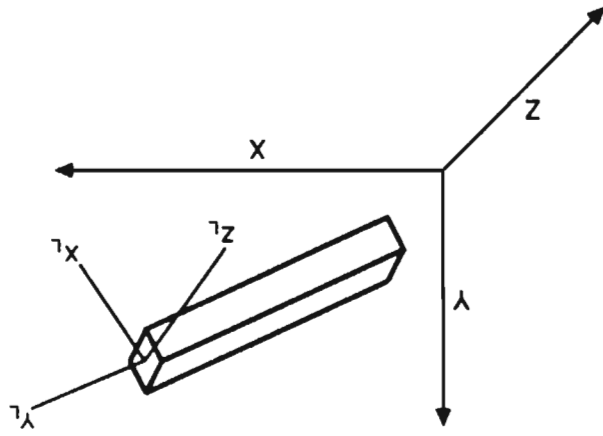
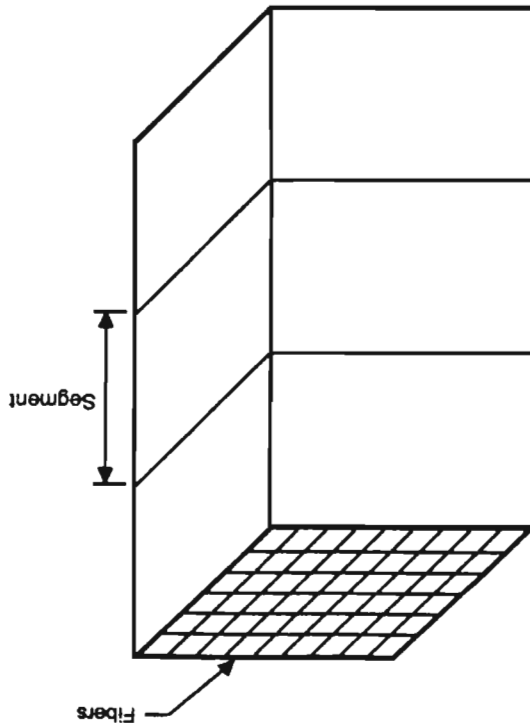
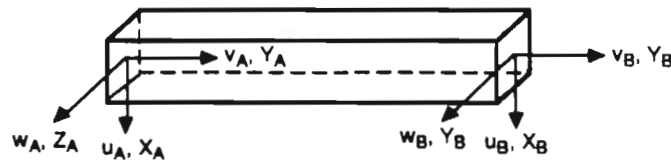
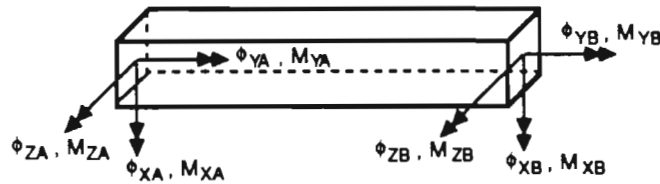


Fig 3.1. Segments and fibers in a member.





(a) Forces and displacements



(b) Moments and rotations

Fig 3.3. Nodal forces and deformations in local coordinates.

$$f_3 = 3 \left[\frac{y}{L} \right]^2 - 2 \left[\frac{y}{L} \right]^3$$

$$f_4 = y \left\{ - \left[\frac{y}{L} \right] + \left[\frac{y}{L} \right]^2 \right\}$$

In matrix form, equations (3.4) through (3.6) can be written as

$$u = \begin{bmatrix} v \\ -u \\ w \end{bmatrix} = N U \quad \dots \quad (3.7)$$

$$\text{where } N = \begin{bmatrix} 0 & g_1 & 0 & 0 & 0 & 0 & 0 & g_2 & 0 & 0 & 0 & 0 \\ -f_1 & 0 & 0 & 0 & 0 & f_2 & -f_3 & 0 & 0 & 0 & 0 & f_4 \\ 0 & 0 & f_1 & f_2 & 0 & 0 & 0 & 0 & f_3 & f_4 & 0 & 0 \end{bmatrix}$$

$$\text{and } U^T = [u_A \quad v_A \quad w_A \quad \phi_{XA} \quad \phi_{YA} \quad \phi_{ZA} \quad u_B \quad v_B \quad w_B \quad \phi_{XB} \quad \phi_{YB} \quad \phi_{ZB}]$$

$$\text{Also } \begin{bmatrix} v' \\ -u'' \\ w'' \end{bmatrix} = B U \quad \dots \quad (3.8)$$

$$\text{where } B = \begin{bmatrix} 0 & g_1' & 0 & 0 & 0 & 0 & 0 & g_2' & 0 & 0 & 0 & 0 \\ -f_1'' & 0 & 0 & 0 & 0 & f_2'' & -f_3'' & 0 & 0 & 0 & 0 & f_4'' \\ 0 & 0 & f_1'' & f_2'' & 0 & 0 & 0 & 0 & f_3'' & f_4'' & 0 & 0 \end{bmatrix}$$

In incremental form, Equations (3.7) and (3.8) become

$$\begin{bmatrix} \Delta v \\ -\Delta u \\ \Delta w \end{bmatrix} = N \Delta U \quad (3.9)$$

$$\text{and } \begin{bmatrix} \Delta v' \\ -\Delta u'' \\ \Delta w'' \end{bmatrix} = B \Delta U \quad (3.10)$$

The small changes in strain can be linearly related to a small change in stress by the following relationship.

$$\Delta \sigma = E \Delta \epsilon \quad (3.11)$$

where

E = tangent modulus of the material under consideration

Also the internal element stress resultants can be related to the normal stresses as

$$\Delta N = \int_{\text{Area}} \Delta \sigma \, dA$$

$$\Delta M_z = \int_{\text{Area}} x \Delta \sigma \, dA$$

$$\Delta M_x = - \int_{\text{Area}} z \Delta \sigma \, dA$$

where

ΔN = increment in axial force

ΔM_z = increment in bending moment about z-axis

ΔM_x = increment in bending moment about x-axis

The above integrals are performed over the cross section of the element. If the member cross section is divided into finite pieces or "fibers" in which the normal strain and stress are constant, the above integrals can be replaced with discrete summations. Using Equations (3.3) and (3.11) the expressions for the stress resultants become

$$\Delta N = \sum_{\text{fibers}} \Delta \sigma A = \sum_{\text{fibers}} (\Delta v' - x \Delta u'' - z \Delta w'') EA$$

$$\Delta M_z = \sum_{\text{fibers}} x \Delta \sigma A = \sum_{\text{fibers}} (\Delta v' - x \Delta u'' - z \Delta w'') x EA$$

$$\Delta M_x = - \sum_{\text{fibers}} z \Delta \sigma A = - \sum_{\text{fibers}} (\Delta v' - x \Delta u'' - z \Delta w'') z EA$$

In matrix form:

$$\Delta Q = \begin{bmatrix} \Delta N \\ \Delta M_z \\ \Delta M_x \end{bmatrix} = D \begin{bmatrix} \Delta v' \\ -\Delta u'' \\ \Delta w'' \end{bmatrix} \quad (3.12)$$

where Q is the vector of stress resultants and

$$D = \begin{bmatrix} \sum EA & \sum EAx & -\sum EAz \\ \sum EAx & \sum EAx^2 & -\sum EAxz \\ -\sum EAz & -\sum EAxz & \sum EAz^2 \end{bmatrix}$$

Substituting Equation (3.10) into (3.12) yields

$$\Delta Q = D B \Delta U \quad (3.13)$$

Equation (3.1) can be rearranged as

$$\int_0^L \int_A \delta \epsilon^T \Delta \sigma \, dA \, dy = \int_0^L \delta u^T (T + \Delta T) \, dy - \int_0^L \int_A \delta \epsilon^T \sigma \, dA \, dy \quad (3.14)$$

Using Equations (3.2), (3.7), (3.8), (3.12) and (3.13) and simplifying yields

$$\int_A \delta \epsilon^T \Delta \sigma \, dA = \delta U^T B^T D B \Delta U$$

$$\int_A \delta \epsilon^T \sigma \, dA = \delta U^T B^T Q$$

$$\int_0^L \delta u^T (T + \Delta T) \, dy = \int_0^L \delta U^T N^T (T + \Delta T) \, dy$$

since U is the vector of nodal displacements and therefore independent of y , Equation (3.14) reduces to

$$\delta U^T \int_0^L B^T D B \, dy \, \Delta U = \delta U^T \int_0^L N^T (T + \Delta T) \, dy - \delta U^T \int_0^L B^T Q \, dy$$

or

$$K \Delta U = (F + \Delta F) - P = \Delta R \quad (3.15)$$

where

$$K = \int_0^L B^T D B \, dy = \text{Tangent stiffness matrix}$$

$$P = \int_0^L B^T Q \, dy = \text{Internal nodal force vector}$$

$$F + \Delta F = \int_0^L N^T (T + \Delta T) \, dy = \text{Applied nodal load vector}$$

$$\Delta R = \text{Residual nodal force vector}$$

The integrals in Equation (3.15) are evaluated numerically using Gaussian quadrature. The selection of the number of integration points depends on the order of the polynomial in the integrands. The degree of the polynomials in Equation (3.15) is dependent upon the shape functions and the variation of stresses and applied loads along the element. For the above mentioned shape functions three integration points would give satisfactory results. It may be noted that the stiffness of an element depends upon the tangent moduli of the materials which may vary considerably along the element length. To monitor the extent of concrete cracking and variation of tangent moduli of steel and concrete over a larger range, five integration points were selected.

Equation (3.15) gives the relationship between the increment in force and the incremental displacements for an element in its local coordinate system as shown in Figure 3.2. Since the bent consists of both horizontal and vertical members, it is convenient to assemble the structure stiffness matrix corresponding to global coordinates as shown in Figure 3.2. The stiffness matrix of each element is formed in its local axes, transformed to the global coordinates and added to the total structure stiffness matrix.

3.3 GEOMETRIC NONLINEARITY

The consideration of this nonlinearity is essential in that equilibrium equations must be written with respect to the deformed geometry, which is not known in advance. If loads are applied to the structure, deformations will result. For the next increment of load, the incremental force-displacement relationship should be corrected for the new position of each element.

In the updated Lagrange approach, a local coordinate system is attached to each element. The local system moves with the element and therefore shares its rigid body motion. Thus, at every step the nodal displacements are added to the previous coordinates of the joints and a new set of local axes are established for each element. Rotation matrices corresponding to the new axes are computed. These matrices are used to transform the forces and stiffness matrix of each element to global coordinates. This approach assumes a straight line between the nodes and makes no allowance for element curvature. Thus, in order to reproduce the deforma-

tions accurately, the structure should be divided into many elements.

Consider the vertical element shown in Figure 3.4a. Figure 3.4b indicates the deformed configuration of the element under some external load. θ_x and θ_z are the rotations about the x and z axes respectively. The transformation matrix for the element can be computed by first rotating the element in the x - y plane and then in the y_1 - z_1 plane. For axes rotated through θ_z , the relationship between the global displacements and the new displacements can be expressed as

$$\begin{aligned} w &= w_1 \\ u &= u_1 \cos\theta_z + v_1 \sin\theta_z \\ v &= -u_1 \sin\theta_z + v_1 \cos\theta_z \end{aligned}$$

where u_1 , v_1 and w_1 are the displacements corresponding to axes rotated by θ_z and u , v and w are global displacements. If the element is now rotated in the y_1 - z_1 plane, the local displacements u_L , v_L and w_L are given as

$$\begin{aligned} u_1 &= u_L \\ v_1 &= v_L \cos\theta_x - w_L \sin\theta_x \\ w_1 &= v_L \sin\theta_x + w_L \cos\theta_x \end{aligned}$$

Simplifying the above equations yields

$$u = u_L \cos\theta_z + v_L \cos\theta_x \sin\theta_z - w_L \sin\theta_x \sin\theta_z \quad (3.16a)$$

$$v = -u_L \sin\theta_z + v_L \cos\theta_x \cos\theta_z - w_L \sin\theta_x \cos\theta_z \quad (3.16b)$$

$$w = v_L \sin\theta_x + w_L \cos\theta_x \quad (3.16c)$$

Equation (3.16) relates the displacements in local axes to global displacements. A similar transformation holds true for rotational degrees of freedom. In matrix form, the transformation of coordinates can be expressed as

$$U_G = R_V U_L$$

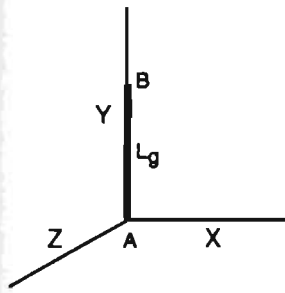
where

$$R_V = \begin{bmatrix} C_1 & C_2 C_3 & -C_2 C_4 & 0 & 0 & 0 \\ -C_2 & C_1 C_3 & -C_2 C_4 & 0 & 0 & 0 \\ 0 & C_4 & C_3 & 0 & 0 & 0 \\ 0 & 0 & 0 & C_1 & C_2 C_3 & -C_2 C_4 \\ 0 & 0 & 0 & -C_2 & C_1 C_3 & -C_2 C_4 \\ 0 & 0 & 0 & 0 & C_4 & C_3 \end{bmatrix}$$

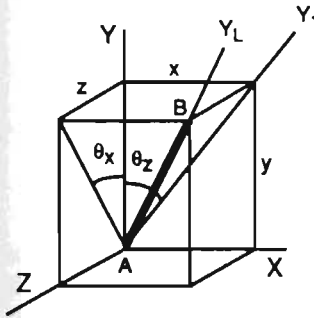
and

$$\begin{aligned} C_1 &= \cos\theta_z \\ C_2 &= \sin\theta_z \\ C_3 &= \cos\theta_x \\ C_4 &= \sin\theta_x \end{aligned}$$

The initial and final positions of a horizontal element are shown in Figure 3.5. The transformation matrix for this element can be derived in a similar fashion. The element is

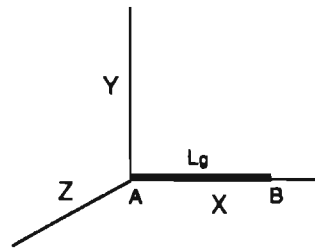


(a) Initial position

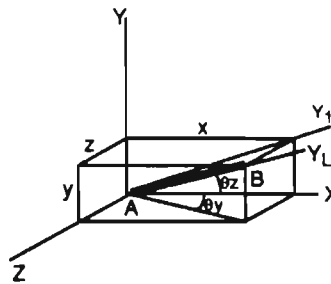


(b) Final position

Fig 3.4. Deformation of vertical members.



(a) Initial position



(b) Final position

Fig 3.5. Deformation of horizontal members.

first rotated in the x - y plane followed by a rotation in the y_1 - z_1 plane. The rotational distortions θ_y and θ_z are chosen for computational convenience. In this case, the transformation of coordinates is related by

$$U_G = R_H U_L$$

where

$$R_H = \begin{bmatrix} C_2 & C_1 C_5 & -C_1 C_6 & 0 & 0 & 0 \\ -C_1 & C_2 C_5 & -C_2 C_6 & 0 & 0 & 0 \\ 0 & C_6 & C_5 & 0 & 0 & 0 \\ 0 & 0 & 0 & C_2 & C_1 C_5 & -C_1 C_6 \\ 0 & 0 & 0 & -C_1 & C_2 C_5 & -C_2 C_6 \\ 0 & 0 & 0 & 0 & C_6 & C_5 \end{bmatrix}$$

and

$$C_5 = \cos\theta_y$$

$$C_6 = \sin\theta_y$$

The correction for the geometry effect is accounted for by transforming the stiffness matrix of the elements to global coordinates as

$$K_G = R^T K_L R$$

where

K_G = stiffness matrix in global coordinates

K_L = stiffness matrix in local coordinates

R = Rotation matrix

3.4 MATERIAL NONLINEARITY

It was mentioned earlier that in the fiber model members are divided into longitudinal fibers and each fiber is subjected to constant normal stress and strain over its area. Thus inclusion of material nonlinearity in the fiber model becomes simple in that only uniaxial stress strain relationship of the materials is required. For a given strain in a fiber, the tangent modulus of the fiber is computed as the slope of the stress-strain curve for that particular type of fiber.

The stress strain relationship for the reinforcing steel is assumed to be elasto-plastic as shown in Figure 3.6. For a known strain, the stress is found by simply multiplying the strain by the elastic modulus of the steel. If the stress is greater than the yield stress, the stress is taken as the yield stress and the elastic modulus as zero. Arbitrarily, the steel is considered to fracture if a fiber strain reaches one percent [25]. There have been many theoretical curves proposed by different authors describing the constitutive relationship of concrete in compression. In this study the stress-strain relationship suggested by Hognestad [16] is adopted and is shown in Figure 3.6. The Hognestad curve has been shown to give good results for concrete not confined by lateral ties [23,25]. The concrete is assumed to have no tensile strength.

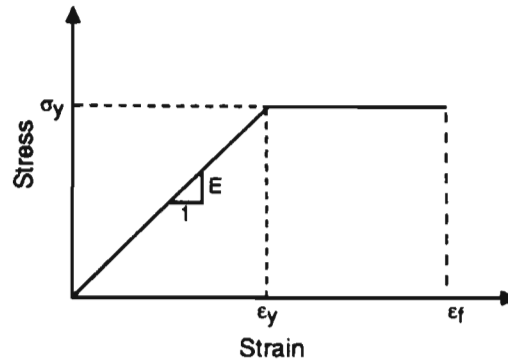


Fig 3.6. Stress-strain relationship for reinforcing steel.

3.5 SOLUTION PROCEDURE

A combination of incremental and iterative solutions with moving coordinates is used to trace the behavior of the structure. The advantage of using moving coordinates is that large deformations can be accommodated. In the general structural equation, given by Equation (3.15), ΔR is the difference between the specified external loadings and the internal nodal forces due to the element distortions. Thus ΔR represents the unbalanced nodal loads which must be zero for equilibrium of the structure. The iterative solution seeks a configuration such that the residual force is zero. The loads are applied in several increments to find the structural behavior at various stages of loading.

3.5.1 Computation of Element Distortions

Under a specified level of external loads, the structure deforms inducing internal nodal loads. Consider a vertical element in global coordinates as shown in Figure 3.4a. Figure 3.4b represents the equilibrium position of the element under a specified load level. From the global displacements of nodes A and B the length and rotation of the element can be computed as

$$\begin{aligned} x &= u_B - u_A \\ y &= v_B - v_A + L_s \\ z &= w_B - w_A \\ L_0 &= \sqrt{(x^2 + y^2 + z^2)} \\ \tan\theta_x &= z / y \\ \tan\theta_z &= x / y \end{aligned}$$

where u, v, w are the global displacements of nodes A and B and L_s is the original length of the element. If the load level is now increased, the structure deforms and appears as in Figure 3.8c. The resulting incremental displacements are a combination of rigid body motion and distortion of the element. As internal forces are developed due to distortions only, the rigid body motion is subtracted and a local axis for the element is established. For the deformed configuration the following relationships hold true.

$$\begin{aligned} x_L &= \Delta u_2 - \Delta u_1 + x \\ y_L &= \Delta v_2 - \Delta v_1 + y \\ z_L &= \Delta w_2 - \Delta w_1 + z \\ L &= \sqrt{(x_L^2 + y_L^2 + z_L^2)} \\ \tan\theta_{x_0} &= z_L / y_L \\ \tan\theta_{z_0} &= x_L / y_L \end{aligned}$$

where $\Delta u, \Delta v$ and Δw are incremental nodal displacements in global coordinates. The distortion corresponding to local coordinates of the element is given by

$$\begin{aligned} \Delta v_{BL} &= L - L_0 \\ \Delta\phi_{xAL} &= \Delta\phi_{xA} + (\theta_x - \theta_{x_0}) \\ \Delta\phi_{xBL} &= \Delta\phi_{xB} + (\theta_x - \theta_{x_0}) \\ \Delta\phi_{xAL} &= \Delta\phi_{xA} - (\theta_z - \theta_{z_0}) \\ \Delta\phi_{xBL} &= \Delta\phi_{xB} - (\theta_z - \theta_{z_0}) \\ \Delta u_{AL} &= \Delta u_{BL} = \Delta v_{AL} = \Delta w_{AL} = \Delta w_{BL} = \phi_{yAL} = \phi_{yBL} \\ &= 0 \end{aligned}$$

In these expressions suffixes A and B are for element nodes, and suffix L indicates the deformations correspond to local coordinates. The distortions for a horizontal member can similarly be derived. Figure 3.5 shows the original and equilibrium positions of a horizontal member. Figure 3.8b represents the deformed configuration under incremental load. The nonzero element distortions for this element are

$$\begin{aligned} \Delta v_{BL} &= L - L_0 \\ \Delta\phi_{xAL} &= -\Delta\phi_{yA} + (\theta_y - \theta_{y_0}) \\ \Delta\phi_{xBL} &= -\Delta\phi_{yB} + (\theta_y - \theta_{y_0}) \\ \Delta\phi_{xAL} &= \Delta\phi_{xA} + (\theta_z - \theta_{z_0}) \\ \Delta\phi_{xBL} &= \Delta\phi_{xB} + (\theta_z - \theta_{z_0}) \end{aligned}$$

In this case

$$\begin{aligned} x &= u_B - u_A + L_s \\ y &= v_B - v_A \\ z &= w_B - w_A \\ \tan\theta_y &= z / x \\ \tan\theta_z &= y / x \\ \tan\theta_{y_0} &= z_L / x_L \\ \tan\theta_{z_0} &= y_L / x_L \end{aligned}$$

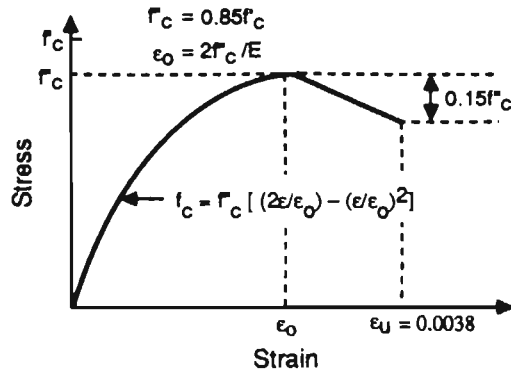


Fig 3.7. Stress-strain curve for concrete in comparison [16].

The incremental strains and curvatures of the sections are computed from local distortions. Strains are updated and the generalized force vector is computed in local axes. The force vector Q is then rotated to global coordinates according to the appropriate transformation matrix.

3.5.2 Iterative Solution

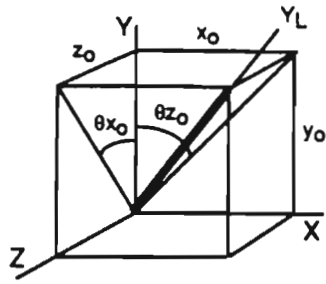
For a known state of stress the stiffness matrix of each element is formed in its local coordinates. The stiffness matrix of each element is then rotated to global coordinates and added to the total structure stiffness matrix. For a specified external load level, incremental global displacements are computed. The updated global displacements are used to establish local axes of each element. Element stiffness matrix and nodal forces due to element distortions are calculated in local coordinates. Unbalanced nodal loads ΔR are computed and the equilibrium of the structure is checked. If a convergence condition is not satisfied, then the stiffness

matrix is assembled and the displacement increments corresponding to the unbalanced forces are calculated. The process is repeated until convergence is achieved. The external loads are then increased and the iteration is started again to find the new equilibrium configuration.

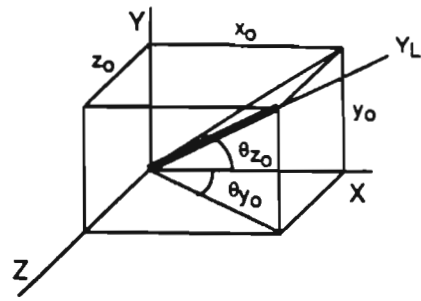
In this way iteration and incremental solutions are combined. Thus in reaching a final load level fewer load steps with more iterations or many load steps with few iterations in each load step can be taken. The equilibrium of the structure is checked by comparing the norms of the external and the internal load vectors corresponding to the unsupported nodal degrees of freedom. Symbolically it is expressed as

$$f(\|F+\Delta F-P\|, \|F+\Delta F\|) \leq \text{Tolerance}$$

The tolerance for the convergence test depends upon the level of desired accuracy. Lower tolerance will yield higher accuracy but at the expense of computational effort. A limit of 0.001 was found to give satisfactory results.



(a) For vertical members



(b) For horizontal members

Fig 3.8. Displaced configuration of members.

CHAPTER 4. VALIDATION OF COMPUTER PROGRAM

4.1 INTRODUCTION

The results of the present nonlinear analysis were checked for a variety of structural configurations and load combinations. Configurations ranged from a single member to frames. The loading was varied from axial load with in-plane loads or moments to biaxial loads. The accuracy of the computer results was established first by checking the effect of the number of segments per member and the size of the load steps. The experimental and analytical results of several investigations were used to verify the predictions of the present formulation.

4.2 EFFECT OF NUMBER OF SEGMENTS PER MEMBER

The monotonic convergence of the computer results was verified by checking the results obtained by refining the mesh. This also established the number of segments or elements required to model the behavior of one member. The results of the typical cases are presented in Figs 4.1 through 4.3.

Figure 4.1 shows the load deflection curves for a cantilever subjected to simultaneous action of axial load and horizontal loads. The length of the member was divided into 2, 4, 8 and 16 segments giving the segment length to section depth ratios of 5, 2.5, 1.25 and 0.625 respectively. No graph is shown for the sixteen segments, as the load deflection values for the eight and sixteen segments were the same. The predicted ultimate compressive axial loads for four, eight and sixteen segments are 305, 300 and 296 kips respectively.

The results for a pin ended column are shown in Fig 4.2. The geometric layout and material properties of the column are essentially the same as the previous case, except for the different support conditions. The column is again divided into 2, 4, 8 and 16 segments. An axial load of 1000 kips was applied first and kept constant while the horizontal loads were increased proportionally until failure. A similar behavior was found for eight and sixteen segments. The ultimate horizontal loads for four, eight and sixteen segments are 134.2, 132.6 and 129.4 kips respectively.

The frame of Fig 4.3 was analyzed to establish the number of segments required for a member accounting the interaction of beams and columns. The vertical members of the frame were divided into 2, 4, 8 and 16 segments giving segment length to depth ratios of 5.4, 2.7, 1.35 and 0.675 respectively. The size of segments were kept constant in both horizontal and vertical members. A total of eight segments implies four elements for the beam and two for each column. The difference between the load deflection values for 32 and 64 segments were negligible. The ultimate horizontal

loads (H) for 16, 32 and 64 segments were 13.31, 12.81 and 12.78 kips respectively.

From the above results, it may be concluded that segments with length to depth ratios of 1.0 to 1.5 would be satisfactory for columns. It is envisaged that a lower ratio would be necessary for beams due to the higher moment gradient.

4.3 EFFECT OF THE SIZE OF LOAD STEPS

To check the effect of the size of the load steps, a specified load level was applied in one step. The solution was then compared with the same load level but applied in several increments. No graphs are shown for these cases as there was no difference between the load deflection values. A combination of incremental and iterative solutions is used in this study. For each load increment, the structural equations are solved using an iterative technique until equilibrium of the structure is established. Therefore the solution is not affected whether a specified load is applied in one step or in several increments. However, to trace the behavior of the structure, loads should be applied in several increments. There are computational advantages in applying relatively larger loads when the effect of nonlinearities are not severe. The size of the load steps should be reduced near the failure of the structure.

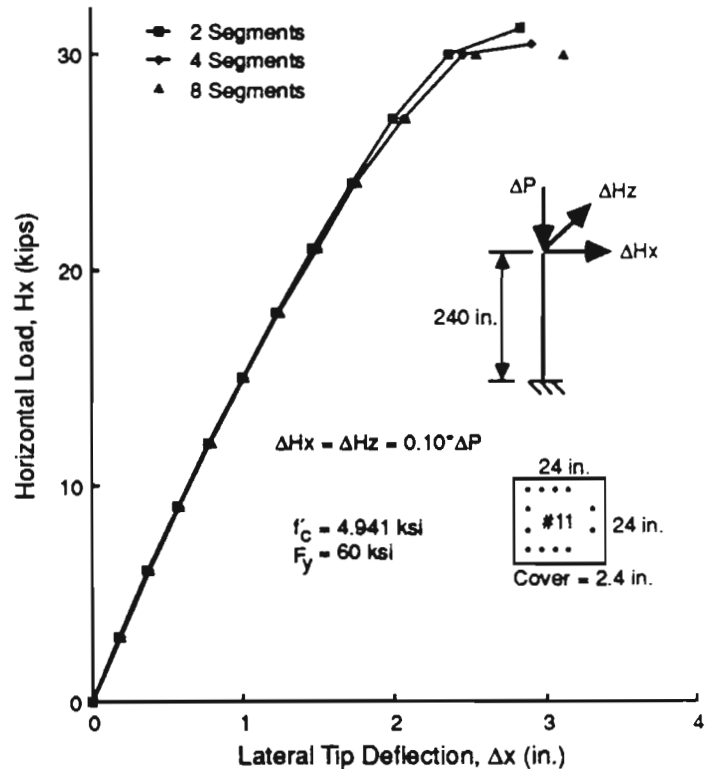


Fig 4.1. Effect of number of segments.

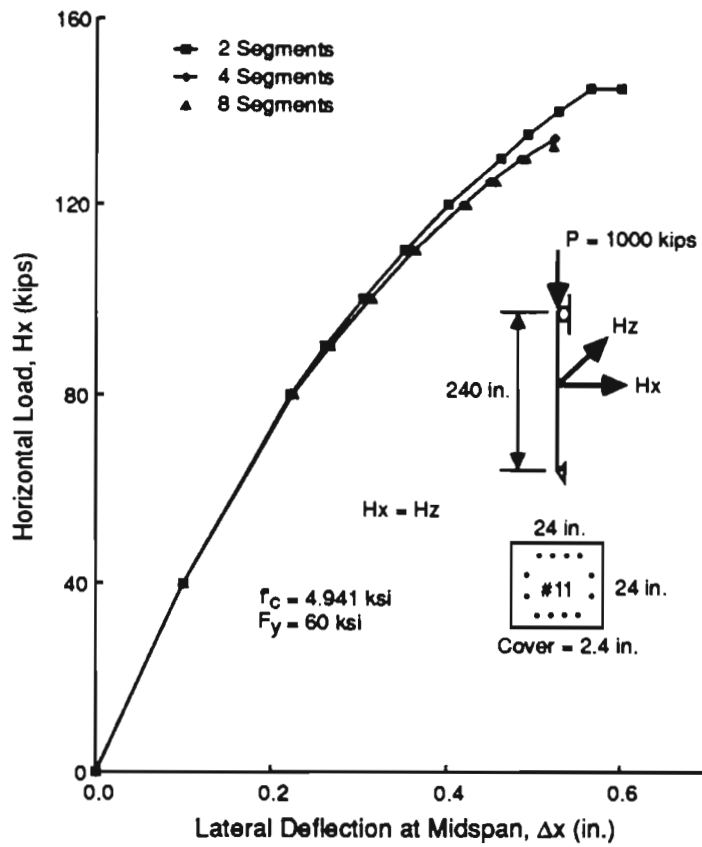


Fig 4.2. Effect of number of segments.

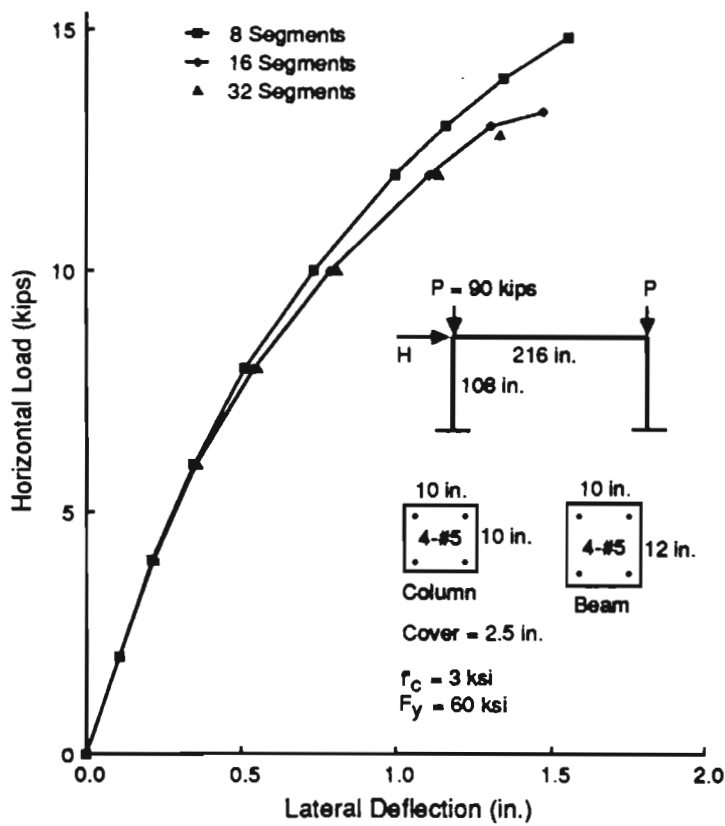


Fig 4.3. Effect of number of segments.

4.4 COMPARISON WITH ANALYTICAL RESULTS

Chen and Atsuta [7] have presented several ultimate strength interaction curves for simply supported square columns under biaxial bending. Their study uses Newmark's method [19] for the numerical integration of the moment-curvature relationships. The results are given for combinations of axial compressive loads (P), reinforcement ratios (A_s/ab), slenderness ratios (L/a), steel ultimate strength (F_y) and the concrete compressive strength (f'_c). The section and the material properties of the column are shown in Fig 4.4. Two ratios of length to section depth (L/a) were selected for comparative study. The results of Chen and Atsuta are compared with the present model and are shown on the same figure. The columns were divided into eight segments while Chen and Atsuta used nine segments. The results are in very good agreement.

Diaz [10] analyzed the frame shown in Fig 4.5 using the complex fiber model. The fiber model of Diaz uses the large deformation theory of beam-columns under uniaxial bending. The results of the complex fiber model are compared with the present formulation and are shown in Fig 4.5. Excellent agreement is found between the two results for the moment M_A . The moment M_B predicted by the present formulation is slightly higher than the one obtained with the complex fiber model.

4.5 COMPARISON WITH EXPERIMENTAL RESULTS

In the absence of experimental results for planar frames under spatial loads, the nonlinear analysis program was used to analyze several rectangular frames under in-plane loads and single columns under biaxial loads. The results for the typical structures are discussed below.

Ferguson *et al.* [13] tested a series of single panel frames. From this series, frame L_3 was chosen for the verification of the computer results. Geometric characteristics and material properties of the frame are shown in Fig 4.6. The proportional loading was used as in the test program. The vertical load versus lateral deflection is also shown on the same figure. The basic shape of the load-deflection curves are almost identical. The ultimate load predicted by the nonlinear analysis was only slightly higher than the measured value.

Ernst *et al.* [11] tested fifteen frames under various combinations of vertical and lateral loads. Two frames were selected to check the accuracy of the program.

Frame 2D12: The geometry and material properties of this frame are shown in Fig 4.7. The frame was loaded with concentrated loads at third

points. The load deflection curve predicted by the present model is in excellent agreement with the test results. The ultimate load predicted is 13.94 kips while the measured value was 14.88 kips.

Frame 2D12H: This frame had the same general properties as frame 2D12 except for the lower concrete strength. In addition to vertical loads, there was a horizontal load applied as shown in Fig 4.8. During the test the vertical load was applied first and kept constant at 7.88 kips while the horizontal load was increased. The same loading sequence was used to predict the behavior of the frame. Except for the initial stages where tension in the concrete plays a major role, the agreement between the predicted and the measured values is good. Since the program shows a good agreement for most frames at early stages, it is envisioned that the omission of the tensile strength of concrete is not the total cause for the difference found in this case. The predicted horizontal load was 2.89 kips. The ultimate load from the experiment was 3.08 kips which differs from the predicted value by 6%.

Farah and Huggins [12] tested a column pinned at the ends with the axial load applied eccentrically. The cross section and material properties of the column are shown in Fig 4.9. In the same figure the deflections measured along the diagonals are shown together with the analytical predictions. The results of the present formulation are in excellent agreement with the test results. The ultimate load predicted is 48.7 kips while the measured value was 48 kips.

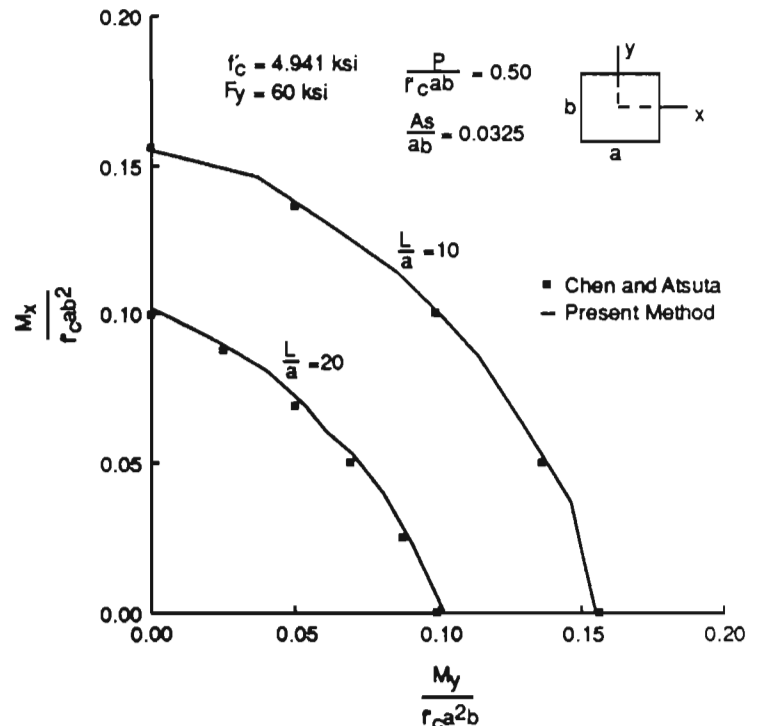


Fig 4.4. Strength interaction curves for square sections.

4.6 SUMMARY

The results presented in this chapter indicate that the present model can be used to predict accurately the behavior of planar concrete frames under spatial loads. In all cases investigated, the analytical predictions were close to the experimentally observed behavior and other analytical results. Although there were some discrepancies between the predicted and the experimental load deformation curves, the ultimate capacity was generally in very good agreement.

The accuracy and monotonic convergence of the computer results were verified by analyzing several structures. It was found that segments of length to depth ratios of 1.0 to 1.5 would be satisfactory for both vertical and horizontal members. The results for a specified load are independent of the number of load increments in which the desired load level is divided.

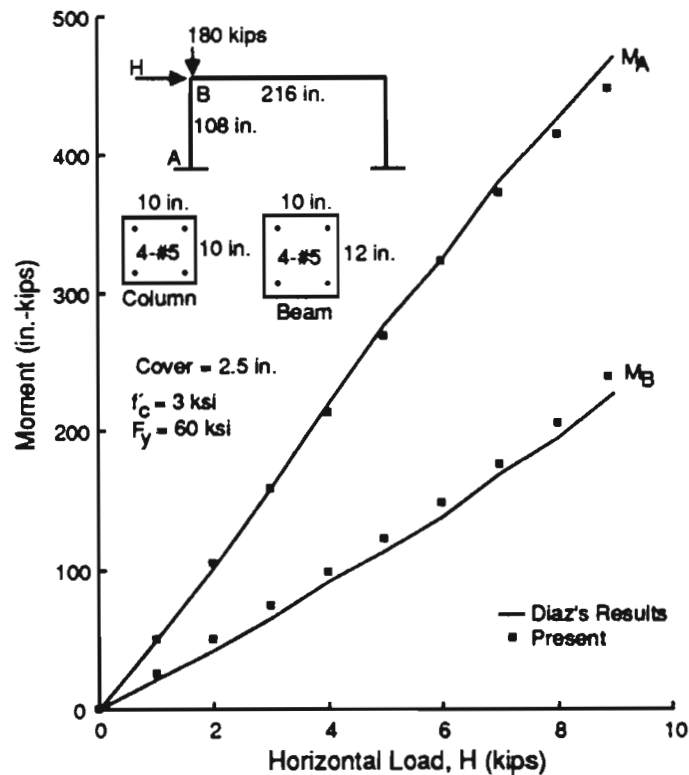


Fig 4.5. Frame C11 (case 2) from Diaz [10].

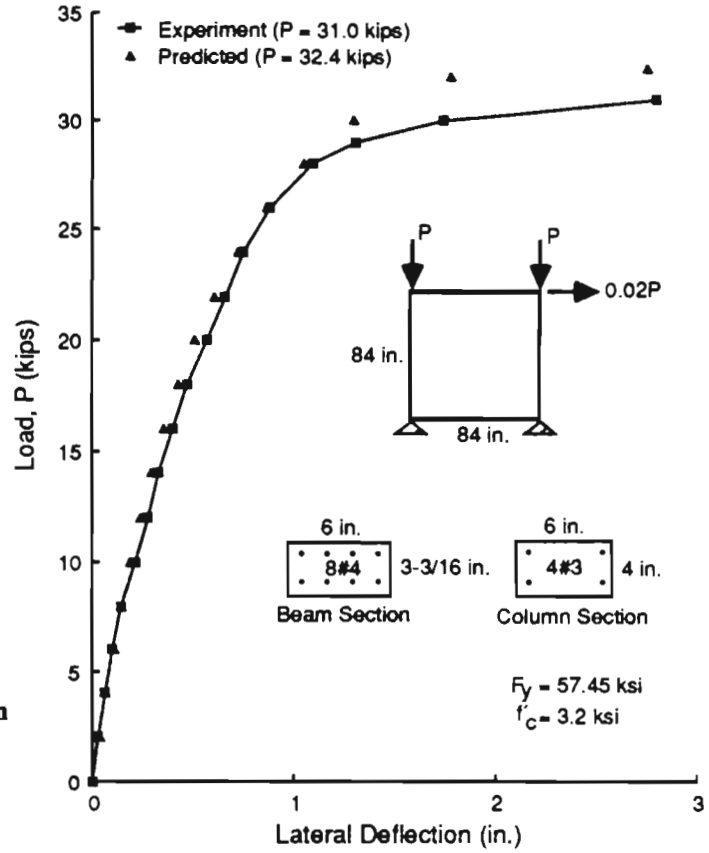


Fig 4.6. Frame L_3 from Ferguson, et al. [13].

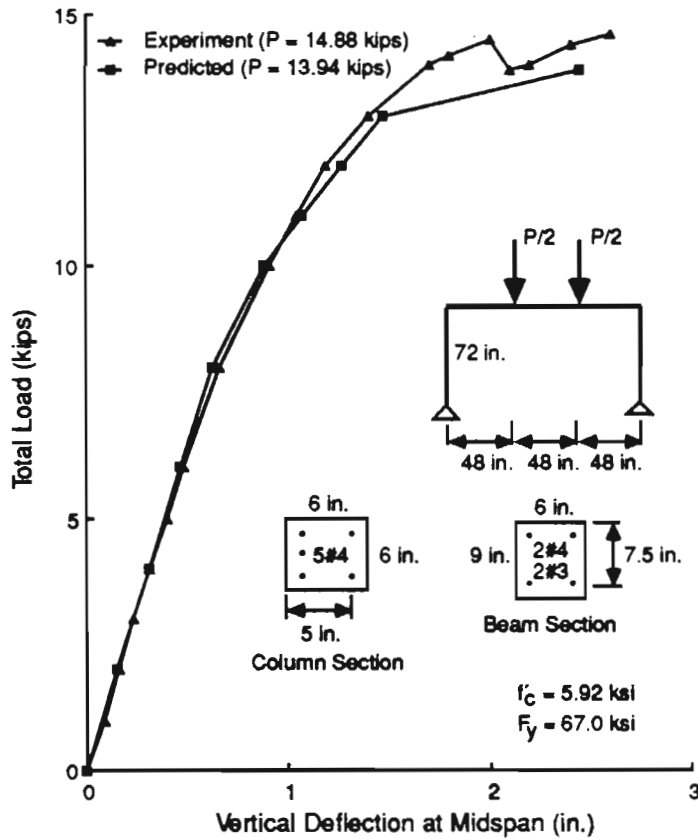


Fig 4.7. Frame 2D12, from Ernst, et al. [11].

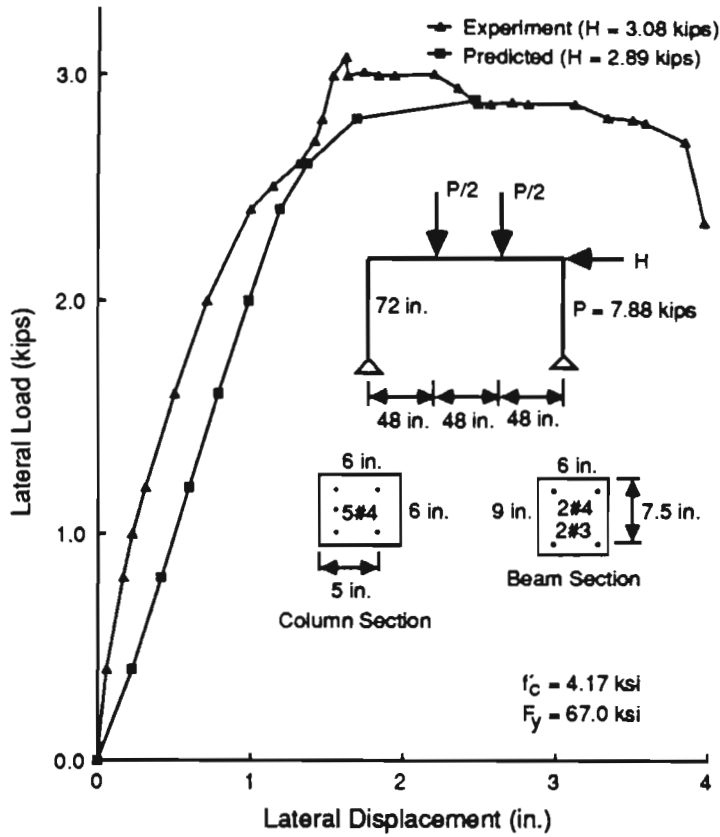


Fig 4.8. Frame 2D12H, from Ernst, et al. [11].

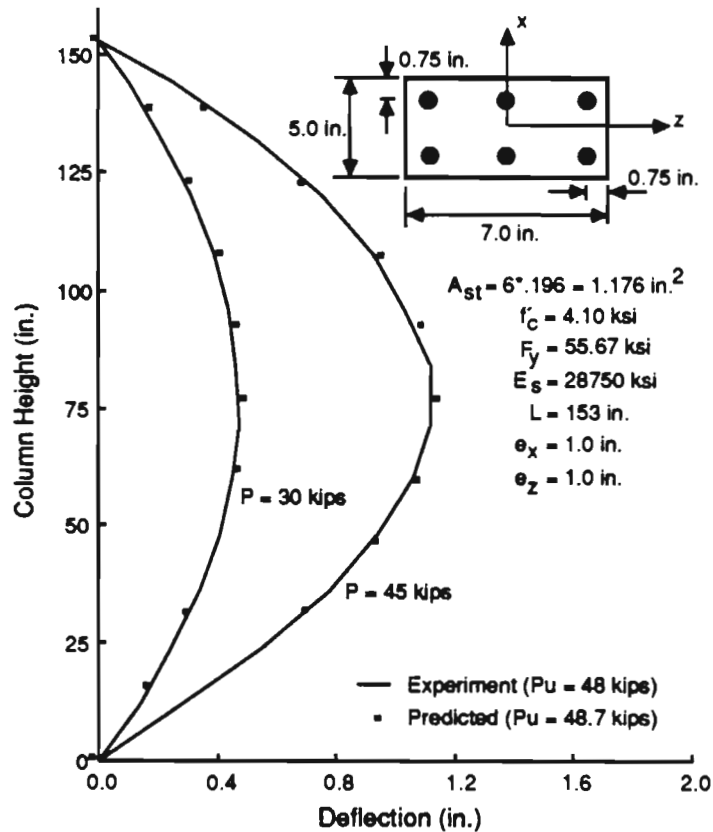


Fig 4.9. Farah and Huggins column [12].

CHAPTER 5. RESULTS AND DISCUSSION

5.1 INTRODUCTION

In Chapter 2, various procedures for analyzing bridge bent columns were described. The details of the second order nonlinear analysis formulation were presented in Chapter 3. The objective of this chapter is to compare the results from the linear and nonlinear analyses with those obtained from the TSDHPT approximate procedure. The current procedure of determining the design column forces and moments is compared with the linear frame analysis. The nonlinear analysis is used to investigate the suitability of the effective length factor used in the approximate procedure. The effect of the foundation flexibility on the overall behavior is finally investigated.

5.2 BENT CONFIGURATION

Five typical bents were selected for the comparative study. These bents are either in service or will be built in the near future. The geometric characteristics and material properties of these bents are shown in Figs 5.1 through 5.10. Bents 1 and 2 are identical except for the number of girders and their spacing. Also, the arrangement of girders is not exactly symmetrical in bent 2. Bents 3 and 4 consist of five and four columns respectively, with eleven girders arranged symmetrically. Bent 5 consists of three columns with an unsymmetrical arrangement of girders. The skew angle of these bents represents the angle between the normal to the longitudinal center line of the bridge and the plane of the bent.

5.3 LOADS ON BENTS

As mentioned earlier, the TSDHPT has identified AASHTO load groups I, II and III as the critical load combinations for the design of typical Texas highway bridge bents. These load groups are used in computing the column axial forces and bending moments in all analysis procedures. The computation of these loads is carried out in accordance with the AASHTO specifications. The capacity reduction factor of 0.70 is used in computing the nominal design loads [29]. The gravity and lateral loads for various bents are summarized in Table 5.1. The design wind velocity was assumed 80 miles per hour in computing the wind loads. The wind loads (Table 5.1) correspond to the wind direction perpendicular to the longitudinal axis of the bridge. The AASHTO HS20-44 standard truck and lane loads are used in computing the live loads on the bridge. In computing the gravity loads of Table 5.1, the live loads on the bridge were distributed equally between the beams. A dead load combination factor β_D of 1.0 is used in this study. H_x and H_z are in-plane and out of plane horizontal loads respectively. These forces are equivalent loads at the bent cap level. L represents the column unsupported length (including depth to fixity)

and the minimum radius of gyration of the column section is designated by r .

In the linear frame analysis, wind loads corresponding to five AASHTO specified wind directions were used. The live loads were computed using the two approaches described in Chapter 2. The first method distributes the live loads evenly between the beams. The second approach considers the variable live load positions on the bridge deck.

5.4 APPROXIMATE PROCEDURE VS LINEAR FRAME ANALYSIS

The results of the linear frame analysis are compared with the column design moments and forces of the current TSDHPT approximate procedure. The moment magnification method of the ACI code is used to approximate second order effects. The method requires the selection of an effective length factor (k) for both axes of bending. Since the bent is treated as a cantilever for the out of plane loads, it would be appropriate to use a k -factor of 2.0 for out of plane bending. For inplane bending, the k -factor should be computed using either the alignment charts or empirical equations [15] recommended by the code. The moments computed for both the inplane and out of plane loads are amplified independently according to their associated magnification factors. This procedure of moment magnification, recommended by the code, will be considered later in this chapter. The approximate procedure assumes an effective length factor of 1.25 for both inplane and out of plane bendings. The same k values are also used in computing the amplified design moments in the linear frame analysis. The resultant of the inplane and out of plane moments is found using the Pythagorean theorem. The results obtained in this study are presented in the next subsections.

5.4.1 Group I Loads

The column axial forces predicted by the approximate and linear frame analysis procedures are shown in Figs 5.11 and 5.12. Each data point on the graph represents a column. The linear analysis yields axial load and associated moment for each column. For example, bent 1 with three columns will yield three data points since only one value of β_D is used in this study. The data points are reduced considering the symmetry of results. The column axial loads from the linear analysis in Fig 5.11 were obtained by distributing the total live loads equally between the beams. Figure 5.12 indicates the effect of variable truck position across the deck. No graph is shown for bending moments in this load group, as minimum eccentricity criterion of AASHTO was found to govern in all cases.

The column axial forces from the two analysis procedures are in good agreement for bents 1 through 4 (Fig 5.11),

the maximum difference being less than 10%. For bent 5, the column axial load predicted by the linear frame analysis is about 35% higher than the results of the approximate analysis. The approximate procedure generally underestimates the design axial forces (Fig 5.12) when the effect of variable truck positioning is considered. For bent 5, the difference is about 50%.

5.4.2 Group II Loads

Figures 5.13 and 5.14 represent the ratios of the column axial forces and moments predicted by the two analysis procedures. For each column, five data points are obtained, one for each wind direction. (AASHTO specifies five wind directions to be considered in computing the design wind loads). It may be noted that the live load is absent in this load group. It is observed (Figs 5.13 and 5.14) that the approximate procedure underestimates axial forces in some columns and overestimates the associated inplane bending moments for bents 1 through 4. For one column of bent 5, the approximate procedure underestimates both the column moment (20%) and axial forces (32%). However, for another column of this bent the axial load predicted by the approximate procedure is almost twice that from the linear analysis. The moments predicted by both procedures are within 5%.

5.4.3 Group III Loads

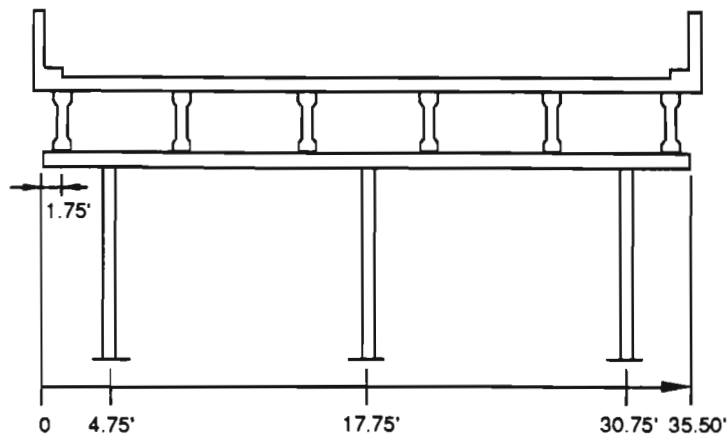
The results obtained for this load combination are shown in Figs 5.15 through 5.18. The column axial forces and bending moments from the linear analysis procedure (Figs 5.15 and 5.16) are based on the live loads distributed equally between the girders. In this load group, the approximate procedure generally overestimates the design moments (bents 1 through 4). The ratio of axial loads predicted by the two procedures are within 10%. The ratios of the column moments and axial loads for bent 5 are similar to those for load group II. Figures 5.17 and 5.18 represent the effect of variable live load position. The maximum column moments and corresponding axial loads are included in these figures. It may be seen that the column moments and axial forces, computed using the two analysis procedures, are generally in good agreement (within 10%) for bents 1

through 4. The results from the approximate procedure are unconservative for bent 5, in terms of either higher moment and low axial load or high axial load and associated moments when compared with the linear frame analysis values.

5.4.4 Discussion of Results

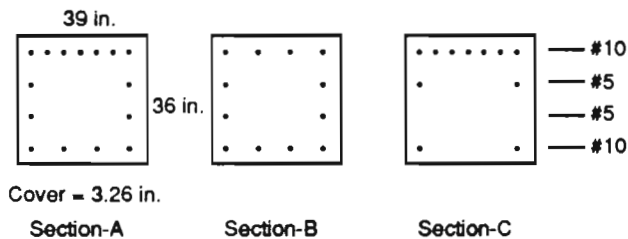
For load group I, the axial forces predicted by the TSDHPT approximate procedure agree well with the linear frame analysis values (bent 1 through 4), when live loads on the bridge are distributed equally between the girders. For bent 5, the approximate procedure underestimates the axial force in one column which is balanced by overestimating the force in another column. The current office procedure, however, generally underestimates the axial forces when the variation in live load positions over the deck is considered. The implication of these results depends on the AASHTO load combination controlling the design. If the design is controlled by this load group, the larger column axial forces and minimum moment would be the critical situation as the design is governed by the axial strength of the column.

For load combinations II and III, the design or strength of columns is typically governed by the bending action as the axial loads in columns are generally less than the corresponding axial loads at the balanced condition. (The balanced condition is defined as a combination of axial load and moment when the yielding of steel and the crushing of concrete occur simultaneously). Therefore, the higher moments and lower axial loads predicted by the approximate procedure are conservative for bents 1 through 4. For bent 5, the approximate procedure overestimates the axial force in a column resulting in an unconservative design situation. As the bent geometry deviates from the typical geometries, the uncertainty relating to the approximate procedure increases. The amounts by which the inplane bending moment is overestimated and the axial force is underestimated by the approximate method are unpredictable. For the range of variables investigated, it was observed that for the load group III, varying the live load positions on the bridge deck does not drastically change the results compared with the values for live loads distributed equally between the beams. This may be attributed to the low percentage of gravity loads contributed by live loads in this load group.



Forward Span Length	= 105.30 ft	Number of Lanes	= 3
Backward Span Length	= 105.30 ft	Number of Beams	= 6
Skew Angle	= 0.00 Degrees	Number of Columns	= 3
Degree of Curve	= 0.00 Degrees	Depth of Beam	= 4.5 ft
Rail Height	= 2.0 ft	Slab Depth	= 7.75 in.
Weight of Rail	= 0.300 kips/ft	Slab Width	= 38.25 ft
Weight of Beam	= 0.516 kips/ft	Beam Spacing	= 6.4 ft
Cap Length	= 35.5 ft	Column Spacing	= 13.0 ft
Column Height	= 22.0 ft	Depth to Fixity	= 5.0 ft
Strength of Concrete	= 3600 psi	Steel Yield Stress	= 60 ksi

Fig 5.1. Layout and material properties of Bent 1.



Bent Cap Sections

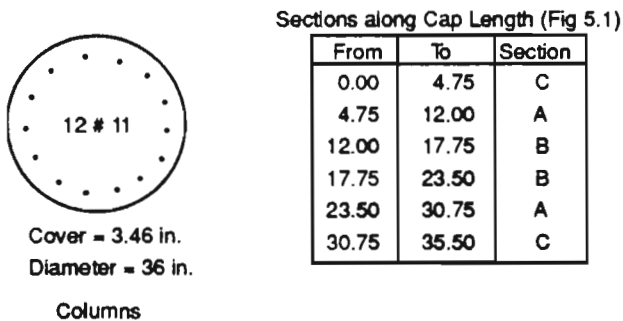
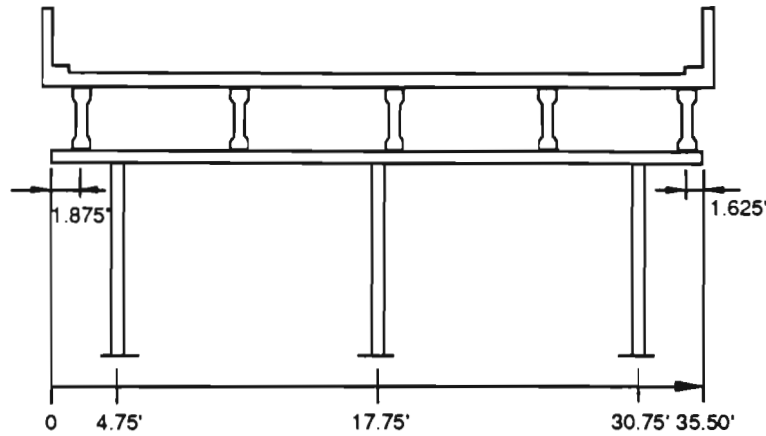
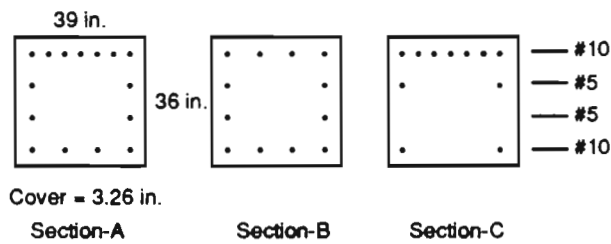


Fig 5.2. Cross sections of bent cap and columns of Bent 1.

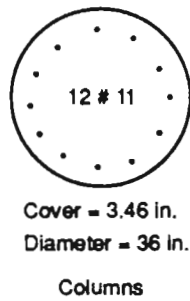


Forward Span Length	= 105.30 ft	Number of Lanes	= 3
Backward Span Length	= 105.30 ft	Number of Beams	= 6
Skew Angle	= 0.00 Degrees	Number of Columns	= 3
Degree of Curve	= 0.00 Degrees	Depth of Beam	= 4.5 ft
Rail Height	= 2.0 ft	Slab Depth	= 7.75 in.
Weight of Rail	= 0.300 kips/ft	Slab Width	= 38.25 ft
Weight of Beam	= 0.516 kips/ft	Beam Spacing	= 8.0 ft
Cap Length	= 35.5 ft	Column Spacing	= 13.0 ft
Column Height	= 22.0 ft	Depth to Fixity	= 5.0 ft
Strength of Concrete	= 3600 psi	Steel Yield Stress	= 60 ksi

Fig 5.3. Layout and material of Bent 2.



Bent Cap Sections

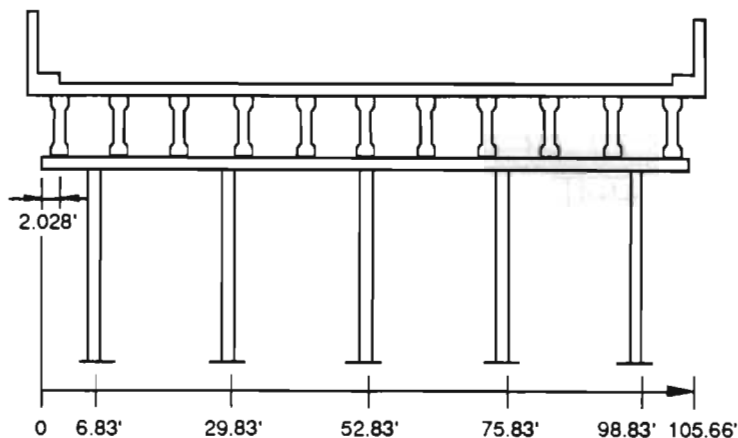


Columns

Sections along Cap Length (Fig 5.3)

From	To	Section
0.00	4.75	C
4.75	14.25	A
14.25	17.75	B
17.75	21.25	B
21.25	30.75	A
30.75	35.50	C

Fig 5.4. Cross sections of bent cap and columns of Bent 2.



Forward Span Length	= 80.0 ft	Number of Lanes	= 6
Backward Span Length	= 75.0 ft	Number of Beams	= 11
Skew Angle	= 30.0 Degrees	Number of Columns	= 5
Degree of Curve	= 0.00 Degrees	Depth of Beam	= 3.33 ft
Rail Height	= 2.0 ft	Slab Depth	= 8.0 in.
Weight of Rail	= 0.330 kips/ft	Slab Width	= 94.0 ft
Weight of Beam	= 0.516 kips/ft	Beam Spacing	= 10.161 ft
Cap Length	= 105.60 ft	Column Spacing	= 23.0 ft
Column Height	= 24.0 ft	Depth to Fixity	= 5.0 ft
Strength of Concrete	= 3600 psi	Steel Yield Stress	= 60 ksi

Fig 5.5. Layout and material properties of Bent 3.

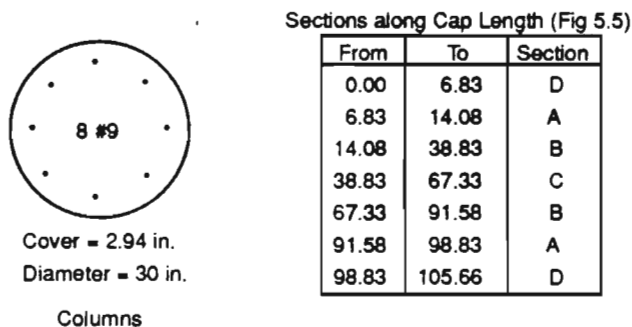
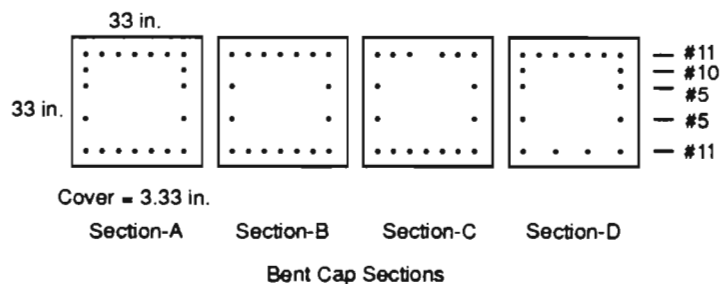


Fig 5.6. Cross sections of bent cap and columns of Bent 3.

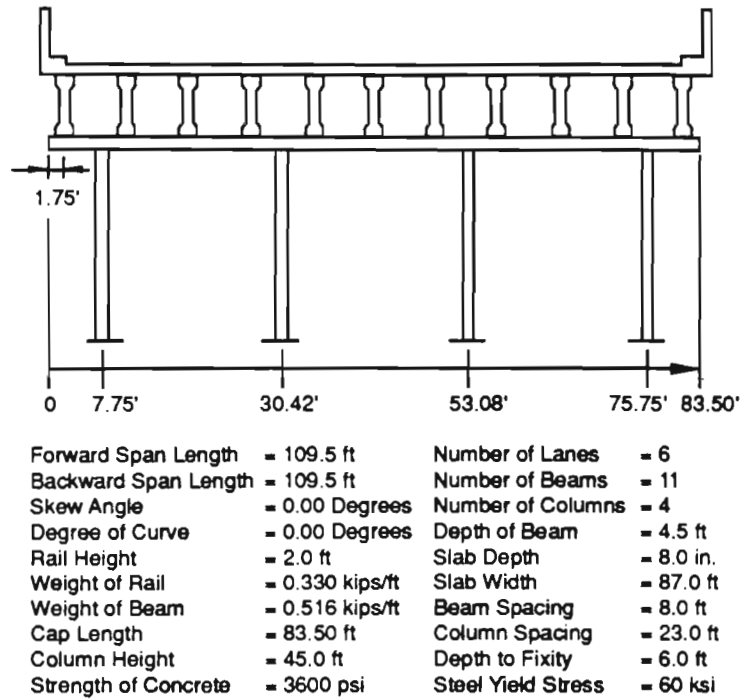
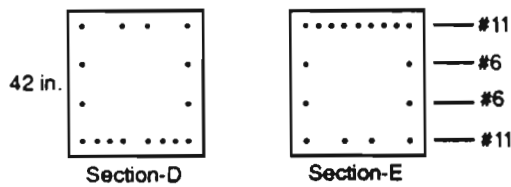
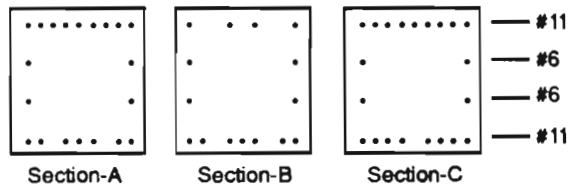
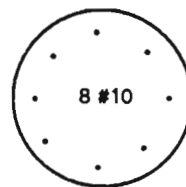


Fig 5.7. Layout and material properties of Bent 4.



Bent Cap Sections

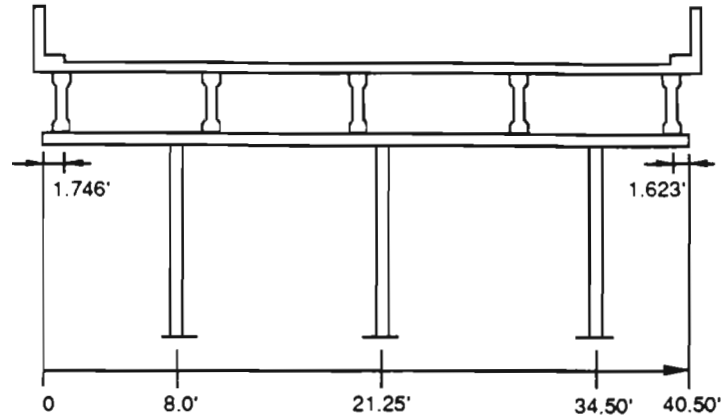


Cover = 3.25 in.
Diameter = 36 in.
Columns

Sections along Cap Length (Fig 5.7)

From	To	Section
0.00	7.75	E
7.75	16.25	A
16.25	22.42	B
22.42	30.42	A
30.42	38.42	C
38.42	45.08	D
45.08	53.08	C
53.08	61.08	A
61.08	67.25	B
67.25	75.75	A
75.75	83.50	E

Fig 5.8. Cross sections of bent cap and columns of Bent 4.



Forward Span Length	= 80.03 ft	Number of Lanes	= 3
Backward Span Length	= 80.03 ft	Number of Beams	= 5
Skew Angle	= 14.2 Degrees	Number of Columns	= 3
Degree of Curve	= 0.00 Degrees	Depth of Beam	= 4.17 ft
Rail Height	= 2.0 ft	Slab Depth	= 10.0 in.
Weight of Rail	= 0.330 kips/ft	Slab Width	= 42.0 ft
Weight of Beam	= 0.516 kips/ft	Beam Spacing	= 9.28 ft
Cap Length	= 40.50 ft	Column Spacing	= 13.25 ft
Column Height	= 23.0 ft	Depth to Fixity	= 5.0 ft
Strength of Concrete	= 3600 psi	Steel Yield Stress	= 60 ksi

Fig 5.9. Layout and material properties of Bent 5.

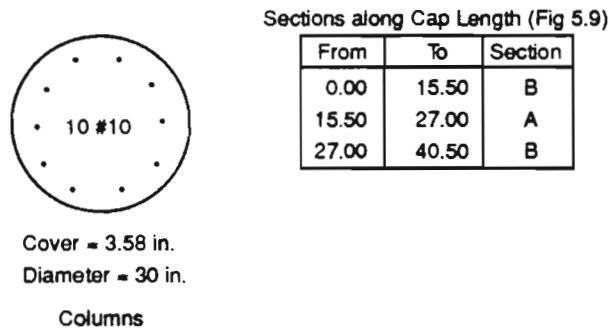
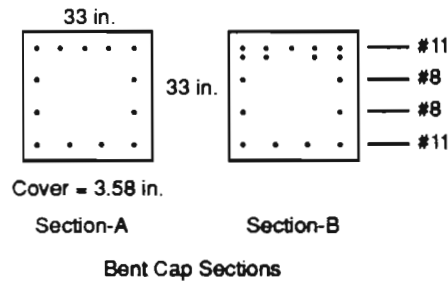


Fig 5.10. Cross sections of bent cap and columns of Bent 5.

Bent	L/r	Load Group	Gravity Load		Design Load Hx (kips)
			per Beam (kips)	H _z /H _x	
1	36.0	I	402.3	---	0
		II	257.6	0.0	49.09
		III	344.4	0.450	48.52
2	36.0	I	462.6	---	0
		II	289.0	0.0	49.09
		III	393.2	0.450	48.52
3	46.4	I	333.2	---	0
		II	226.4	0.657	29.33
		III	290.2	0.862	46.06
4	68.0	I	437.6	---	0
		II	302.0	0.0	56.02
		III	383.2	0.680	47.39
5	44.8	I	413.5	---	0
		II	269.4	0.243	35.64
		III	355.7	0.606	40.54

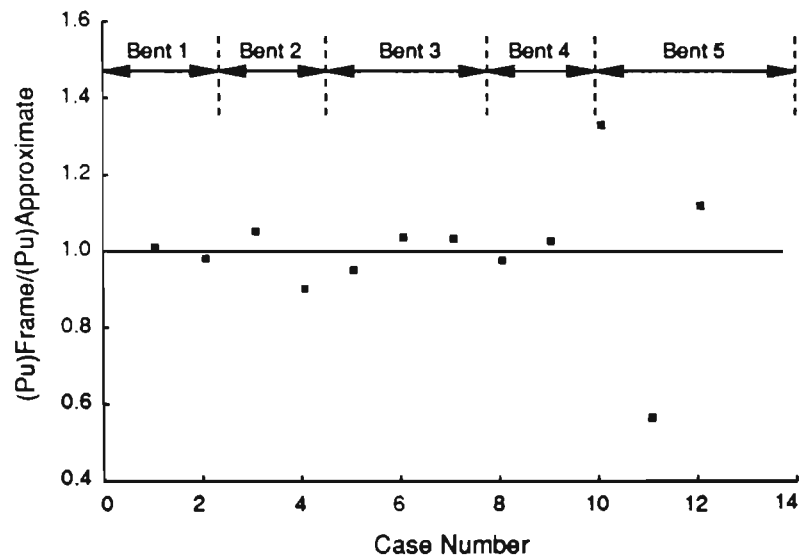


Fig 5.11. Column axial forces for group I loads (equal live load per beam).

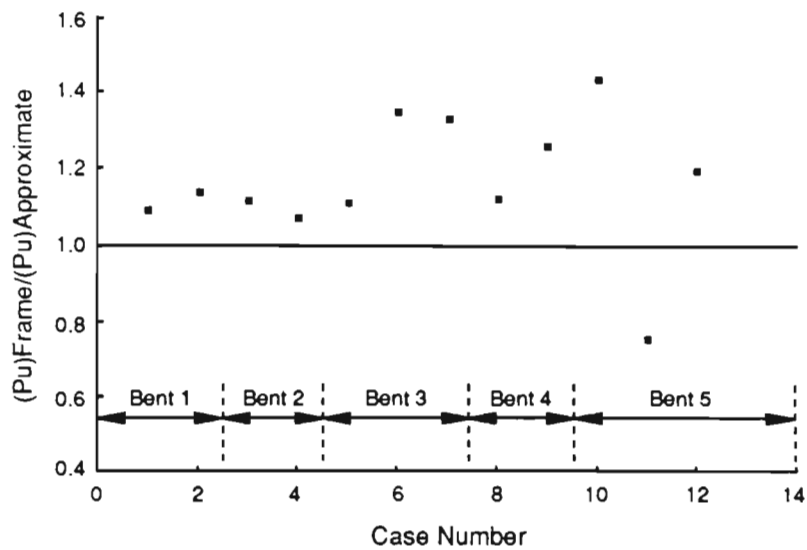


Fig 5.12. Column axial forces for group I loads (variable live load position).

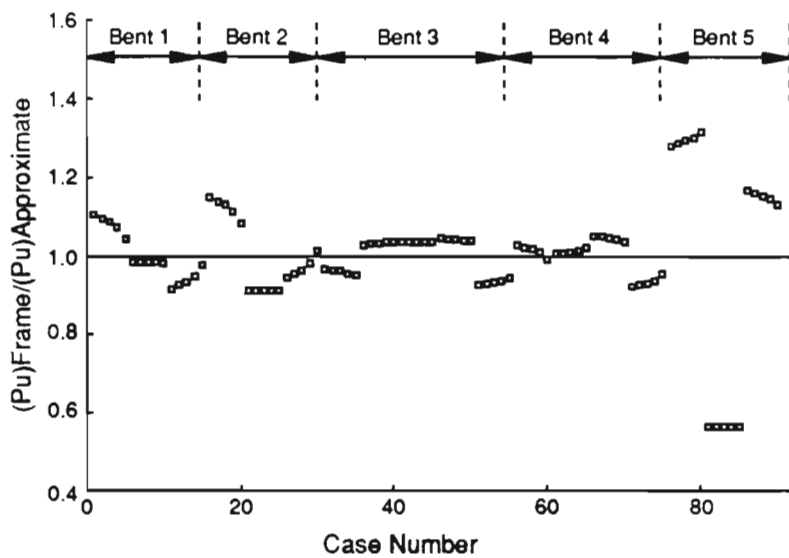


Fig 5.13. Design axial forces for group II loads.

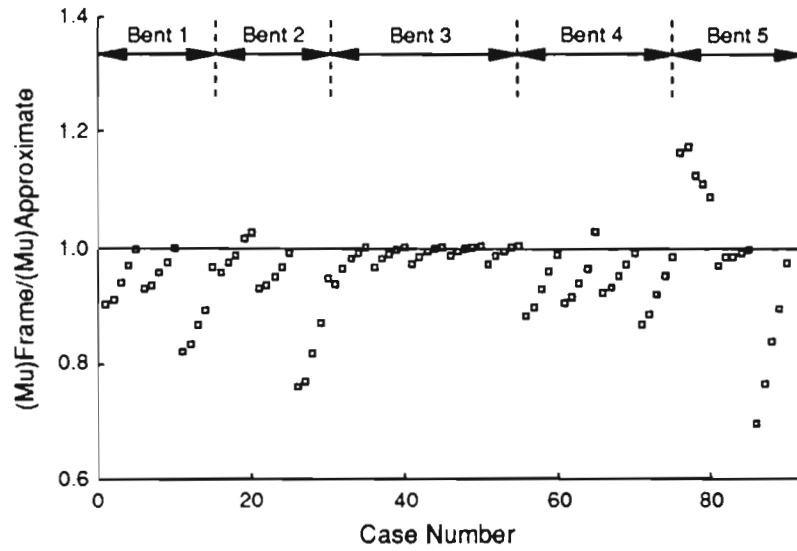


Fig 5.14. Design forces for load combination II.

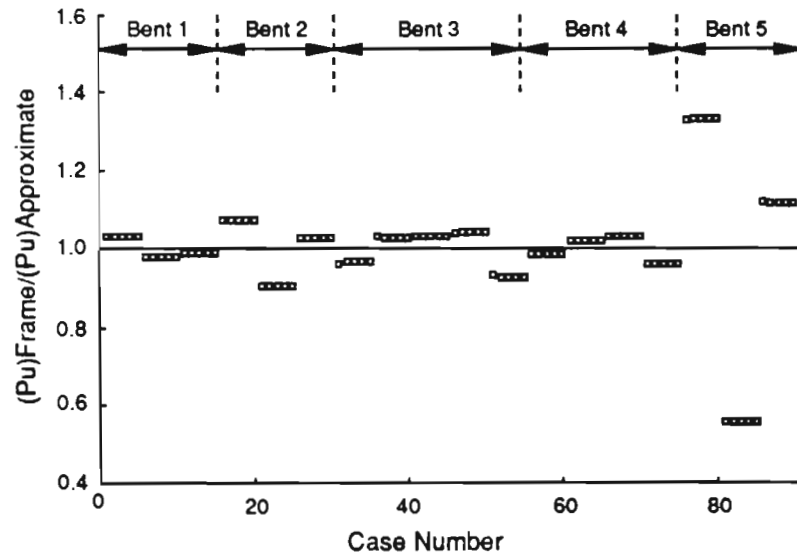


Fig 5.15. Design axial forces for load group III (equal live load per beam).

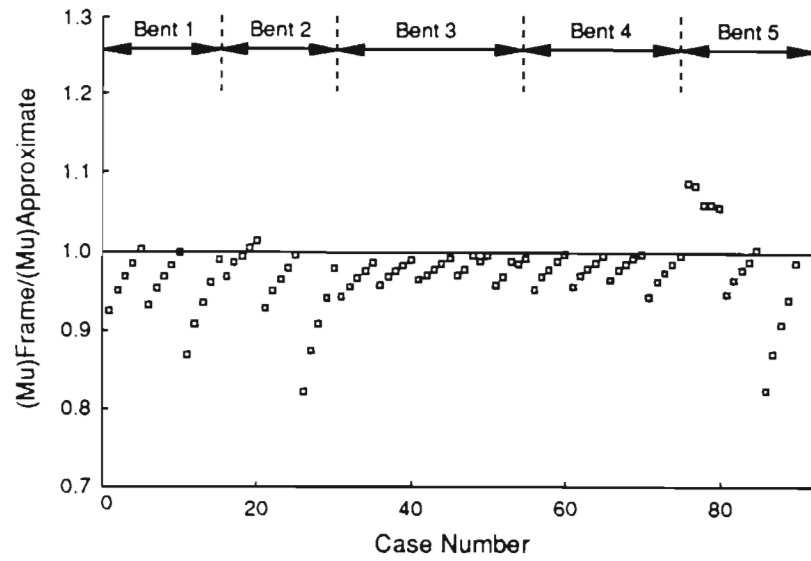


Fig 5.16. Design moments for load group III (equal live load per beam).

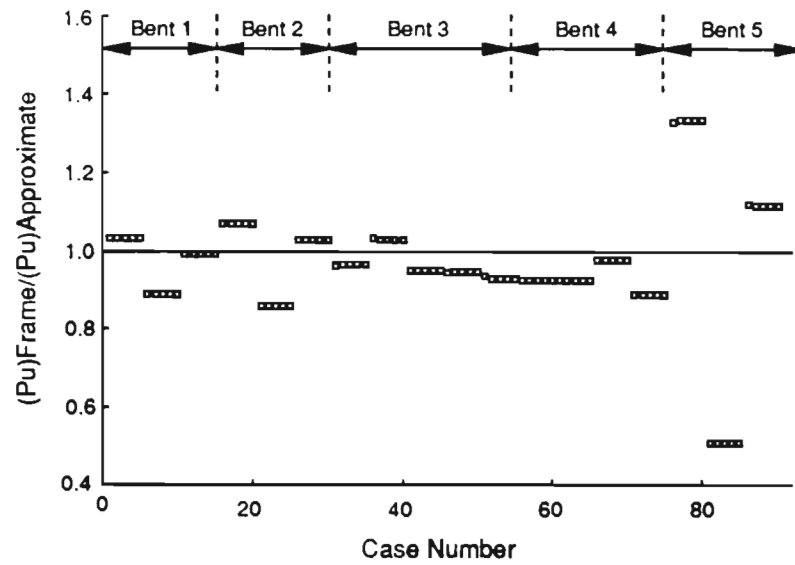


Fig 5.17. Design axial forces for load group III (variable live load position).

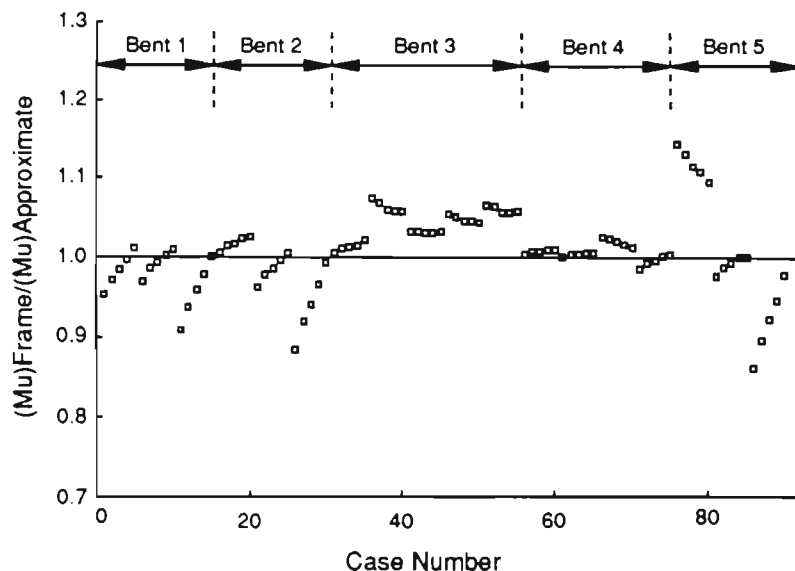


Fig 5.18. Design moments for load group III (variable live load position).

5.5 APPROXIMATE PROCEDURE VS NONLINEAR ANALYSIS

In this section, the results predicted by the nonlinear analysis are compared with those obtained from the TSDHPT approximate procedure and the ACI moment magnifier method. The moment magnification method of ACI assumes an effective length factor of 2.0 for out of plane bending. The k factor for inplane bending was computed using the alignment chart of the Code [2]. In the nonlinear analysis, the gravity loads on the bridge were divided equally between the girders. The gravity loads on beams were applied first and kept constant. The biaxial lateral loads were then increased proportionally until failure. Three modes of failure are recognized: (a) compression failure when the specified compressive strain of concrete is reached; (b) tension failure when the specified steel ultimate strain is reached; and (c) stability failure when the tangent stiffness matrix of the system becomes singular or negative. The loads applied on bents are given in Table 5.1.

5.5.1 Load-Deformation Curves

The load-deflection curves for all five bents and for load combinations II and III are presented in Figs 5.19 through 5.28. The inplane and out of plane lateral deformations are plotted against the inplane horizontal loads (H_x). It may be observed that for a given load, the out of plane deflections are generally higher than the inplane deflections. This is due to the cantilever action in the out of plane direction, in addition to the relative magnitude of the lateral loads. The maximum lateral loads and the failure modes for various bents, predicted by the nonlinear analysis are summarized in Table

5.2. The analysis of each case is as expected. The change in the initial slope of the load deflection curve is an indication of the initiation of flexural cracks in concrete. The yielding of rebars may be responsible for a subsequent change in the slope. It may be seen that bents 3 and 4 (Figs 5.23, 5.24 and 5.26) experienced a large deflection prior to failure. The program showed a material failure in the structure. It is envisioned that such a large deformation may be an indication of the stability failure.

5.5.2 Predicted Axial Loads vs Design Axial Forces

The variation of the column axial forces with the gravity loads on beams for various bents is presented in Figs 5.29 through 5.33. The column axial forces computed using the TSDHPT approximate procedure are also included. From Figs 5.29 through 5.32, it may be seen that the axial forces predicted by the approximate procedure are in close agreement with the analytical predictions. For bent 5, the approximate procedure underestimates the analytical predictions for one column. This is balanced by overestimating the axial force in another column. Recall that the bent 5 consists of five girders arranged unsymmetrically over the bent cap. These results are similar to those obtained from the linear frame analysis where live loads were distributed equally between the beams.

5.5.3 Predicted Moments vs Design Moments

The moments from the nonlinear analysis procedure are compared with the predictions of the ACI moment magnifier method and the TSDHPT approximate procedure. The results of this study are presented, for each bent and for load groups II and III, in the following subsections. In load

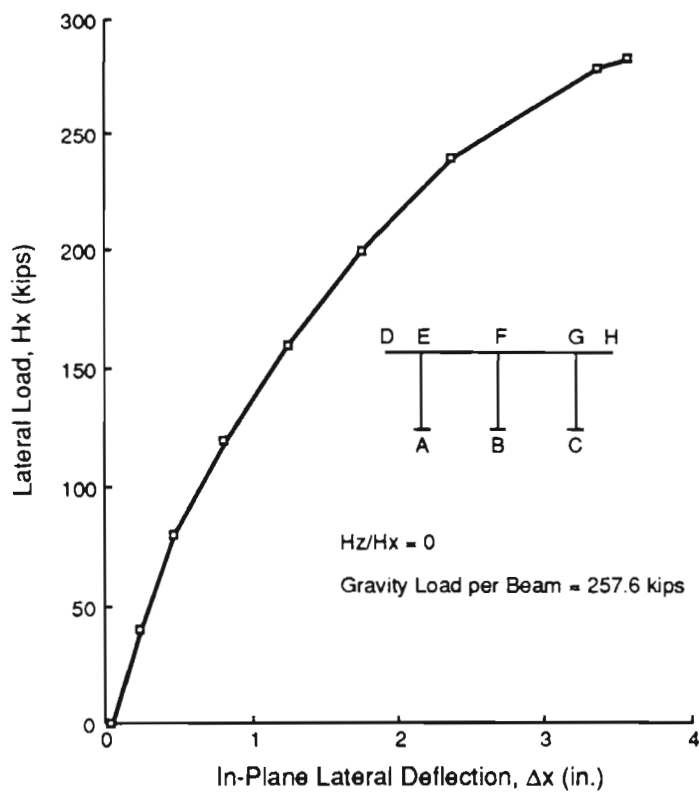


Fig 5.19. Load-deformation curve for Bent 1 (load group II).

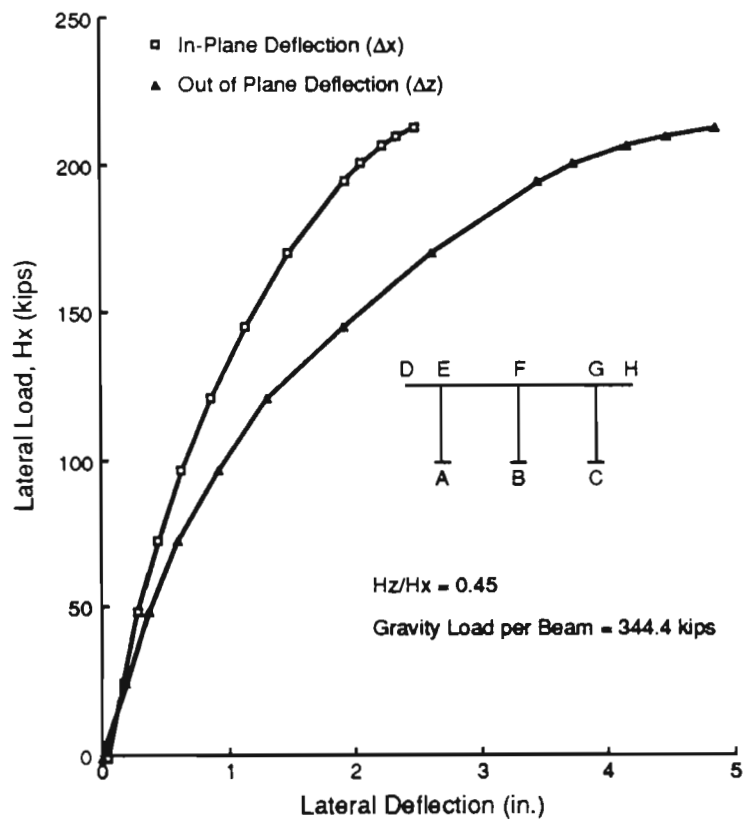


Fig 5.20. Load-deformation curve for Bent 1 (load group III).

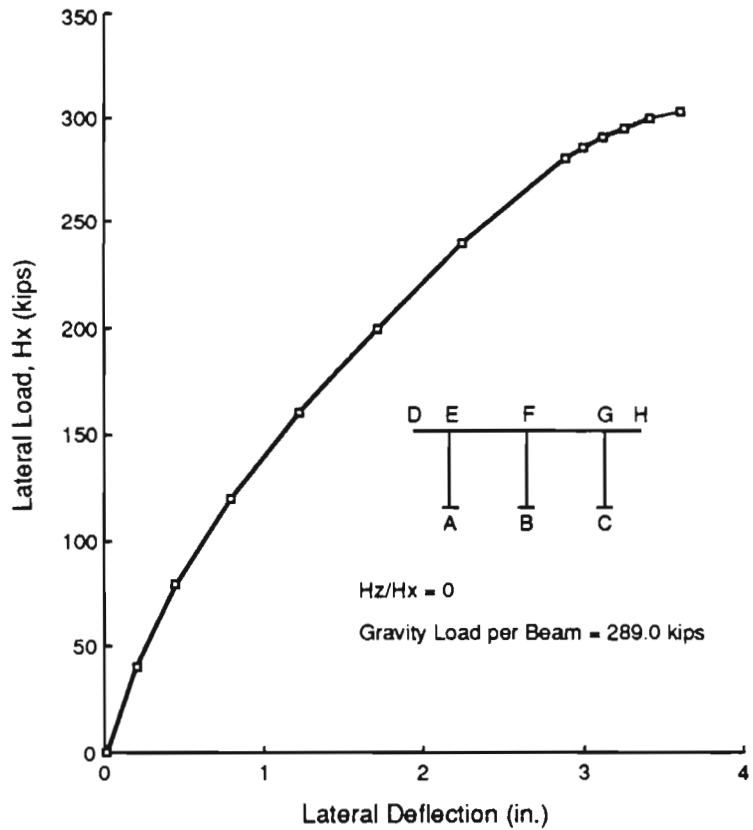


Fig 5.21. Load-deformation curve for Bent 2 (load group II).

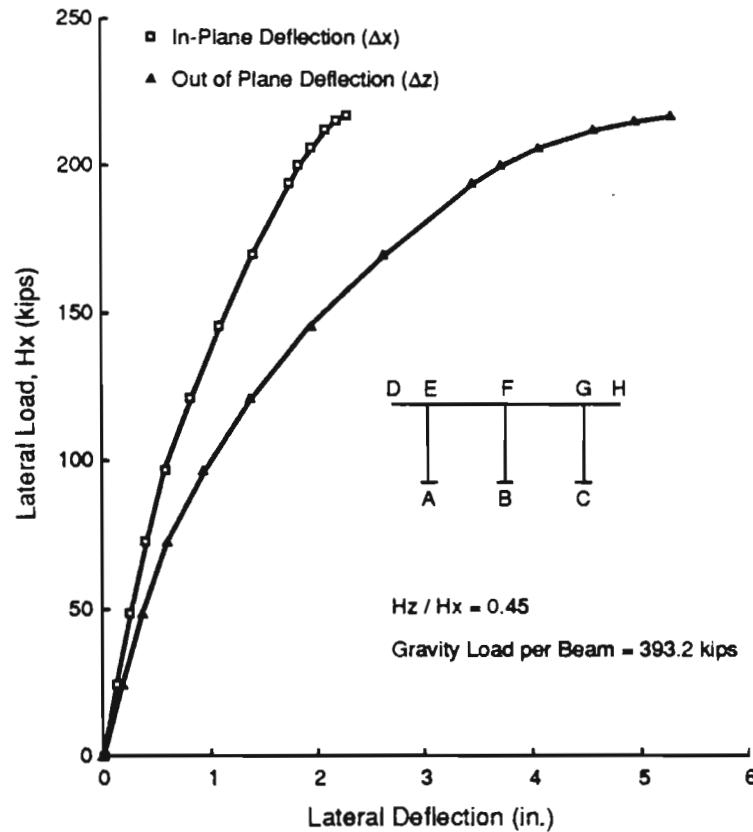


Fig 5.22. Load-deformation curve for Bent 2 (load group III).

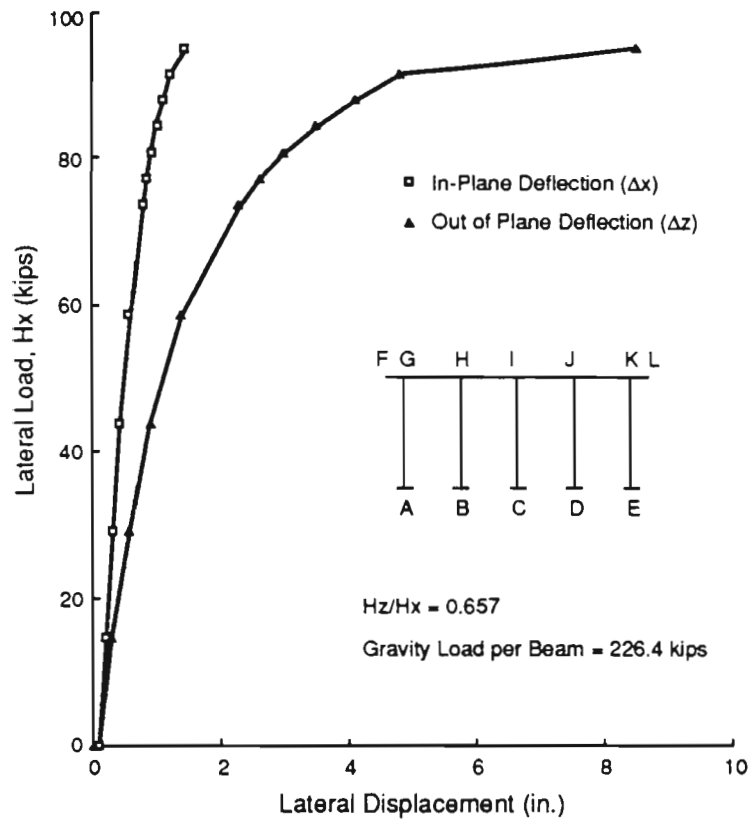


Fig 5.23. Load-deformation curve for Bent 3 (load group II).

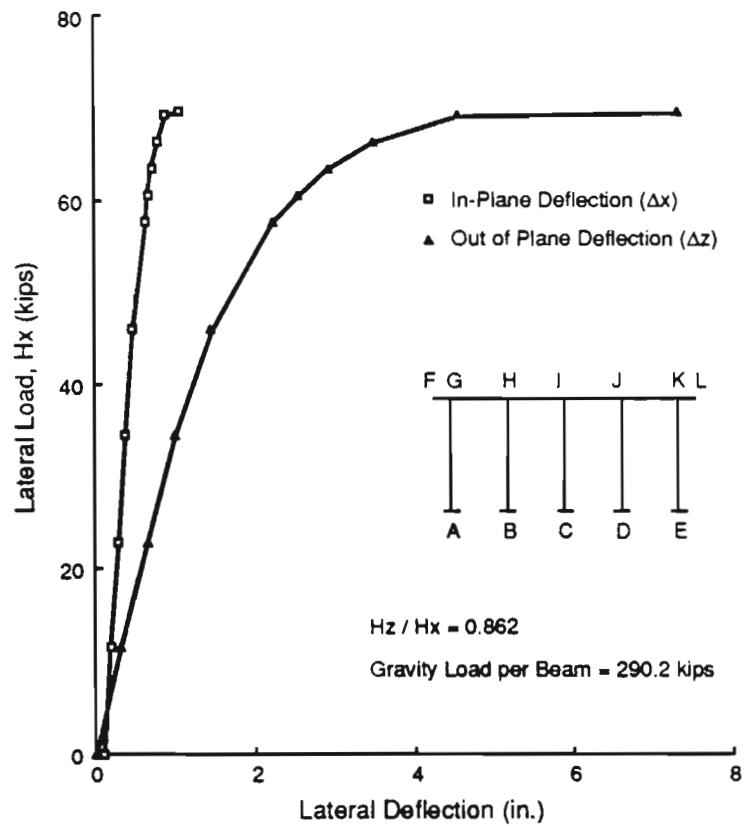


Fig 5.24. Load-deformation curves for Bent 3 (load group III).

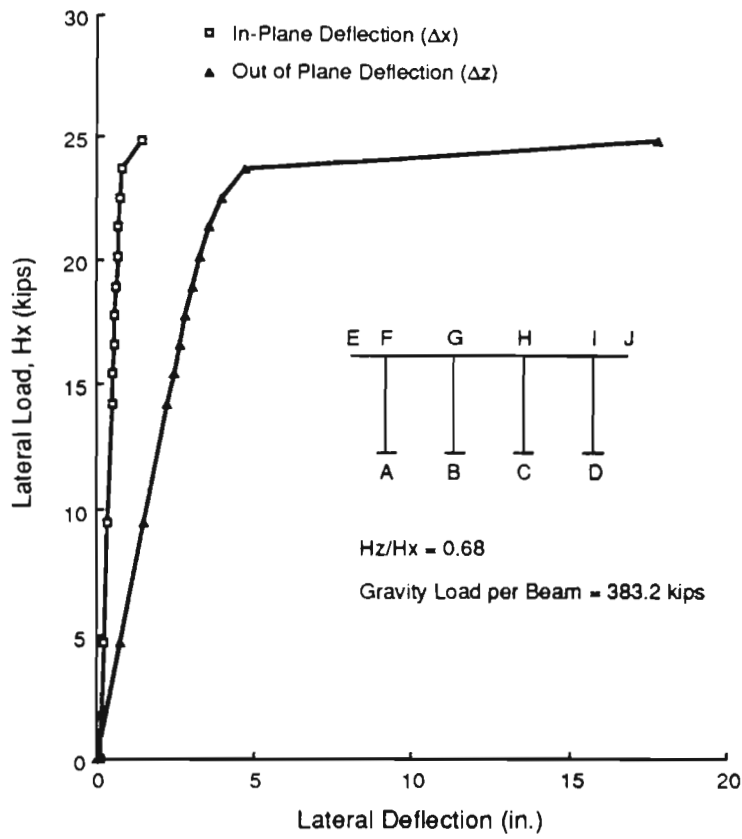


Fig 5.25. Load-deformation curve for Bent 4 (load group II).

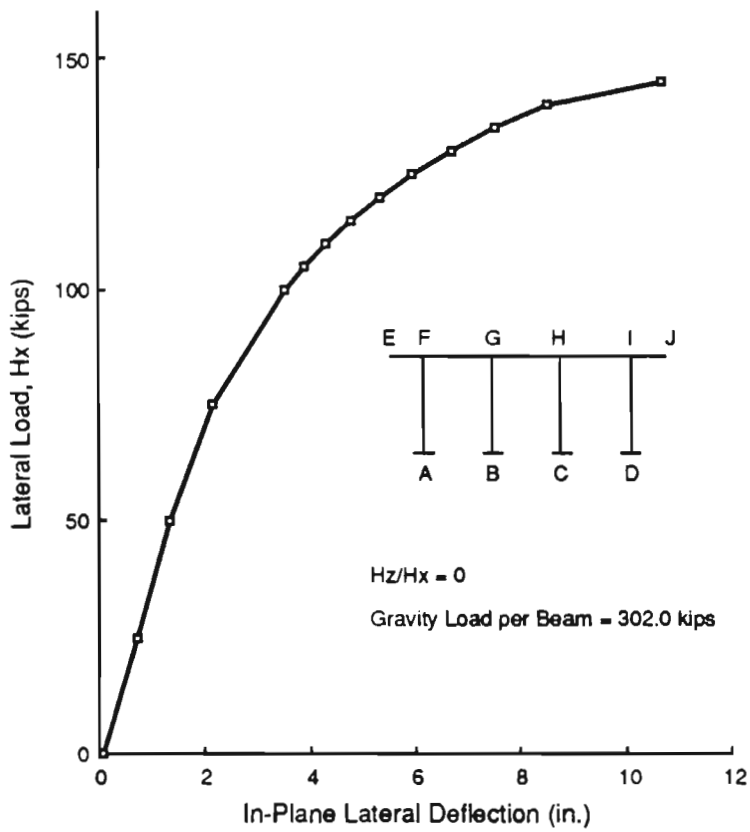


Fig 5.26. Load-deformation curves for Bent 4 (load group III).

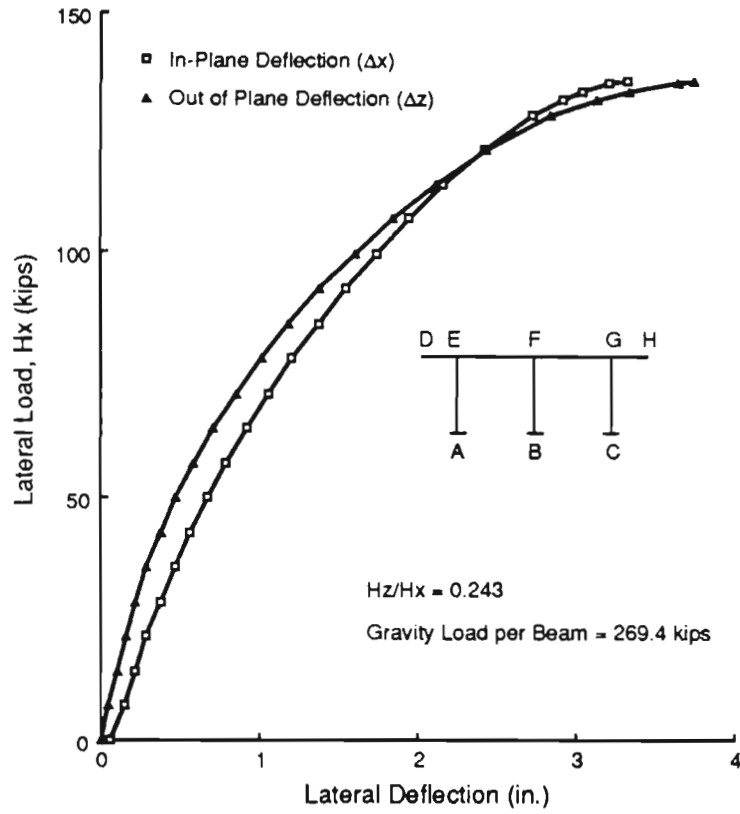


Fig 5.27. Load-deformation curves for Bent 5 (load group II).

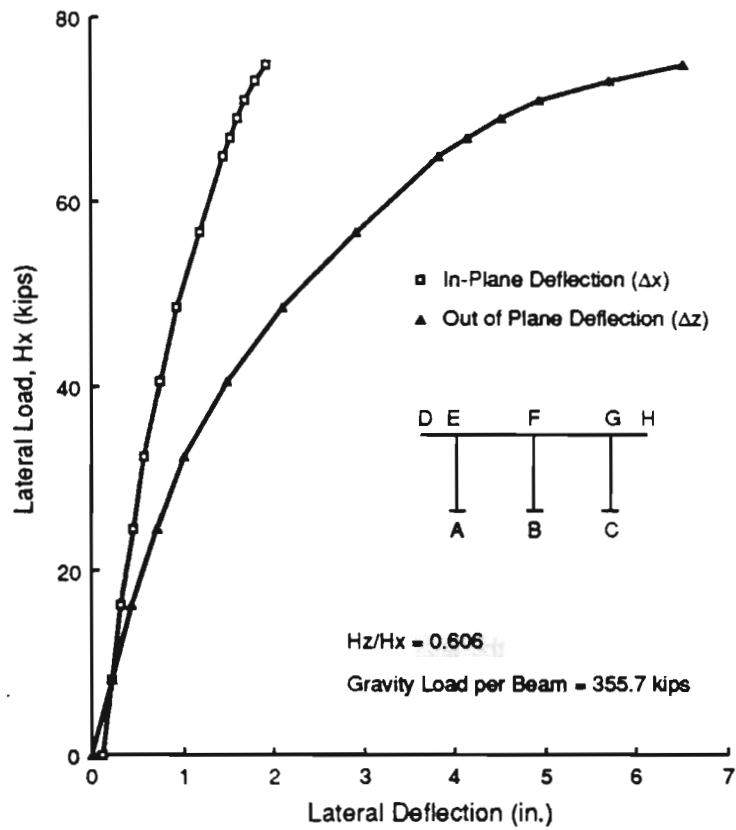


Fig 5.28. Load-deformation curves for Bent 5 (load group III).

TABLE 5.2. ULTIMATE LATERAL LOADS FOR BENTS

Bent	Load Group	Ultimate Load Hx (klips)	Failure Mode
1	II	284.5	Tension Failure in Beam EF*
	III	212.4	Compression Failure in Column BF
2	II	303.0	Compression Failure in Column AE
	III	217.5	Compression Failure in Column CG
3	II	95.2	Compression Failure in Column EK
	III	69.6	Compression Failure in Column CI
4	II	145.0	Compression Failure in Column CH
	III	24.9	Compression Failure in Column AF
5	II	133.5	Compression Failure in Column CG
	III	74.8	Compression Failure in Beam EF

* Members are indicated on corresponding figures.

combination I, the design moments were controlled by the minimum eccentricity criterion of the ACI code and are not presented here. Only one wind direction, perpendicular to the bridge longitudinal axis, is considered in computing the design wind loads (Table 5.1).

5.5.3.1 Bent 1

Figure 5.34 shows the variation of the inplane moments with the applied inplane horizontal loads for load combination II. The predicted inplane and out of plane moments for load group III are shown in Figures 5.35 and 5.36. The design moments estimated by the ACI and TSDHPT procedures are also shown in these figures. It may be seen that for uniaxial bending under inplane loads (Fig 5.34), the results from all three analysis procedures are in good agreement. When the bent is subjected to biaxial lateral loads, the inplane moments from the approximate and ACI methods are slightly higher (Fig 5.35) than the analytical predictions. The out of plane moments (Fig 5.36) calculated by the nonlinear analysis agree well with the results from the approximate procedure for low values of lateral loads (up to 50% of the predicted failure load). In the higher load range, the approximate procedure underestimates the out of plane moments of the nonlinear analysis. The operating load ranges on the bridges are generally less than half of the ultimate loads (for a safety factor of 2.0). Thus it may be concluded that the moments computed by the approximate procedure are reasonable for service load conditions. The ACI method estimates out of plane moments greater than the analytical values. The difference between the out of plane moments from the ACI method and the nonlinear analysis reduces near failure of the structure. The difference between the failure loads of the three analysis procedures is within 10%.

5.5.3.2 Bent 2

The results for this bent are presented in Figs 5.37 through 5.39 for load groups II and III. The slenderness ratio of the bent is 36. Bents 1 and 2 are identical except for the number of girders on the bridge and their spacing. The trend of results for this bent is similar to the previous case. The ultimate lateral loads predicted by the analytical procedure agree well with the approximate and the ACI procedures. Again the TSDHPT procedure is in better agreement with the analysis results in the range of service loads than the ACI procedure. As loads increase toward failure the effective length factor (k) increases and the results approach of the ACI method.

5.5.3.3 Bent 3

The moments from the nonlinear analysis, the TSDHPT approximate procedure and the ACI method are shown in Figs 5.40 through 5.43. It may be noted that the bent is subjected to both inplane and out of plane lateral loads for load group II. The angle of skew for this bent is 30 degrees (Fig 5.5). As stated earlier, the skew angle is defined as the angle between the plane of the bent and the longitudinal axis of the bridge. The wind direction is considered as the normal to the bridge longitudinal axis. This resulted in forces parallel and perpendicular to the plane of the bridge bent. The column slenderness ratio for this bent is 46.4.

From Figs 5.40 and 5.41, it may be observed that for low values of the lateral loads the approximate procedure underestimates the analytical inplane moments. This deviation is due to the contribution of gravity loads on inplane moments. The approximate procedure neglects the moments developed by the gravity loads. The out of plane moments predicted by the approximate and nonlinear analyses are in

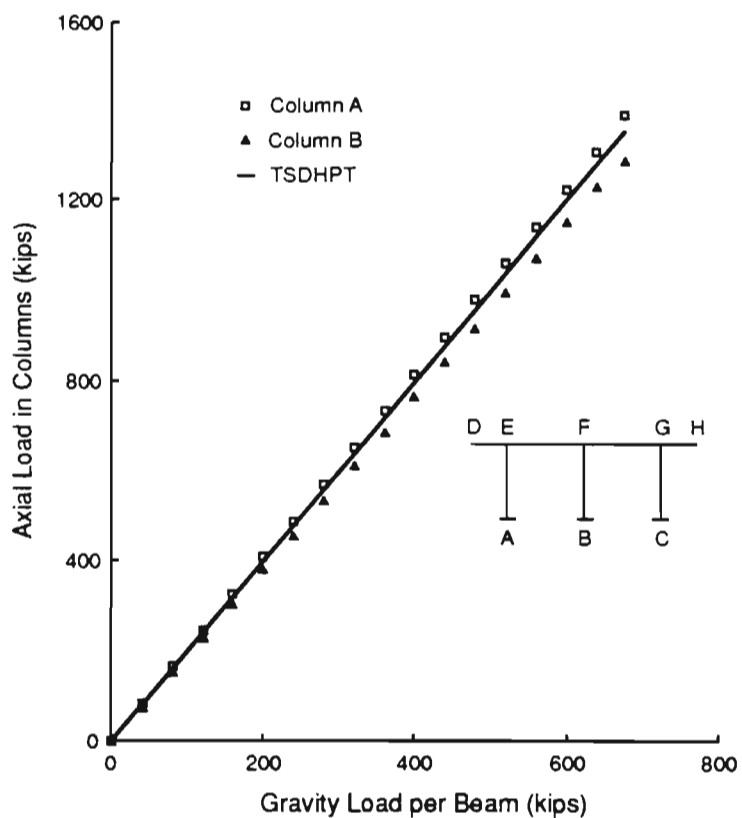


Fig 5.29. Column axial forces for Bent 1 (load group I).

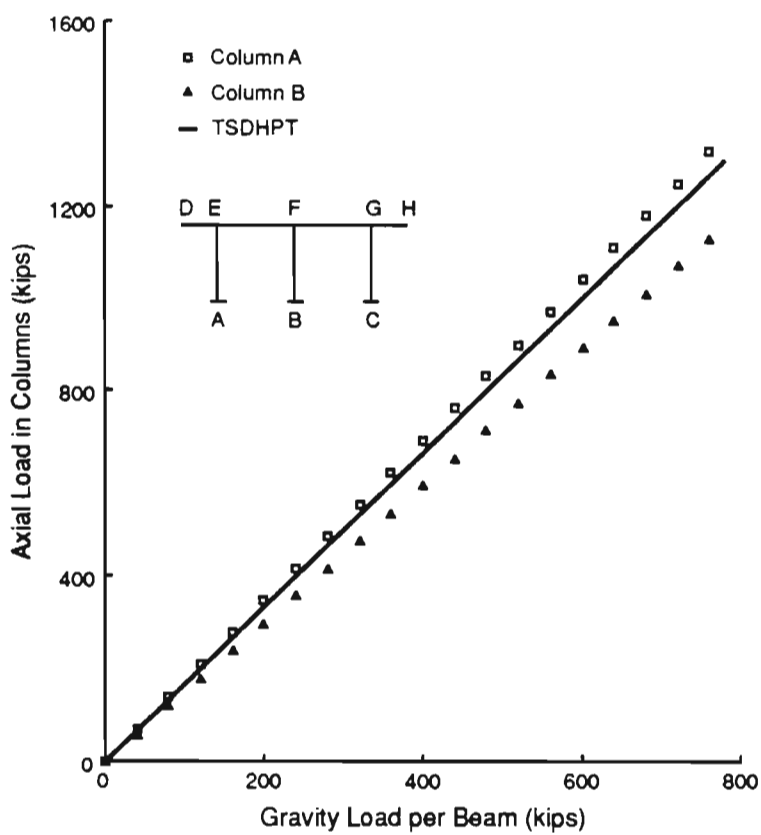


Fig 5.30. Column axial forces for Bent 2 (load group I).

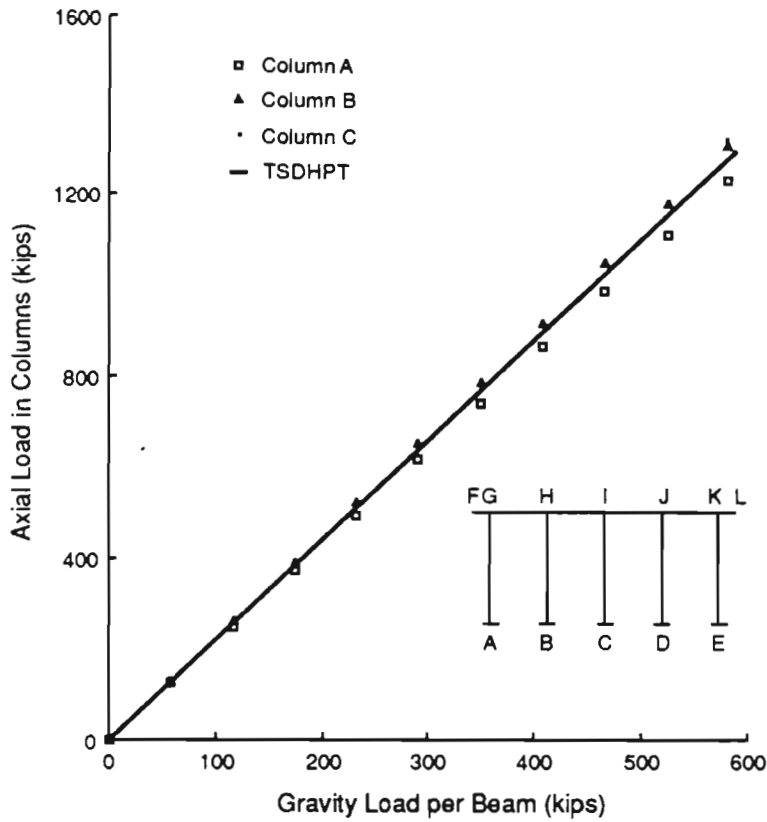


Fig 5.31. Column axial forces for Bent 3 (load group I).

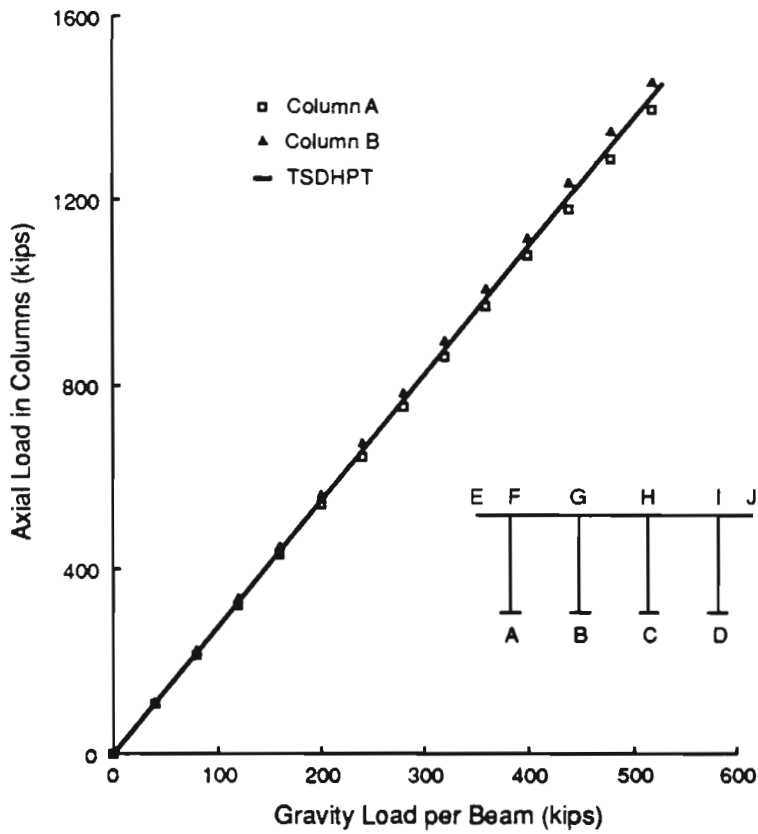


Fig 5.32. Column axial forces for Bent 4 (load group I).

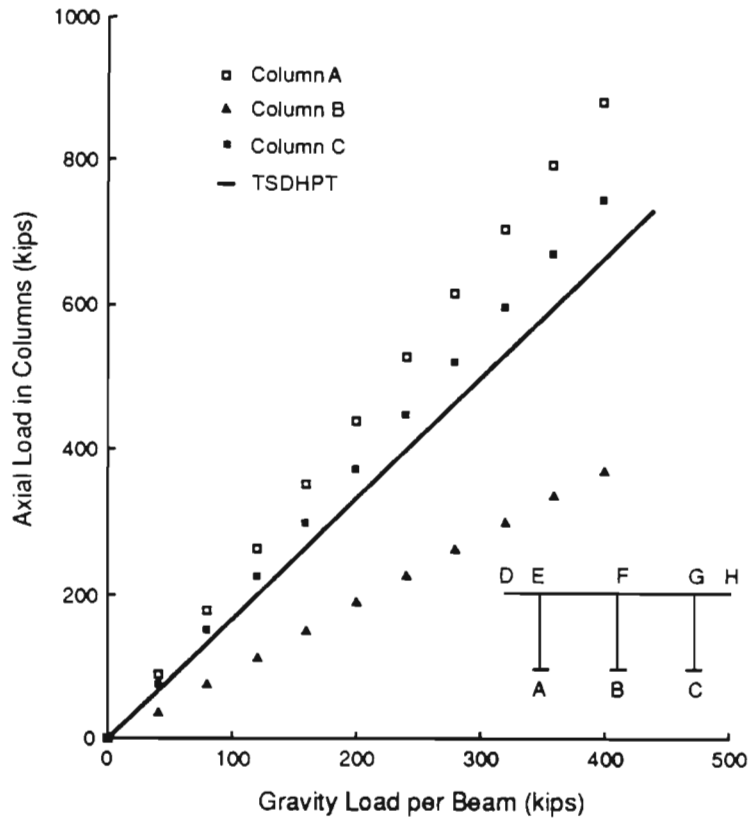


Fig 5.33. Column axial forces for Bent 5 (load group I).

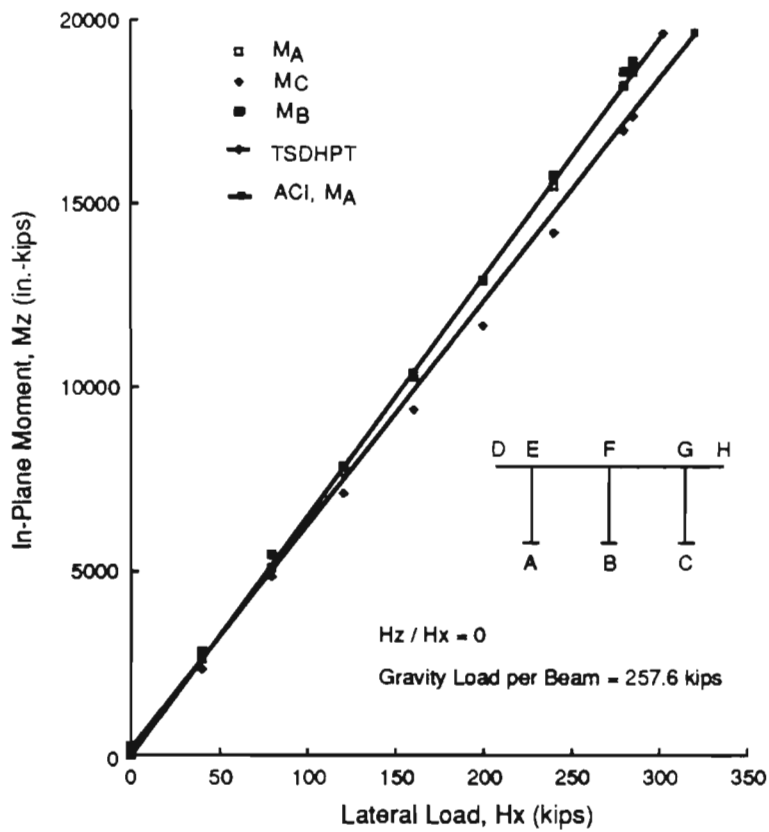


Fig 5.34. Column axial forces for Bent 1 (load group II).

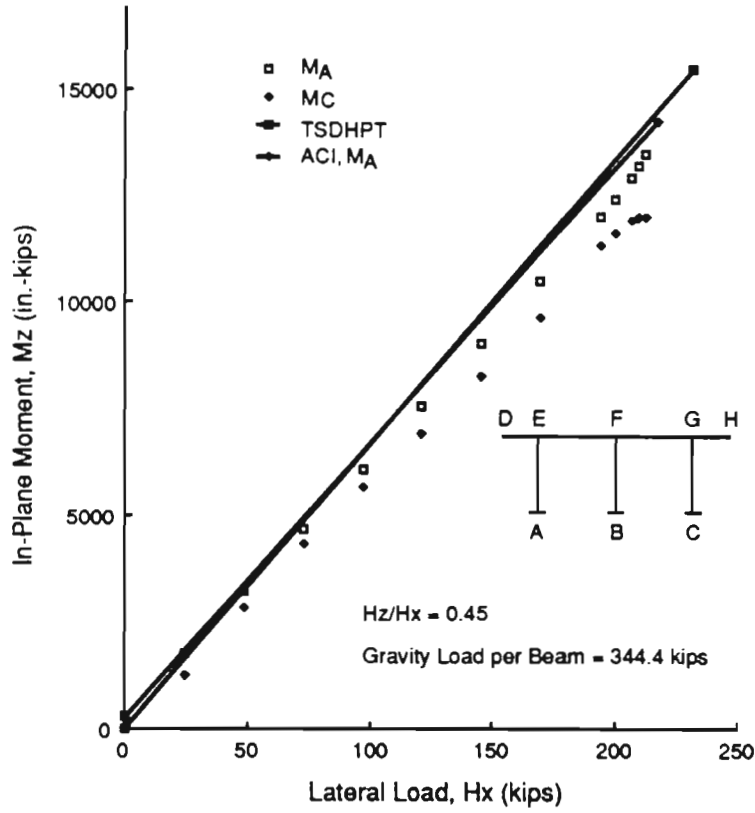


Fig 5.35. Design moments for Bent 1 (load group III).

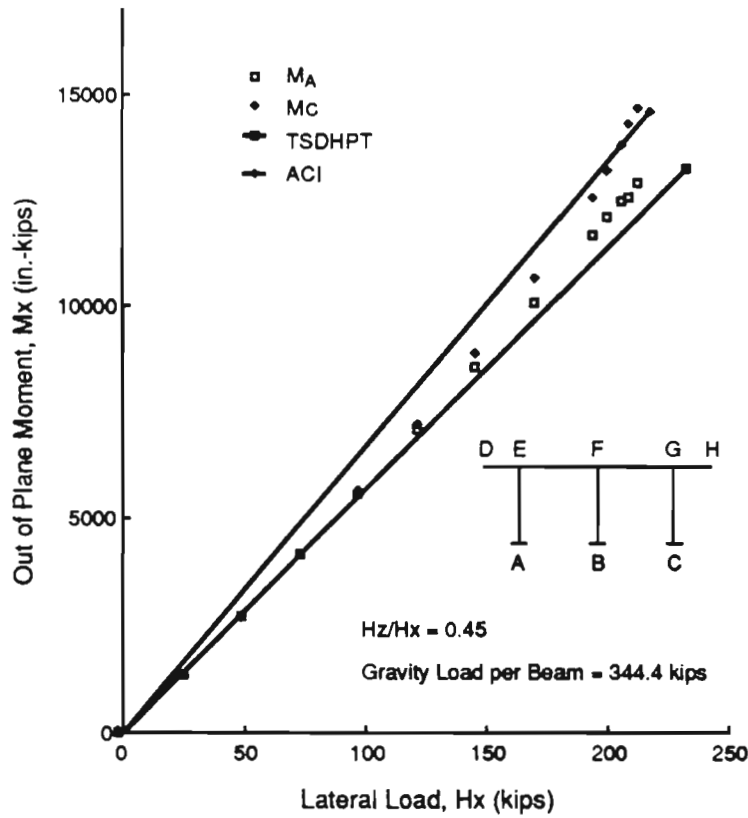


Fig 5.36. Design moments for Bent 1 (load group III).

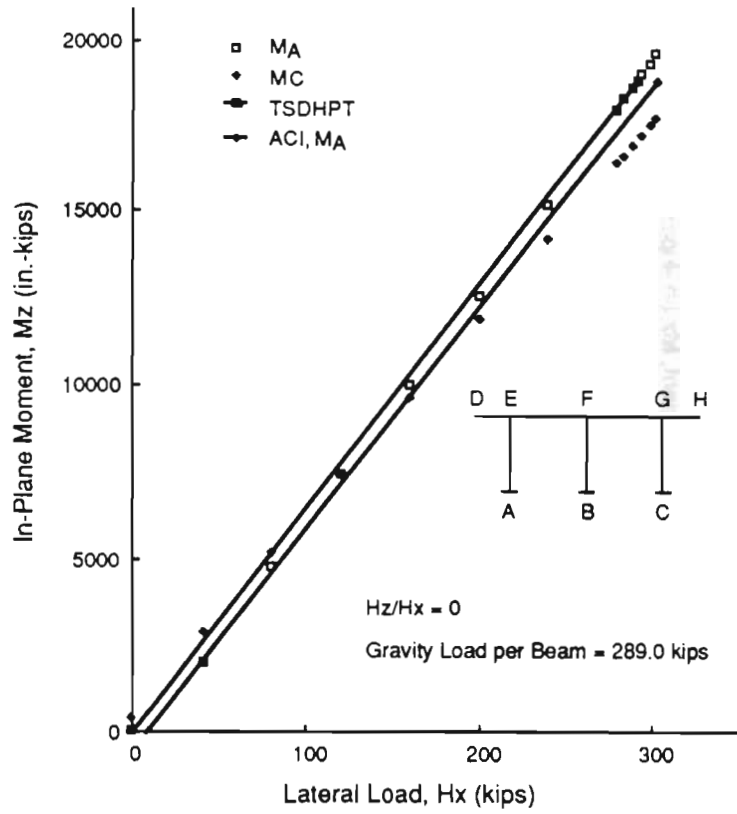


Fig 5.37. Design moments for Bent 2 (load group II).

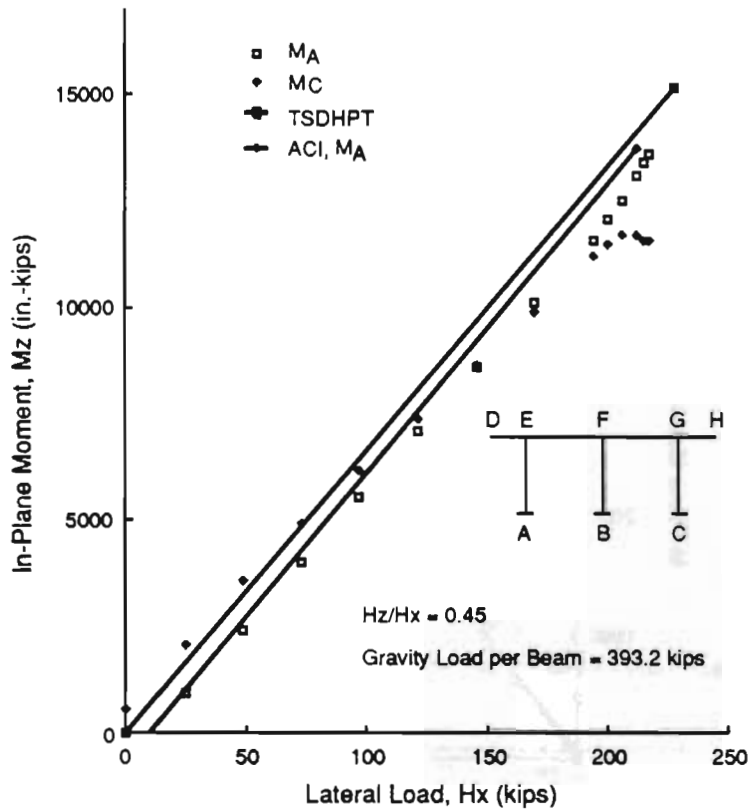


Fig 5.38. Design moments for Bent 2 (load group III).

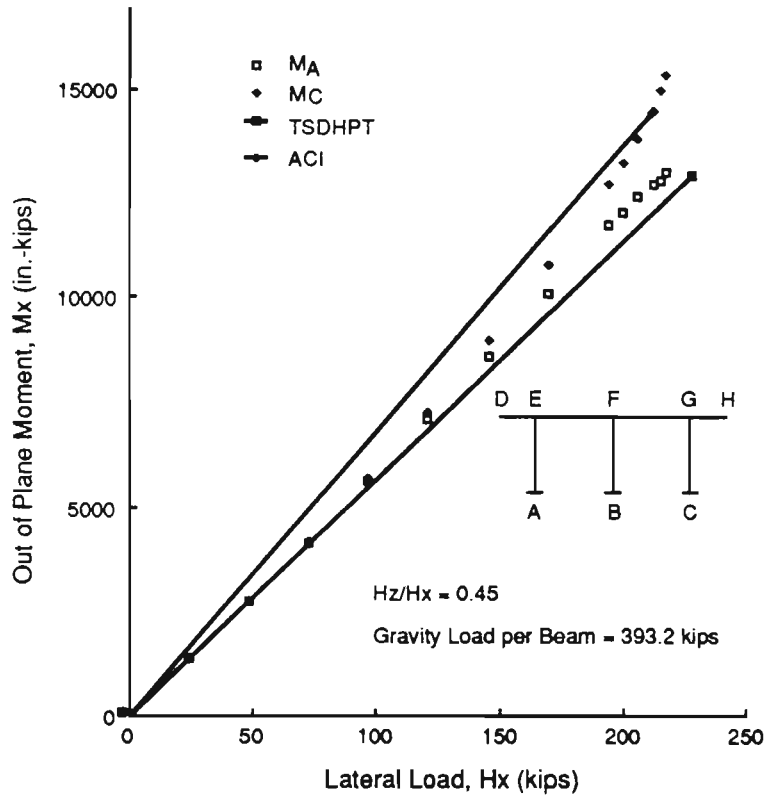


Fig 5.39. Design moments for Bent 2 (load group III).

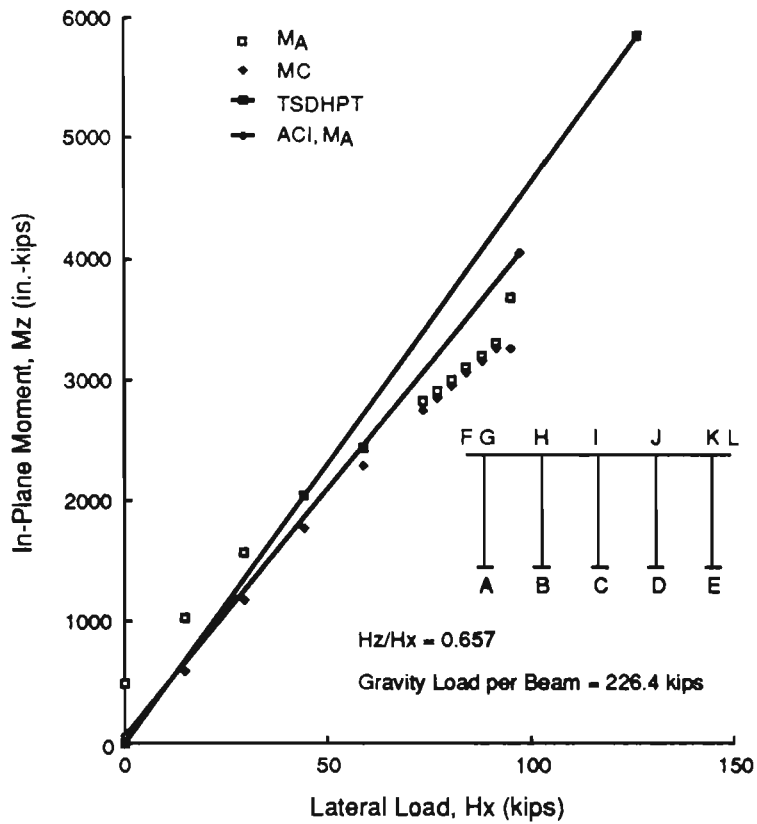


Fig 5.40. Design moments for Bent 3 (load group II).

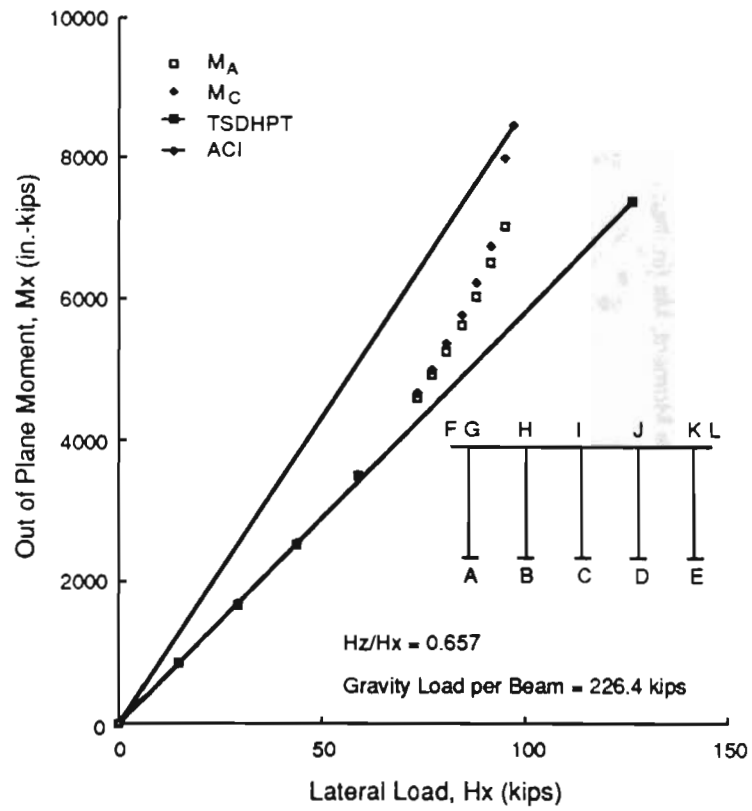


Fig 5.41. Design moments for Bent 3 (load group II).

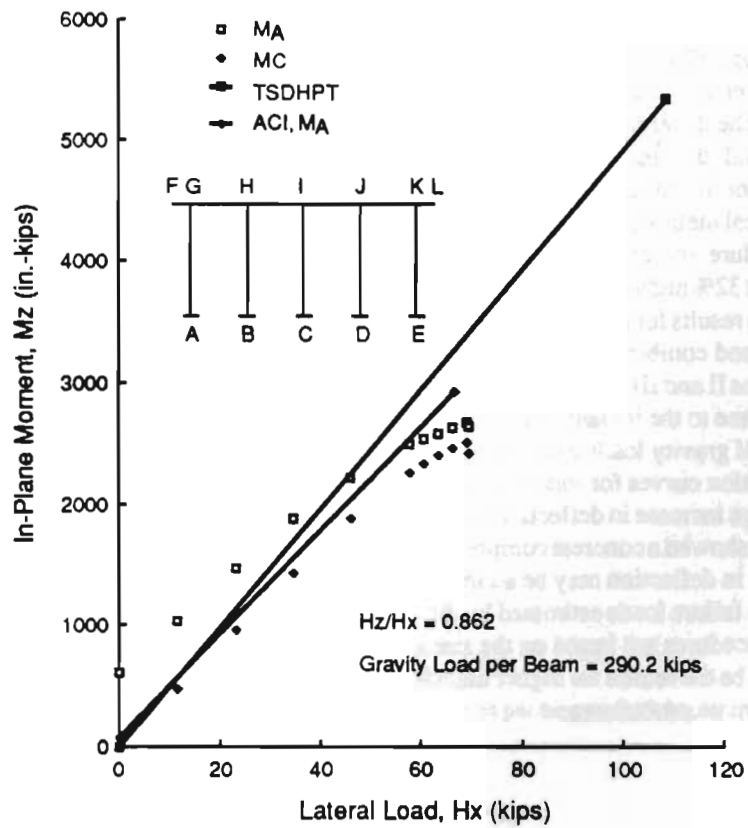


Fig 5.42. Design moments for Bent 3 (load group III).

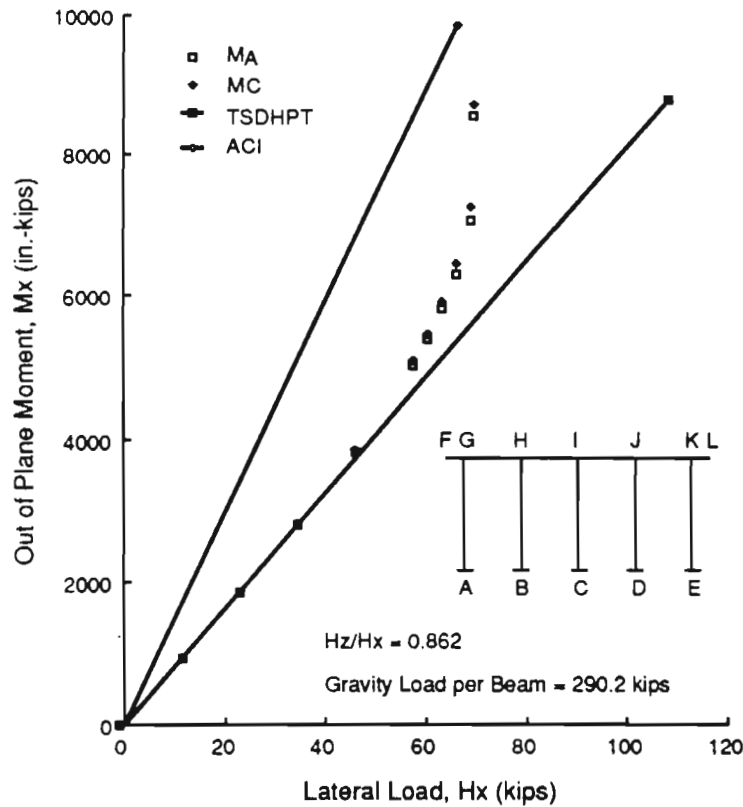


Fig 5.43. Design moments for Bent 3 (load group III).

close agreement up to 50% of the predicted failure load. The ACI method, however, overestimates the results for the out of plane moments. The difference between the results from the ACI method and the analytical procedure becomes smaller near failure of the structure. The failure loads from the ACI and analytical methods are in close agreement. The approximate procedure indicates a capacity of the bent ($H_x=126$ kips) about 32% higher than the analytical capacity ($H_x=95.2$ kips). The results for group III loads are similar to those obtained for load combination II. The applied forces for load combinations II and III differ mainly in terms of the ratio of the out of plane to the inplane lateral loads (H_z/H_x) and the magnitude of gravity loads over the girders.

The load deflection curves for this bent (Figs 5.23 and 5.24) indicated a large increase in deflection prior to failure. Although the results showed a concrete compression failure, this sudden increase in deflection may be an indication of a stability failure. The failure loads estimated by the ACI and the approximate procedures are based on the strength consideration. This may be the reason for higher ultimate lateral loads of the approximate procedures.

5.5.3.4 Bent 4

The slenderness ratio of this bent is 68, larger than those of the other four bents. The results for group II loads obtained from the three analysis procedures are shown in Fig 5.44. In this case, the inplane moments from the ACI method agree reasonably well with the analytical moments. For a specified lateral load, the approximate procedure of TSDHPT estimates higher inplane moments than those obtained from the nonlinear analysis. The ultimate loads from the ACI method and the analytical procedure are the same. The approximate procedure indicates a capacity of the bent smaller than the nonlinear analysis predictions.

Figures 5.45 and 5.46 show the variation of the moments for group III loads. The ACI method indicated instability of the system, as the applied gravity load on columns is greater than the column critical buckling load (out of plane direction). It may be seen that the inplane moments are reduced near the failure of the structure. This reduction is accompanied by a sudden increase in the out of plane moments. The load-deformation curves (Fig 5.26) showed a sudden increase in deflection indicating instability

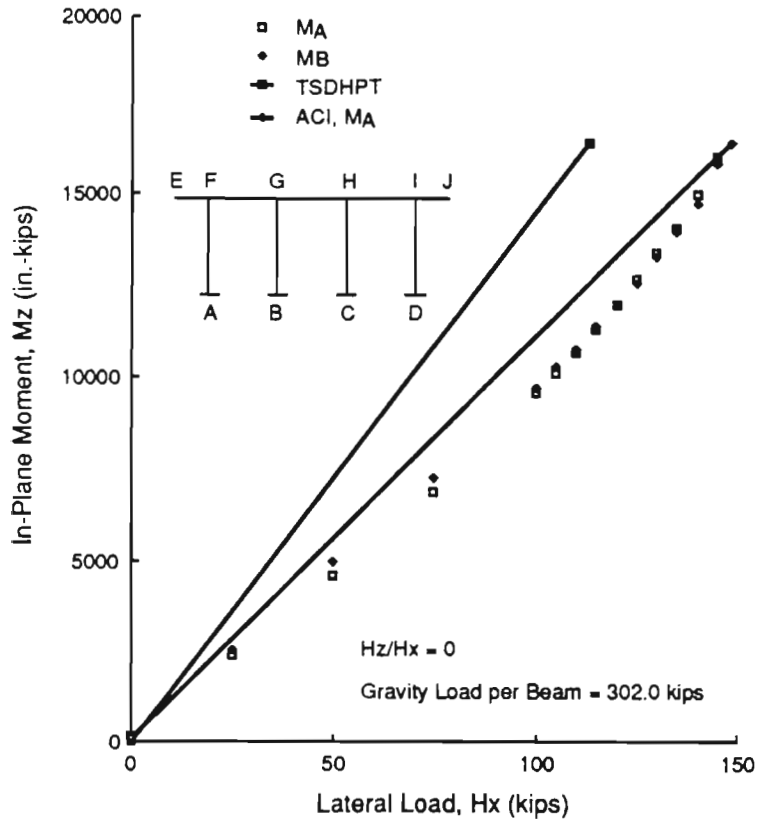


Fig 5.44. Design moments for Bent 4 (load group II).

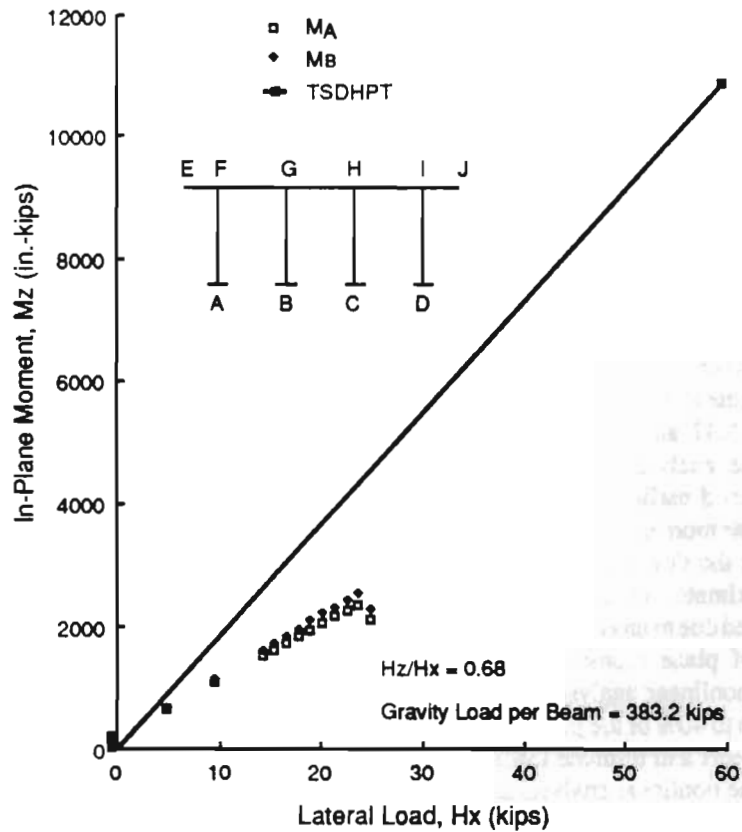


Fig 5.45. Design moments for Bent 4 (load group III).

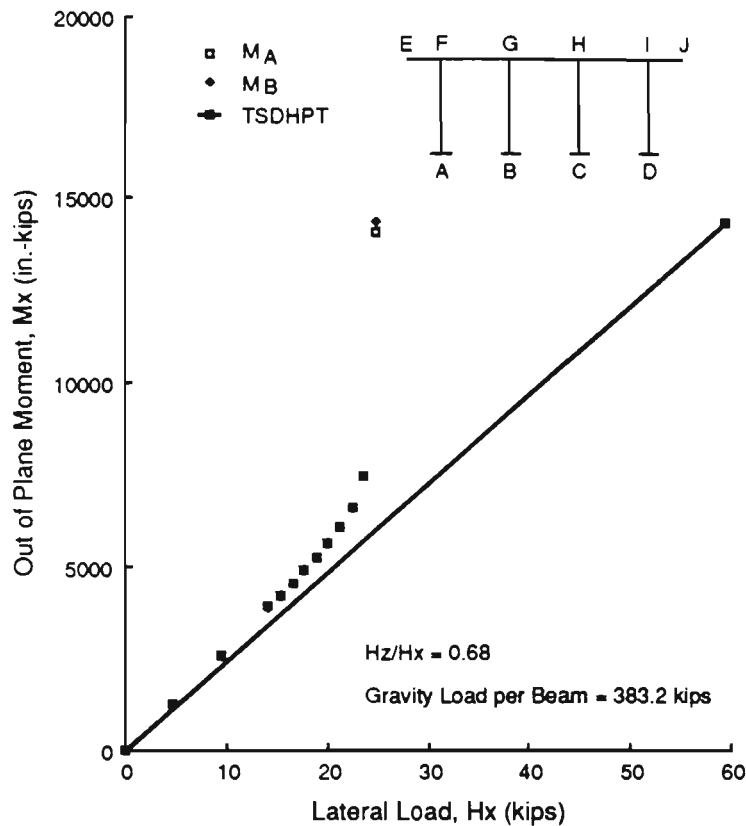


Fig 5.46. Design moments for Bent 4 (load group III).

failure. The approximate procedure overestimates the in-plane moments and underestimates the out of plane moments compared with the analytical values. The failure load predicted by the approximate procedure ($H_x=59.6$ kips) is more than twice the analytical prediction ($H_x=24.9$ kips). This may again be attributed to the higher column slenderness and instability failure mode.

5.5.3.5 Bent 5

The bent consists of girders positioned unsymmetrically over the bent cap. The slenderness ratio of the bent columns is 44.8 and the skew angle is 14 degrees. The results for this bent are presented in Figs 5.47 through 5.50. For group II loads (Figs 5.47 and 5.48), the ultimate loads predicted by the three analysis procedures are in good agreement. As mentioned earlier, the approximate procedure neglects the inplane moments due to gravity loads. This may be the reason for the deviations between the inplane moments of the approximate and the analytical procedures. The effect is pronounced due to unsymmetrical arrangement of girders. The out of plane moments predicted by the approximate and the nonlinear analysis procedures are in excellent agreement up to 40% of the predicted failure load.

The inplane moments and ultimate loads predicted by the ACI method and the nonlinear analysis are within 10% for load combination III. The ACI method overestimates the

analytical results for the out of plane moments. The predictions of the approximate procedure are similar to the results for group II loads. The ultimate load predicted by the approximate procedure ($H_x=105$ kips) is approximately 40% higher than the analytical predictions ($H_x=74.8$ kips). It may be noted that the structure failed due to crushing of concrete in the beam EF (Fig 5.49). From the variation of the out of plane moments, it is seen that the column was also on the verge of failure.

5.5.4 Effect of Slenderness Ratio of Bent Columns

In the previous section, the results for five bents were presented. These bents had different geometrical properties, layout and slenderness ratios. The objective of this section is to investigate the effect of slenderness ratio on the predicted behavior. Bent 2 of the previous section (Fig 5.3) was analyzed with slenderness ratios of 40, 60 and 80. This was achieved by varying the length of the columns. The gravity load per beam was taken as 450 kips. A ratio of the out of plane lateral loads to inplane horizontal loads of 0.75 was assumed. The results from the nonlinear analysis and the TSDHPT approximate procedures are discussed below.

5.5.4.1 Bents under Uniaxial Bending: The load-deflection behavior of the bent for slenderness ratios of 40, 60 and 80 are shown in Fig 5.51. As expected, the lateral deflections

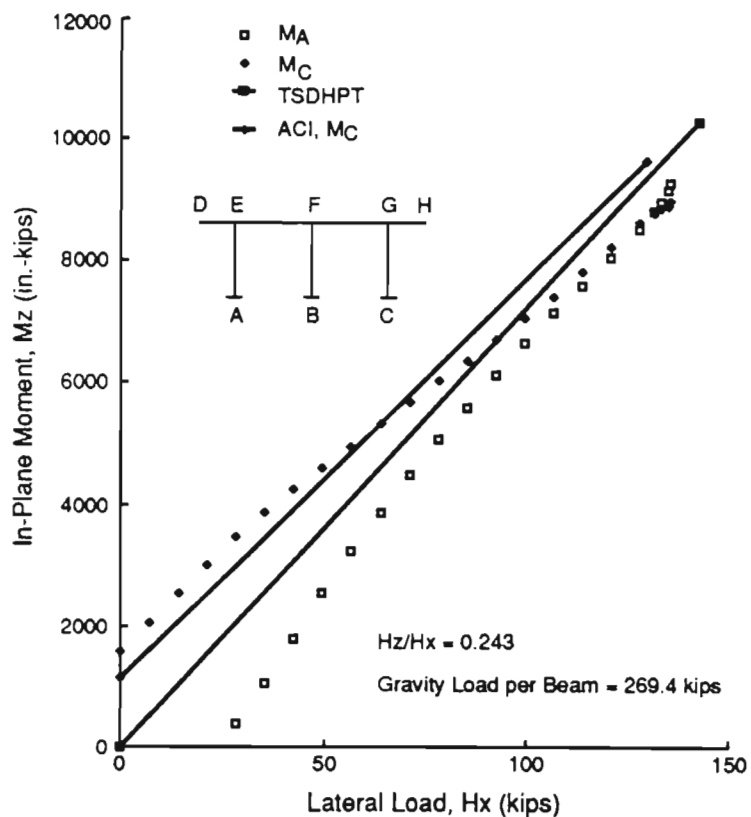


Fig 5.47. Design moments for Bent 5 (load group II).

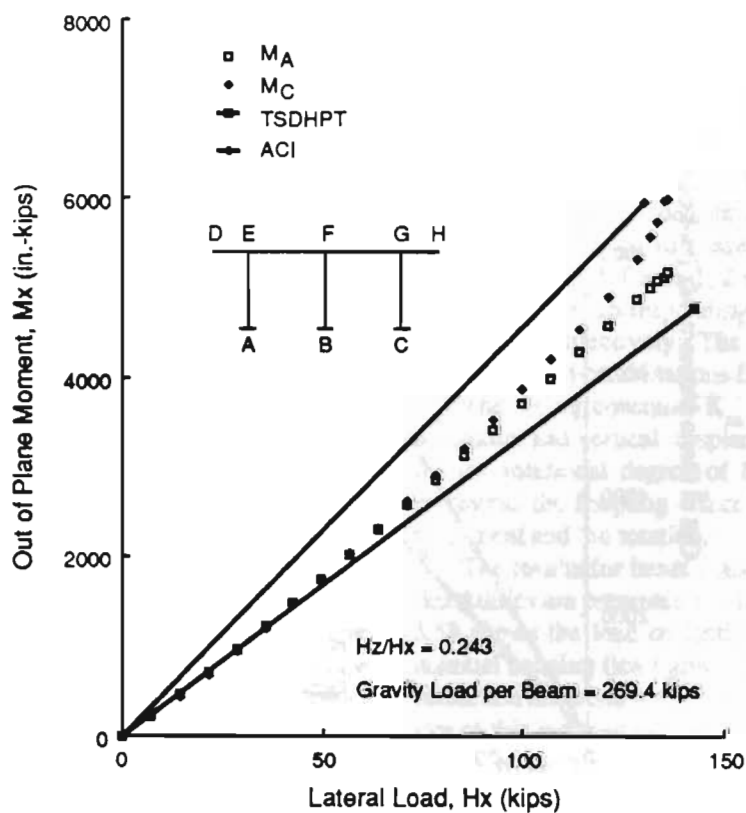


Fig 5.48. Design moments for Bent 5 (load group II).

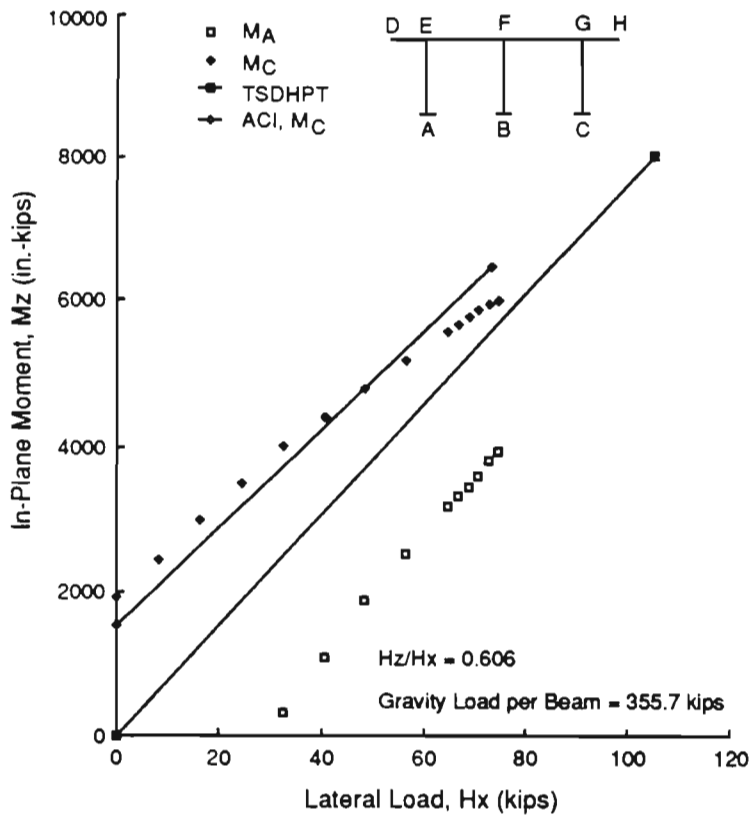


Fig 5.49. Design moments for Bent 5 (load group III).

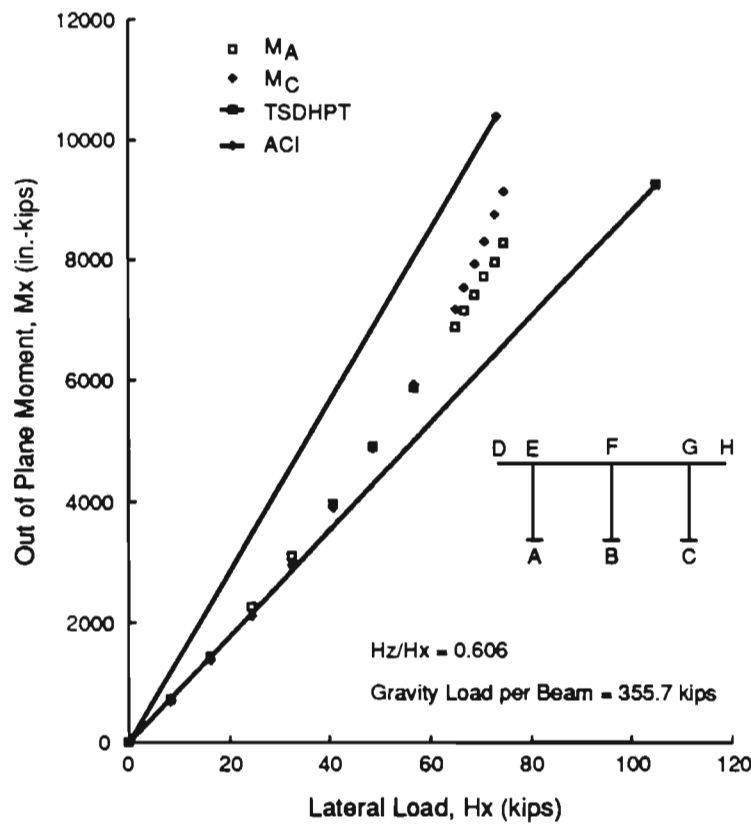


Fig 5.50. Design moments for Bent 5 (load group III).

for a prescribed lateral load increase with the increase in the column slenderness. The ultimate lateral loads predicted by the nonlinear analysis procedure are 283.2, 169.6 and 103.9 kips for L/r ratios of 40, 60 and 80 respectively. For slenderness ratio of 40, the structure failed due to crushing of concrete in column AE. For L/r ratios of 60 and 80, the compression mode of failure was observed in the beam EF.

The moments predicted by the analysis and the TSDHPT approximate procedures are shown in Fig 5.52. For low slenderness ratios (up to 40 or 50), the results from the approximate procedure are in excellent agreement with the analytical predictions. For the range of slenderness values investigated, the ultimate lateral loads predicted by the two analysis procedures are in close agreement. The approximate method, however, is conservative in estimating the moments in the higher slenderness range. This is mainly due to the effect of relative flexural stiffnesses of beams and columns on the inplane moments. (the approximate procedure assumes the column effective length factor of 1.25 irrespective of the relative sizes of beams and columns).

5.5.4.2 Bents under Biaxial Loads: Figures 5.53 through 5.55 represent the load deformation curves for bents under biaxial loads. The horizontal displacements are plotted against the inplane lateral loads. The crushing of concrete in column CG was observed at failure for the slenderness ratio of 40. The bents with slenderness ratios of 60 and 80 indicated instability failure.

The variation of moments with the lateral loads are shown in Figs 5.56 through 5.58. For slenderness ratio of 40 (Fig 5.56), the inplane moments estimated by the approximate procedure are within 10% of the analytical results. The out of plane moments calculated by the TSDHPT approximate procedure are in very good agreement with the analytical values up to 50% of the predicted failure load. The approximate procedure underestimates the analytical moments in the higher load range. The ultimate lateral loads from the approximate and the nonlinear analysis procedures are 153 and 139.1 kips respectively. The capacity of the bent with L/r ratio of 60, estimated by the approximate procedure is 90.8 kips which is about twice the predicted capacity (48 kips). The ratio of the ultimate lateral loads from the nonlinear analysis and the approximate procedures (16.4 and 56.2 kips) is 3.4 for the bent with slenderness ratio of 80.

For the range of variables investigated, the inplane moments from the approximate procedure are generally in good agreement with the analytical predictions, except for low values of the loads where moments due to gravity loads are dominant. The approximate procedure underestimates the out of plane moments for slender bents. From the above results, it may be concluded that the approximate procedure is reasonable for low values of slenderness ratios (less than 40). For slender bents (L/r greater than 60), the approximate procedure is unconservative in predicting the moments and failure loads for bents subjected to biaxial loads. For uniaxial bending, the results from the approximate procedure are

always conservative compared with the ACI method and the nonlinear analysis results. The ACI method is very conservative, for slender bents under biaxial bending.

5.5.5 Effect of Foundation Flexibility

As mentioned earlier, the TSDHPT approximate procedure uses an increased column length (depth to fixity) to account for the degree of fixity at the foundation level. The results of this section, from the nonlinear analysis, are based on the actual column lengths. The effect of foundation is incorporated in terms of appropriate spring stiffnesses. The plans of typical Texas highway bridges indicated prevalent use of pile foundations. In many cases, a single pile is used for each bent column. The equivalent spring stiffnesses for a single pile, for various ratios of elastic modulus of pile to that of the soil (E_p/E_s), have been presented by several authors [5,6,22]. A critical review of various results is given by Sanchez-Salinero and Roesset [27]. The spring constants of Poulos [26] are considered in this study. The soil modulus (E_s) depends upon the shear wave velocity which in turn is a function of soil properties. It is realized that the exact determination of the shear wave velocity is a formidable task. The use of a shear wave velocity as 50 times the number of blow counts has been suggested [28]. The ratio E_p/E_s under normal soil conditions, typically lies in the range of 200 to 400.

The objective of this part of the study is to investigate the bent behavior under varying foundation stiffnesses in order to determine the soil-structure interaction effects. The results are then compared with the previous values where the bents were analyzed with fixed base but increased column length. In this research, spring stiffnesses corresponding to E_p/E_s ratios of 100, 500 and 1000 are used. The higher E_p/E_s ratio indicates softer soil.

Bents 1 and 4 (Figs 1 and 7) were analyzed with actual column lengths and added spring stiffnesses at the foundation level. The spring stiffnesses for these bents are summarized in Table 5.3. Cases 1, 2 and 3 are designated for the spring constants corresponding to E_p/E_s ratios of 100, 500 and 1000 respectively. The bents were analyzed for AASHTO load combinations II and III (Table 5.1)

The spring constants K_{xx} and K_{yy} correspond to the horizontal and vertical displacements respectively. $K_{\phi\phi}$ is for the rotational degree of freedom. The constant $K_{x\phi}$ represents the coupling effect between the horizontal displacement and the rotation.

The results for bents 1 and 4 with various foundation flexibilities are presented in Figs 5.59 through 5.70. Figure 5.59 shows the load deflection behavior of bent 1 under uniaxial bending (load group II). For a specified load, the deflection increases with the increase in the E_p/E_s ratio. The rate of this increase becomes larger for higher E_p/E_s ratio. However, there is no significant difference (less than 10%) between moment values (Fig 5.60) for the three foundation flexibilities investigated. The maximum difference in

ultimate loads is less than 10% (Table 5.4). When the bent is subjected to biaxial loading, the trend of results (Figs 5.61 through 5.64) is somewhat similar to that for the uniaxial bending case.

Figure 5.65 shows the variation of the inplane horizontal deflection with the inplane lateral loads for bent 4 under uniaxial bending (load combination II). The deflection values for three cases of foundation flexibilities indicate a similar trend as observed for bent 1. The variation of inplane moments (Fig 5.66) indicates no difference in moment values for the three cases, except near failure of the structure. The difference between the ultimate loads for the three foundation flexibilities are within 10% (Table 5.4). When bent 4 is subjected to group III loads, a substantial reduction in ultimate loads is observed with the increase in E_p/E_s ratio. The ratio of the ultimate lateral loads (Table 5.4) for cases 1 and 3 is 1.65. The load-deflection curves and the variation of the inplane and out of plane moments are presented in Figs 5.65 through 5.68. It may be noted that bent 4 experienced a large deflection before failure indicating an instability of the system. This may be one of the reasons for the drastic reduction in ultimate loads.

The previous two paragraphs summarized the results for bents 1 and 4 for three cases of foundation flexibilities. As stated earlier, the approximate procedure of the TSDHPT uses an increased column length to simulate the foundation conditions. This so called "depth to fixity" varies from 4 to 10 feet depending upon soil properties and engineering judgment. The ultimate load predicted for bents 1 and 4 for various foundation flexibilities are shown in Table 5.4. The results for these bents obtained earlier are also included. Earlier analyses were based on an increased column length and fixed base. For bent 4 under biaxial bending, the values corresponding to E_p/E_s ratio of 1000 show the best agreement. It is observed that the bents with foundation springs generally show higher capacity and less deflections than their counterparts where the analysis is based on the increased column length. From these results, it may be concluded that the current approach of accounting for the foundation conditions by increasing the column length yields conservative results.

5.6 SUMMARY

The bent column design forces and moments computed using the TSDPHT approximate procedure and the linear frame analysis were presented in section 5.4. It was found that the approximate procedure estimates reasonably well the column axial forces and underestimates the moments (bent 1 through 4) when the live loads are distributed evenly between the beams. In one column of bent 5, the moments predicted by the approximate procedure were comparable with the moments from the linear frame analysis. The corresponding axial force in that column predicted by the

approximate procedure (load group II and III) was about half of the linear analysis value. However, in another column of bent 5, the axial load and moment were underestimated by the approximate procedure. The approximate procedure generally underestimates column axial forces and estimates moments reasonably well when the variation in the live load position is considered.

The implications of the above results depend upon the criteria governing the design of bent columns. If the design is controlled by the axial strength of concrete then the high axial load and minimum moment constitute critical design forces. For this situation, the approximate procedure underestimates the design axial forces (group I loads) when the variation in live load positions is considered. For group II and III loads, the higher moments and low axial loads predicted by the approximate procedure are conservative. An unconservative design situation (in the approximate procedure) was observed in a column of bent 5, where the moments from the two procedures were the same but the axial force from the approximate procedure was almost 50% of the linear frame analysis value. The results indicated that varying the live load positions on the deck has no significant influence compared with the live loads distributed equally between the beams for group III loads.

The results from the nonlinear analyses were compared with the values calculated by the ACI moment magnifier method and the TSDHPT approximate procedure (section 5.5). The load-deflection curves for various bents indicated higher out of plane deflections than the inplane deflections. This was explained in terms of cantilever action in the out of plane direction and the relative magnitude of lateral loads. The column axial forces (due to gravity loads on beams) calculated using the approximate procedure and the nonlinear analysis were in good agreement for bents 1 through 4. For bent 5, the nonlinear analysis showed scattering in column axial forces compared with the approximate analysis.

For bents under uniaxial bending (due to inplane lateral loads), inplane moments predicted by the three analysis procedures were generally in good agreement. For low lateral loads, the inplane moments from the approximate procedure show some deviations from the nonlinear analysis results. This discrepancy appeared as the approximate procedure neglects the effect of gravity loads on the inplane moments. The deviations in predicted moments were substantial for bent 5 in which the girders were arranged unsymmetrically over the bent cap.

For bents under biaxial lateral loads, the inplane moments calculated by the ACI method were in good agreement with the analytical moments. The ACI method overestimates the out of plane moments. The difference between the two results for out of plane moments become smaller near failure. The ultimate loads estimated by the ACI method

agree very well with the analytical predictions except for bent 4. For bent 4, the ACI approach was very conservative in predicting the failure load.

The results from the nonlinear analysis and the approximate procedure indicated a good agreement for inplane moments. The out of plane moments from the two analysis procedures, for low to moderate slenderness ratios (less than 45), were in excellent agreement up to 50% of the predicted failure loads. For high lateral loads, the approximate procedure underestimates the analytical out of plane moments. For slender bents (L/r greater than 60), the out of plane moments computed by the approximate procedure were smaller than those obtained from nonlinear analysis. The difference between the ultimate loads predicted by the approximate procedure and the nonlinear analysis were less than 20% for bents with slenderness ratio less than 45. For slender bents, the approximate procedure is unconservative in estimating the failure loads. It was found that the approximate procedure reasonably estimates moments (both inplane and out of plane) in bents with the column slenderness ratios (L/r) less than 40.

The effect of foundation flexibility on the overall bent behavior was presented in section 5.5.5. The load deflection curves indicated a higher rate of increase in deflection for

higher ratios of elastic moduli of pile and soil (E_p/E_s). The difference between inplane moments for the three foundation flexibilities was less than 10%. For bent 1, the predicted out of plane moments for three foundation flexibilities were within 10%. However, bent 4 showed a drastic reduction in the out of plane moments with increasing E_p/E_s ratio. The ultimate lateral loads predicted for three foundation conditions were essentially the same for bent 1 under uniaxial and biaxial bendings (load groups II and III) and bent 4 with inplane loads (load group II). The predicted ultimate load for bent 4 for case 3 ($E_p/E_s=1000$) was 60% of the ultimate load corresponding to E_p/E_s ratio of 100. The results for various foundation conditions were compared with the results where the degree of fixity at the foundation level is approximated by an increased column length and fixed base. For the range of variables investigated, it was concluded that the current approach of simulating the foundation condition is conservative.

TABLE 5.3. EQUIVALENT SPRING STIFFNESS

Bent	Case	K_{xx} (lb/in.)	K_{yy} (lb/in.)	$K_{\phi\phi}$ (in.-lb/rad)	$K_{x\phi}$
1	1	$.369 \cdot 10^7$	$.715 \cdot 10^7$	$.854 \cdot 10^{10}$	$.111 \cdot 10^9$
	2	$.212 \cdot 10^7$	$.406 \cdot 10^7$	$.653 \cdot 10^{10}$	$.711 \cdot 10^8$
	3	$.554 \cdot 10^6$	$.978 \cdot 10^6$	$.451 \cdot 10^{10}$	$.321 \cdot 10^8$
4	1	$.307 \cdot 10^7$	$.594 \cdot 10^7$	$.496 \cdot 10^{10}$	$.773 \cdot 10^8$
	2	$.177 \cdot 10^7$	$.338 \cdot 10^7$	$.379 \cdot 10^{10}$	$.494 \cdot 10^8$
	3	$.503 \cdot 10^6$	$.815 \cdot 10^6$	$.262 \cdot 10^{10}$	$.223 \cdot 10^8$

TABLE 5.4. ULTIMATE LATERAL LOADS FOR BENTS

Bent	Load Group	Case	With Springs (klps)	Without Springs (klps)
1	II	1	341.0	284.5
		2	331.0	
		3	308.7	
	III	1	273.3	212.4
		2	270.7	
		3	254.8	
4	II	1	165.2	145.0
		2	163.5	
		3	153.0	
	III	1	39.1	24.9
		2	34.5	
		3	23.7	

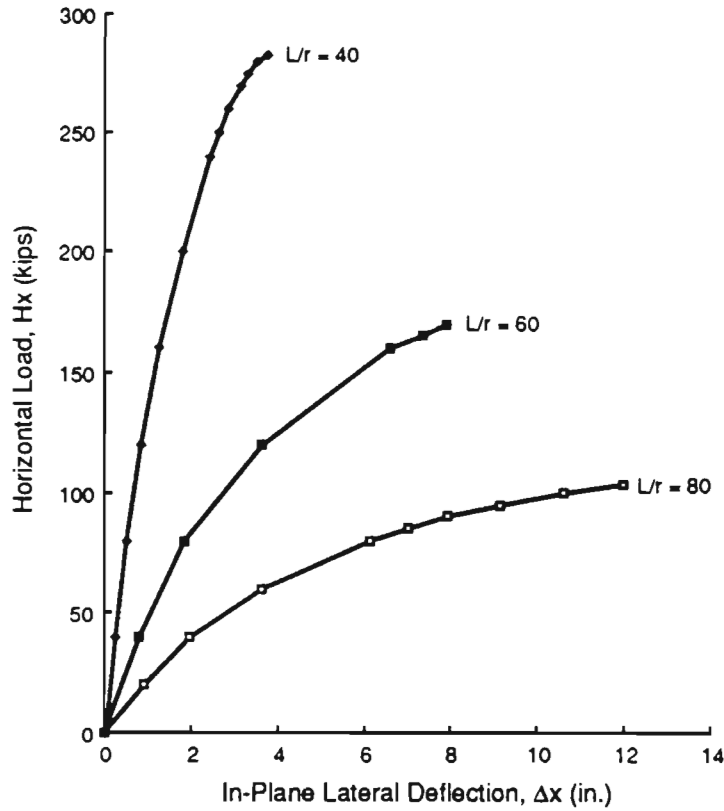


Fig 5.51. Load-deflection curves for Bent 2 with various slenderness ratios (uniaxial bending).

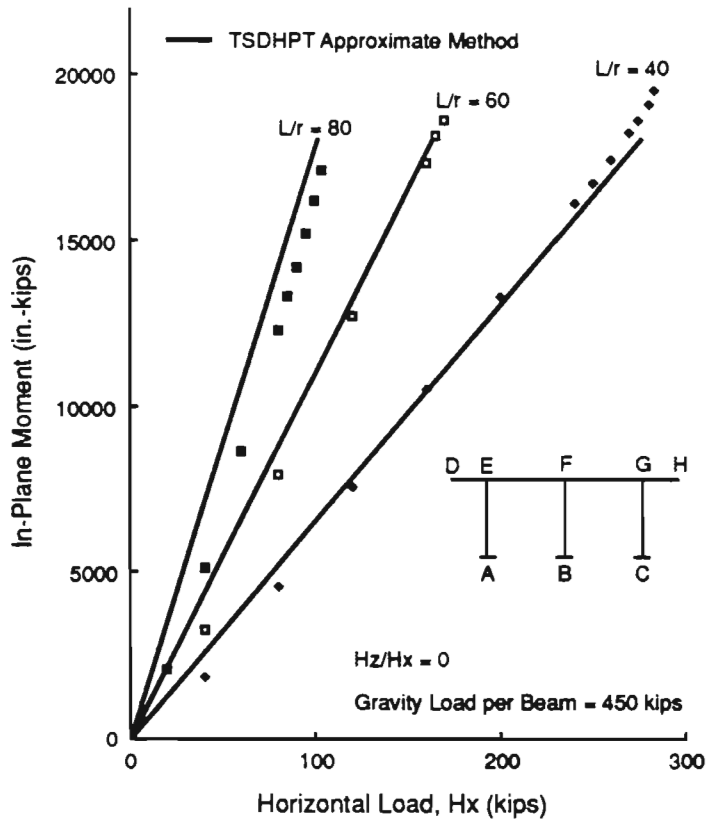


Fig 5.52. Inplane moments for Bent 2 (M_A) with various slenderness ratios (uniaxial bending).

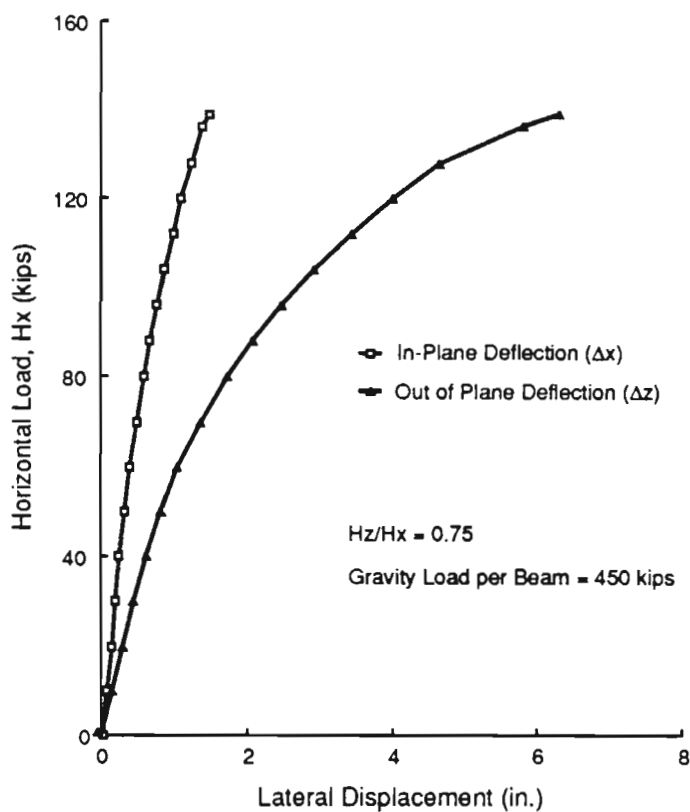


Fig 5.53. Load versus displacement for Bent 2 under biaxial bending ($L/r = 40$).

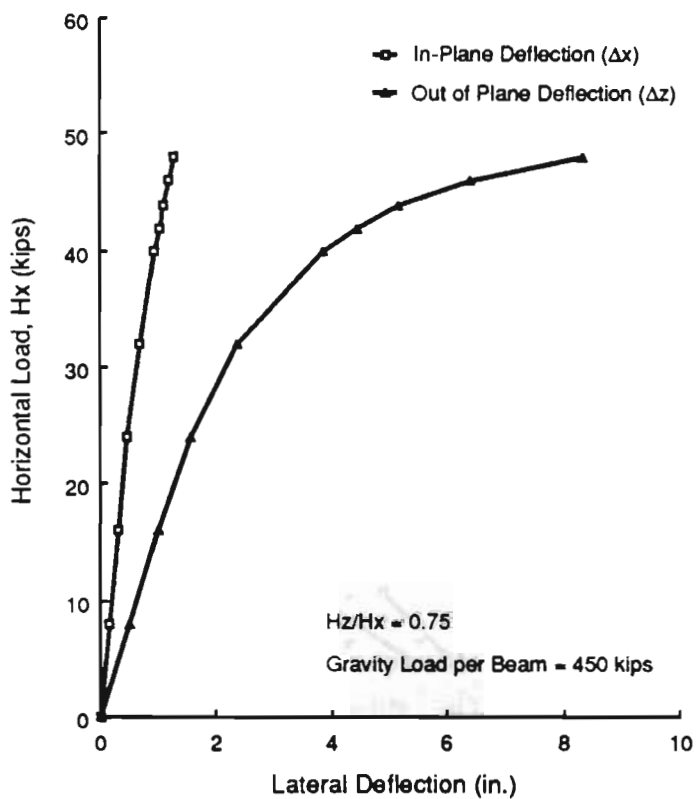


Fig 5.54. Load versus displacement for Bent 2 under biaxial bending ($L/r = 60$).

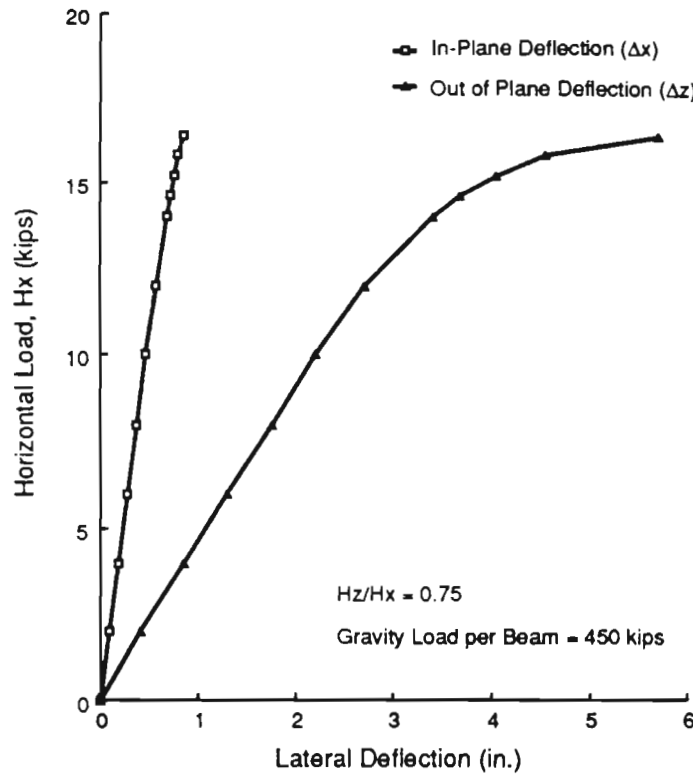


Fig 5.55. Load versus displacement for Bent 2 under biaxial bending ($L/r = 80$).

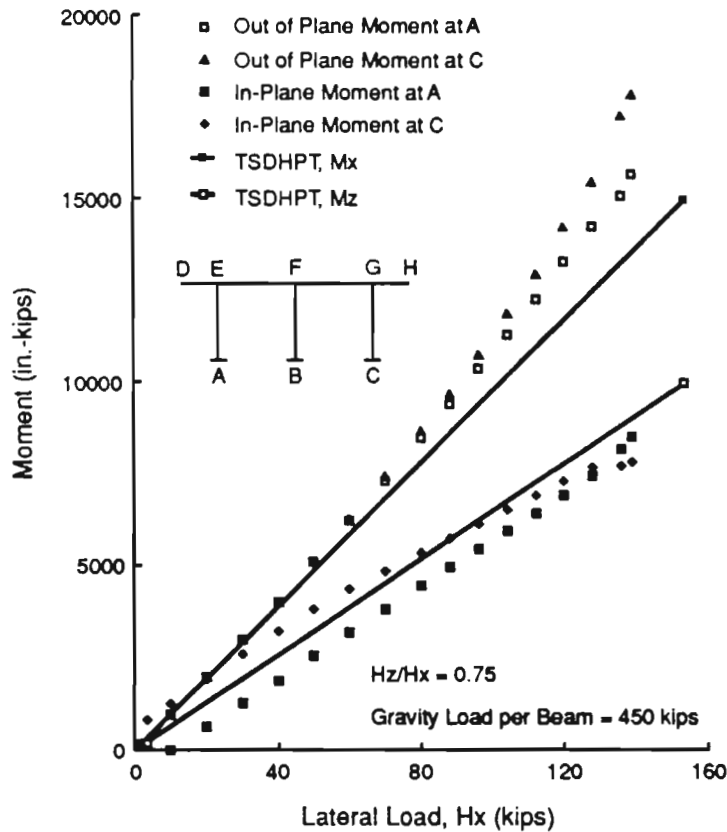


Fig 5.56. Design moments for Bent 2 under biaxial bending ($L/r = 40$).

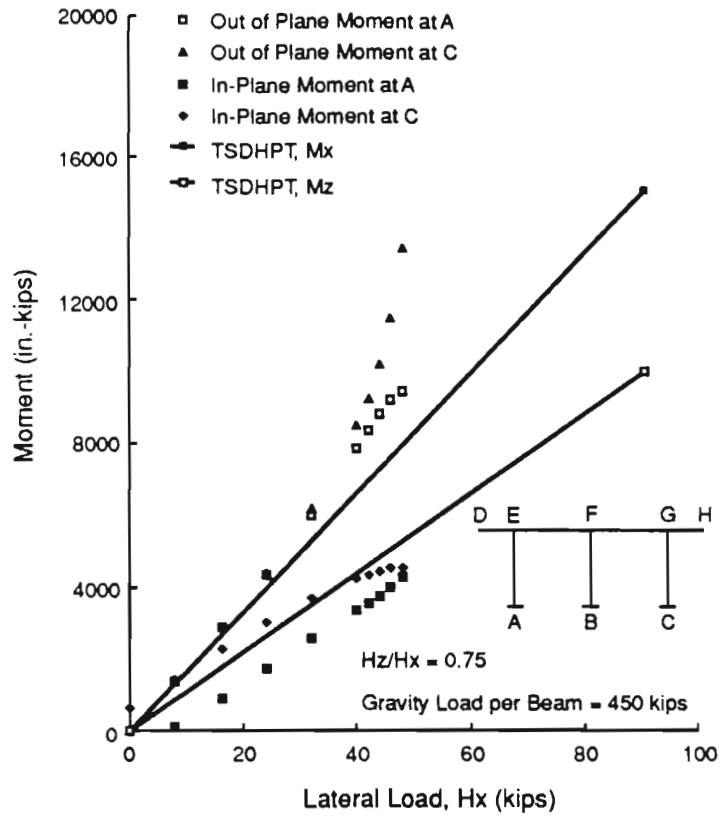


Fig 5.57. Design moments for Bent 2 under biaxial bending ($L/r = 60$).

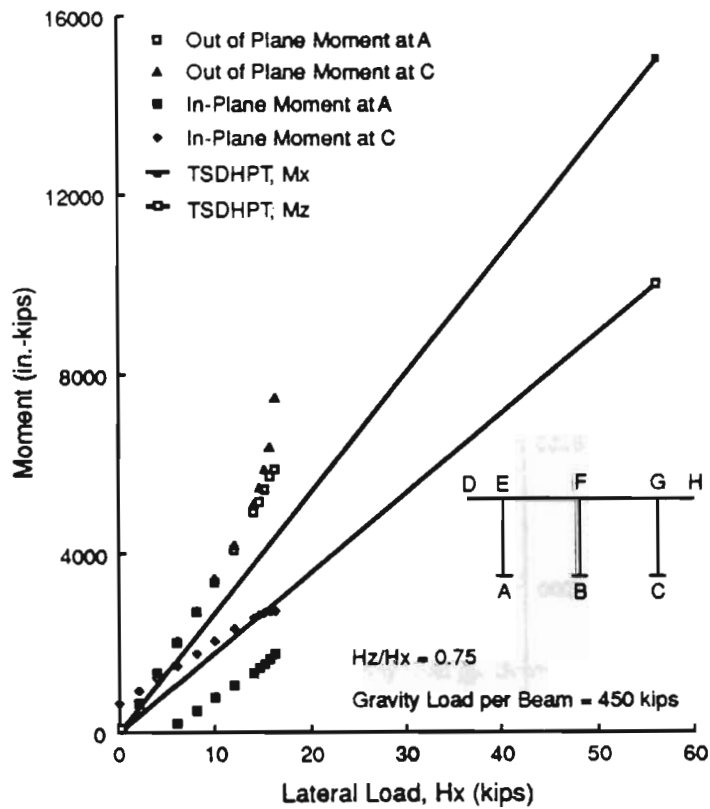


Fig 5.58. Design moments for Bent 2 under biaxial bending ($L/r = 80$).

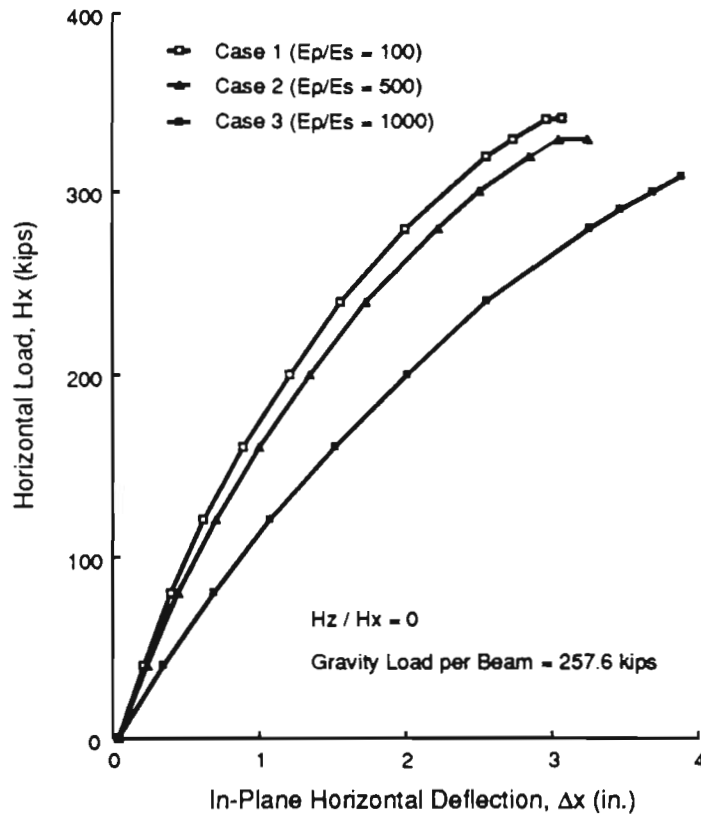


Fig 5.59. Effect of foundation flexibility on lateral deflection (Bent 1 under Group II loads).

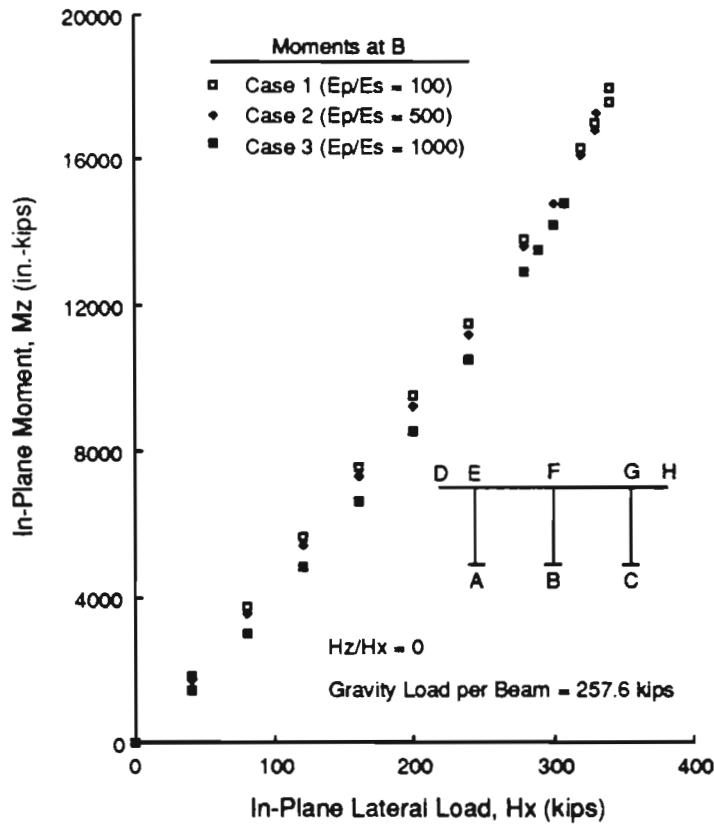


Fig 5.60. Effect of foundation flexibility on design moment (Bent 1 under Group II loads).

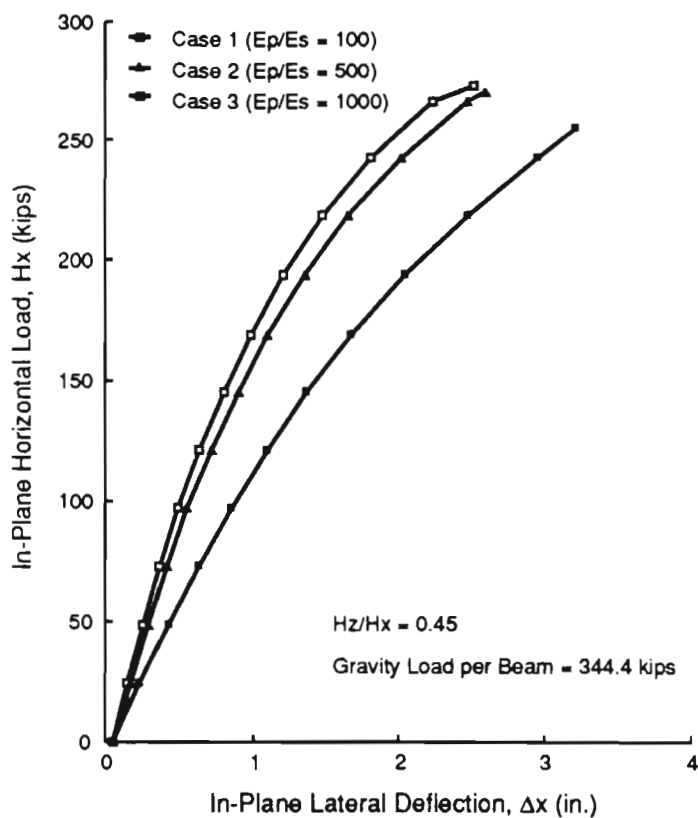


Fig 5.61. Effect of foundation flexibility on inplane deflection (Bent 1 under Group III loads).

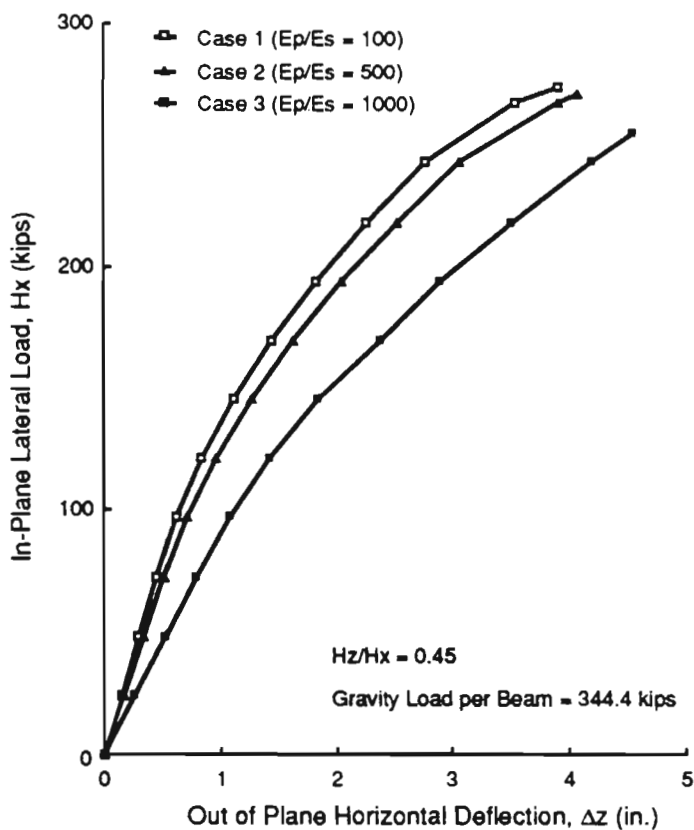


Fig 5.62. Effect of foundation flexibility on out of plane deflection (Bent 1 under Group III loads).

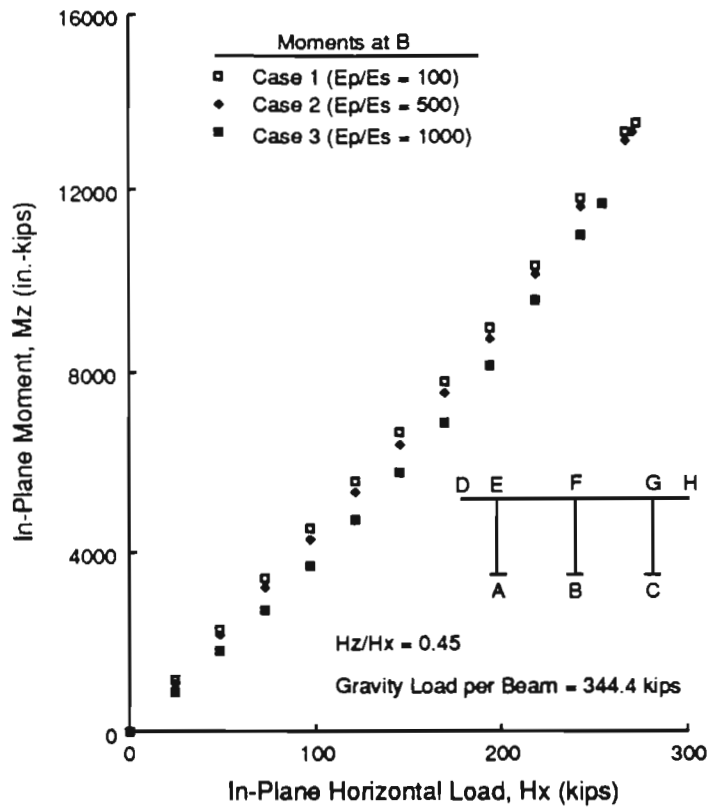


Fig 5.63. Effect of foundation flexibility on inplane moment (Bent 1 under Group III loads).

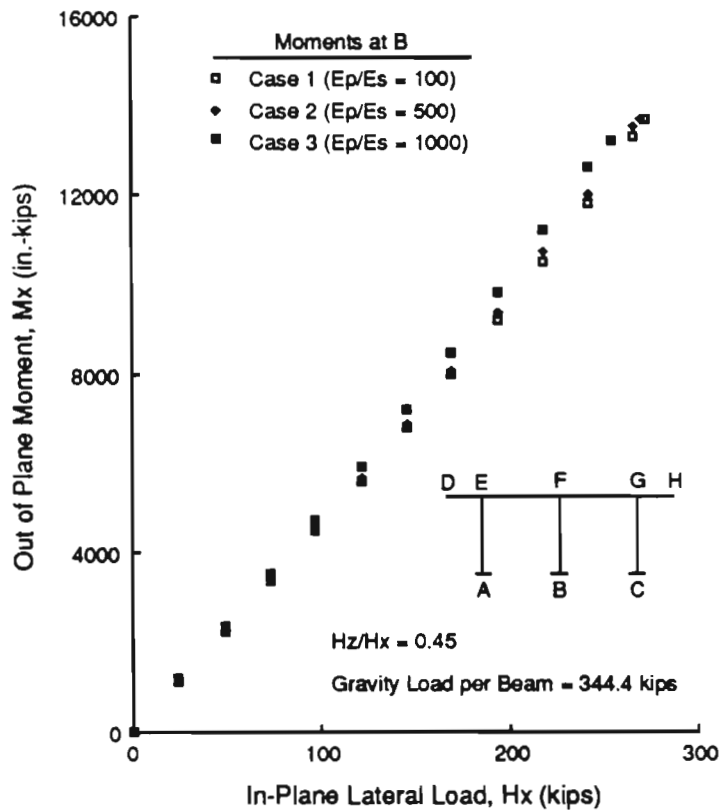


Fig 5.64. Effect of foundation flexibility on out of plane moment (Bent 1 under Group III loads).

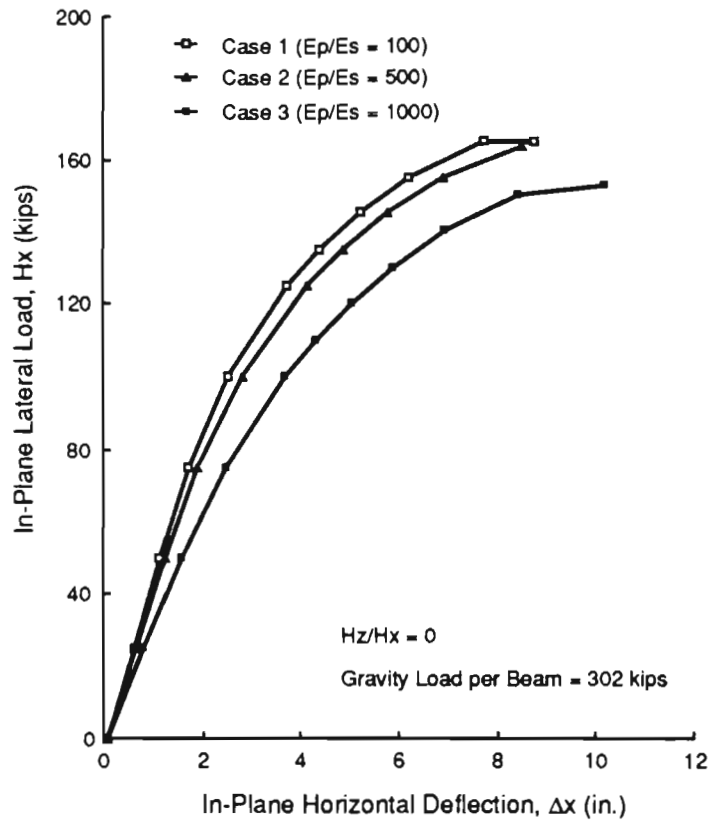


Fig 5.65. Effect of foundation flexibility on lateral deflection (Bent 4 under Group II loads).

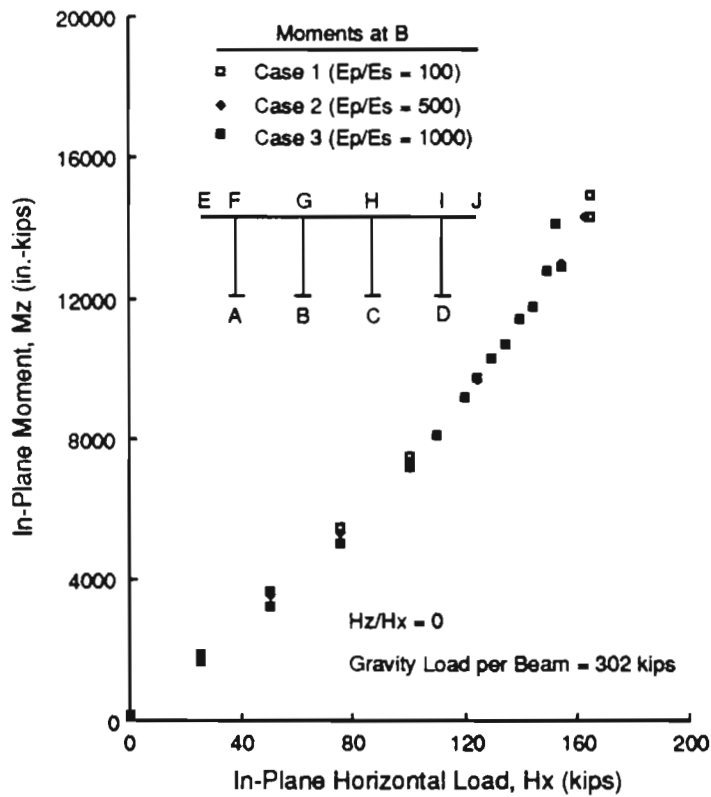


Fig 5.66. Effect of foundation flexibility on design moment (Bent 4 under Group II loads).

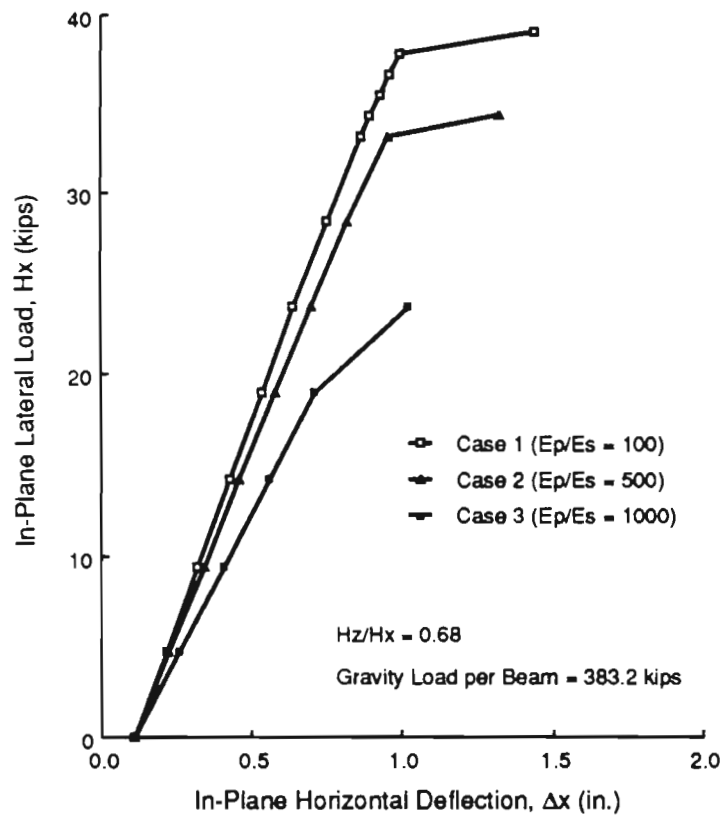


Fig 5.67. Effect of foundation flexibility on inplane deflection (Bent 4 under Group III loads).

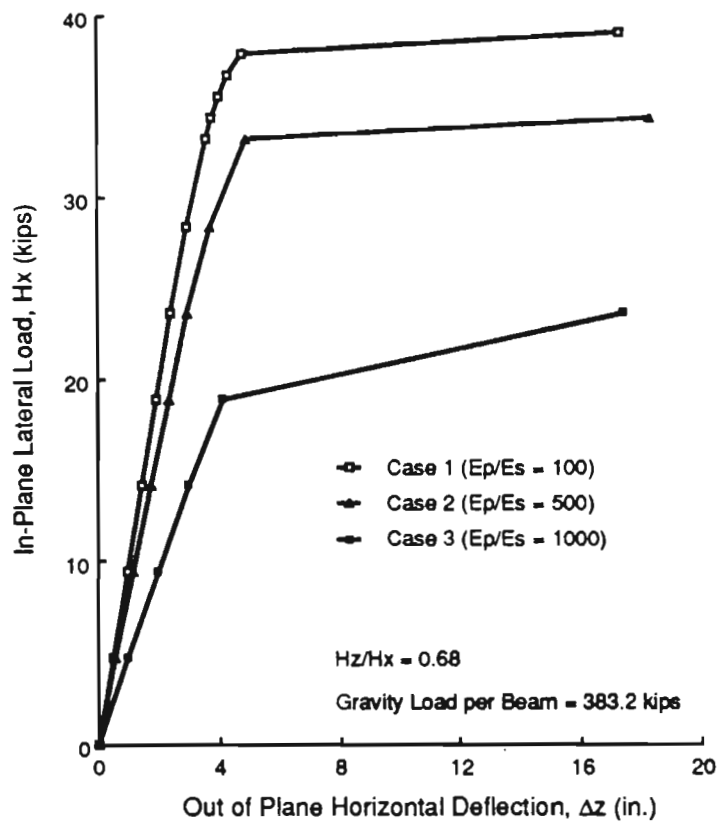


Fig 5.68. Effect of foundation flexibility on out of plane deflection (Bent 4 under Group III loads).

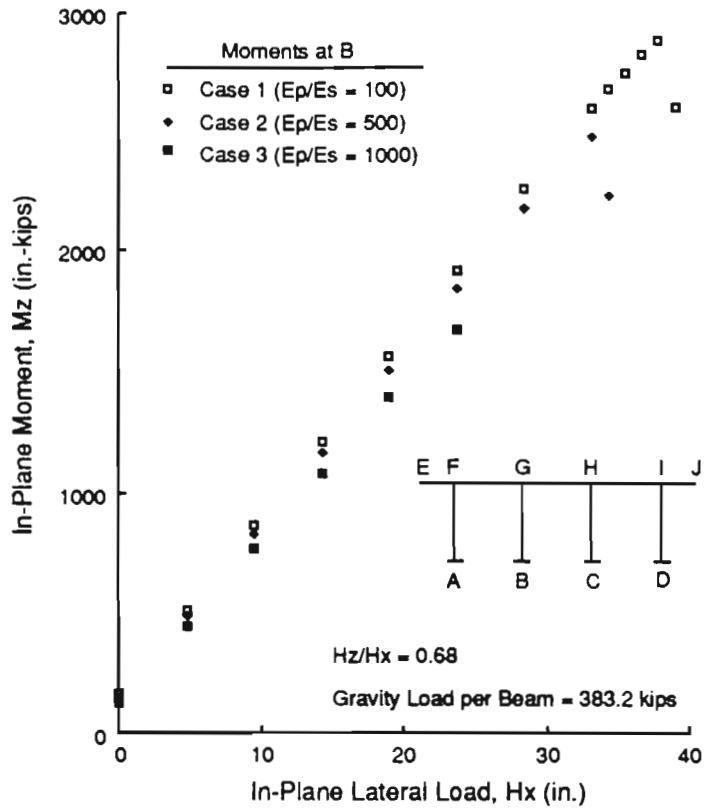


Fig 5.69. Effect of foundation flexibility on inplane moment (Bent 4 under Group III loads).

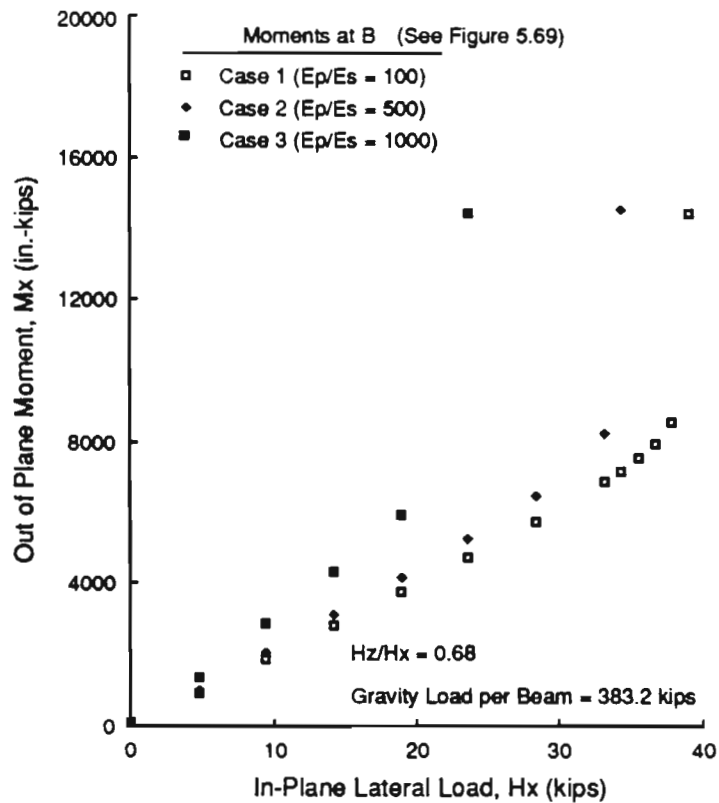


Fig 5.70. Effect of foundation flexibility on out of plane moment (Bent 1 under Group III loads).

CHAPTER 6. CONCLUSIONS AND RECOMMENDATIONS

6.1 SUMMARY OF THE STUDY

The objective of this research was to evaluate the accuracy and suitability of the current office procedure of the Texas State Department of Highways and Public Transportation (TSDHPT) for designing slender bent columns. The study involved developing two computer programs. The linear frame analysis program was developed to evaluate the design forces considering the total gravity load on the bridge divided equally between the girders. The variation in the positions of live loads was also included in the analysis. The moment magnifier method of AASHTO was used to approximate second order effects. The design forces from the linear frame analysis were compared with those obtained from the TSDHPT approximate procedure.

The nonlinear method of analysis, developed in this research, was used to predict the three dimensional behavior of slender reinforced concrete bridge bents. The fiber model and an updated Lagrange finite element formulation were used to model the geometric and material nonlinearities. A variety of problems were solved to determine the accuracy and efficiency of the proposed formulation. The behavior of a number of typical bridge bents was studied. The results from the nonlinear analysis were compared with the predictions of the TSDHPT approximate procedure and the AASHTO moment magnifier method. The sensitivity of the results to column slenderness and foundation flexibilities were evaluated in terms of the predicted bent behavior.

6.2 CONCLUSIONS

6.2.1 *Approximate Procedure vs Linear Frame Analysis*

Comparison of results from the linear frame analysis and the approximate procedure indicated that the current office procedure generally underestimates column axial forces and overestimates associated bending moments in typical highway bridge bents. For AASHTO load combination I, the approximate procedure results in axial forces which are smaller than the real ones. The design of bent columns, in this load group, is governed by high axial load and low bending moment. For group II and III loads, however, the approximate procedure estimates reasonably the design forces for typical bent geometries (bents 1 through 4). As the bent geometry deviates from the typical ones, the uncertainty related to the approximate method increases. In some cases (bent 5), the approximate method estimates unconservative design forces compared with the linear frame analysis values. It was found that varying the position of live loads over the deck does not drastically change the

design forces for load group III although it is a major factor in the discrepancies for load group I.

6.2.2 *Approximate Procedure vs Nonlinear Analysis*

The results from the approximate procedure, the AASHTO moment magnifier method and the nonlinear analysis were compared for slender bents under both uniaxial and biaxial lateral loads. For the range of values investigated, the following conclusions were reached:

(1) For bents under inplane lateral loads (uniaxial bending) and with column slenderness ratios (L/r) less than 50, the moments predicted by the approximate procedure are in good agreement with the analytical values, except for low values of lateral loads (in some cases). This deviation is due to the exclusion of moments developed by gravity loads in the approximate procedure. The failure load predicted by the office procedure was in good agreement with the analytical predictions. For slender bents (say $L/r > 60$), the approximate procedure is conservative in predicting the analytical failure load. The results from the moment magnifier method and nonlinear analysis were in very good agreement for the range of slenderness values investigated.

(2) For bents under biaxial bending, the inplane moments predicted from the nonlinear analysis and approximate procedures were in good agreement except for low values of loads where gravity load moments are dominant. For bents with low to moderate slenderness ratios ($L/r < 40$), the out of plane moments from the approximate procedure and the nonlinear analysis were in excellent agreement up to 50% of the predicted failure load. For higher loads, the approximate procedure underestimates the analytical out of plane moments. The failure loads predicted by the two procedures are within 20%. The inplane moments and failure loads estimated by the AASHTO moment magnifier method were in good agreement with the analytical predictions. The moment magnifier method overestimates the analytical out of plane moments. The difference reduces near the failure of the structure.

(3) For slender bents ($L/r > 60$) under biaxial bending, the approximate procedure overpredicts the analytical ultimate lateral loads. The out of plane moments predicted by the approximate procedure are smaller than the analytical predictions for slender bents. The ACI procedure is very conservative in estimating the failure load for slender bents.

(4) Comparison of results for various foundation flexibilities and the current procedure of assuming fixity depth indicated that the current approach yields conservative results for typical Texas soil conditions.

6.3 RECOMMENDATIONS

For the range of variables examined, it seems appropriate to use the current office procedure for designing typical bridge bent columns of slenderness ratio (L/r) less than 40. For slender bents ($L/r > 60$), the designers are cautioned against the use of the current office procedure. The values of effective length factor need to be critically examined. In the absence of a more sophisticated analysis tool, like the nonlinear analysis program developed in this study, the use of the AASHTO moment magnifier method is recommended although it gives very conservative design values especially for slender bents.

6.3.1 Research Needs

Several research areas in which additional work is needed are:

- Study of multi-story bents under biaxial lateral loads.
- Study of bents with different column cross sections, e.g. hollow shaft, hollow rectangular sections.
- Study of bents with high strength materials.
- Parametric study of heavily loaded slender bents (bridge spans >100 feet).

REFERENCES

1. ACI Committee 318, *Building Code Requirement for Reinforced Concrete (ACI 318-83)*, American Concrete Institute, Detroit, 1983.
2. ACI Committee 318, *Commentary on Building Code Requirement for Reinforced Concrete (ACI 318-83)*, American Concrete Institute, Detroit, 1983.
3. Adams, John, "Nonlinear Behavior of Steel Frames," unpublished Ph. D. dissertation, Massachusetts Institute of Technology, 1973.
4. American Association of State Highway and Transportation Officials, *Standard Specifications for Highway Bridges*, 12th Edition, 1977.
5. Blaney, G. W., Kausel, E., and Roesset, J. M., "Dynamic Stiffness of Piles," *Proceedings, 2nd Intl. Conf. Num. Meth. Geomechanics*, ASCE, pp 1001-1012.
6. Breen, J. E., MacGregor, J. S., and Pfrang, E. O., "Determination of Effective Length Factor for Slender Concrete Columns," *ACI Journal*, Vol 69, No. 11, November 1972, pp 669-672.
7. Chen, W. F., and Atsuta, T., *Theory of Beam-Columns*, Vol 2, McGraw-Hill, 1977.
8. Clough, R. W., and Penzien, J., *Dynamics of Structures*, McGraw-Hill, 1975.
9. Cook, R. D., *Concepts and Applications of Finite Element Analysis*, John Wiley & Sons, Inc., 1974.
10. Diaz, M. A., "Evaluation of Approximate Slenderness Procedures for Nonlinear Analysis of Concrete and Steel Frames," Ph.D. Dissertation, The University of Texas at Austin, December 1984.
11. Ernst, C., Smith, M., Riveland, R., and Pierce, N., "Basic Reinforced Concrete Frame Performance Under Vertical and Lateral Loads," *ACI Journal, Proceedings*, Vol 70, No. 4, April 1973, pp 261-269.
12. Farah, A., and Huggins, M. W., "Analysis of Reinforced Concrete Columns Subjected to Longitudinal Loads and Biaxial Bending," *ACI Journal*, July 1969, pp 569-575.
13. Ferguson, P. M., and Breen, J. E., "Investigation of the Long Concrete Column in a Frame Subject to Lateral Loads," *Symposium on Reinforced Concrete Columns*, SP-13, American Concrete Institute, Detroit, 1966, pp 75-120.
14. Ford, J. S., Chang, D. C., and Breen, J. E., "Design Indications from Tests of Unbraced Multipanel Concrete Frames," *Concrete International*, March 1981, Vol 103, No. 3, pp 37-47.
15. Furlong, R. W., "Column Slenderness and Charts for Design," *ACI Journal, Proceedings*, Vol 68, No. 1, January 1971, pp 9-17.
16. Hognestad, E., "A Study of Combined Bending and Axial Load in Reinforced Concrete Members," *University of Illinois Bulletin, Engineering Experimental Station Bulletin Series No. 399*, November 1951.
17. MacGregor, J. G., and Hage, S. E., "Stability Analysis and Design of Concrete Frames," *Journal of the Structural Division, ASCE*, Vol 103, No. ST10, October 1977, pp 1953-1970.
18. MacGregor, J. G., Breen, J. E., and Pfrang, E. O., "Design of Slender Concrete Columns," *Journal of the American Concrete Institute, Proceedings*, Vol 67, No. 1, January 1970, pp 6-28.
19. Newmark, N. M., "Numerical Procedure for Computing Deflections, Moments, and Buckling Loads," *Transactions, ASCE*, Vol 108, 1943, p 1161.
20. Newmark, N. M., and Rosenbleuth, E., *Fundamentals of Earthquake Engineering*, Prentice-Hall, Inc., 1971.
21. Nixon, D., Beaulieu, D., and Adams, P. F., "Simplified Second-Order Frame Analysis," *Canadian Journal of Civil Engineering*, Vol 2, No. 4, December 1975, pp 602-605.
22. Novak, M., "Dynamic Stiffness and Damping of Piles," *Canadian Geotechnical Journal*, Vol 11, No. 4, 1974, pp 574-598.
23. Poston, R. W., "Computer Analysis of Slender Nonprismatic and Hollow Bridge Piers," M.S. Thesis, The University of Texas at Austin, Texas, May 1980.
24. Poston, R. W., Breen, J. E., Roesset, J. M., "Analysis of Nonprismatic or Hollow Slender Concrete Bridge Piers," *ACI Journal*, Vol 82, No. 5, September-October 1985, pp 731-739.
25. Poston, R. W., Diaz, M., Breen, J. E., and Roesset, J. M., "Design of Slender, Nonprismatic, and Hollow Concrete Bridge Piers," *Research Report 254-2F*, Center for Transportation Research, The University of Texas at Austin, August 1982.
26. Poulos, H. G., "Behavior of Laterally Loaded Piles: I - Single Piles," *Journal of Soil Mechanics and Foundations Division, ASCE*, Vol 97, No. SM5, 1971, pp 711-731.

27. Sanchez-Salineró, I., and Roesset, J. M., "Static and Dynamic Stiffnesses of Single Piles," Geotechnical Engineering Report GR82-31, Geotechnical Engineering Center, Civil Engineering Department, The University of Texas at Austin, August 1982.
28. Schmertmann, J. H., "Use of the SPT to Measure Dynamic Soil Properties? - Yes, But...!" Dynamic Geotechnical Testing, ASTM, STP 654, 1978.
29. Stocks, R. W., "Computer Program for the Analysis of Bridge Bent Columns Including a Graphical Interface," M.S. Thesis, The University of Texas at Austin, December 1987.
30. Sykora, D. W., "Examination of Existing Shear Wave Velocity and Shear Modulus Correlations in Soils," Report, Department of the Army, Waterways Experimental Station, Corps of Engineers, Mississippi, September 1987.
31. Veletsos, A. S., and Wei, Y. T., "Lateral and Rocking Vibration of Footings," ASCE Soil Mechanics Journal, Vol 97, No. SM9, September 1971, p 1227.
32. Wood, B. R., Beaulieu, D., Adams, P. F., "Column Design by P-Delta Method," Journal of the Structural Division, ASCE, Vol 102, No. ST2, February 1976, pp 411-427.
33. Wood, B. R., Beaulieu, D., Adams, P. F., "Further Aspects of Design by P-Delta Model," Journal of the Structural Division, ASCE, Vol 102, No. ST3, March 1976, pp 487-500.